McGill University

A Study of the Effects of Cadaveric Decomposition on Hyperspectral Signatures of Soil and Vegetation

By

Carrie Herzog

Department of Geography
McGill University, Montreal, QC

A thesis submitted to McGill University in partial fulfillment of the requirements of the degree of Master of Science

ABSTRACT

Airborne hyperspectral imagery has shown promise as a viable method to discover clandestine graves in tropical moist forest ecosystems and on grass fields found in a humid continental climate (Kalacska 2009; Leblanc, Kalacska et al. 2012). Nevertheless, a better understanding of how decomposition affects the spectral signature of vegetation and soil is needed in order to minimize false positives. The main aim of the research was to test if the spectral signatures of plants grown in soil with fertilizer treatments such as manure, blood meal and bone meal can be differentiated from the spectral signatures of plants grown in soil with animal tissue (liver) undergoing decomposition. I also examined the effect of the fertilization treatments and common products of decomposition in comparison to the liver treatments on the spectral signature of soil. Results indicate that it is possible to distinguish between plants affected by the decomposition of the liver from fertilized soils. Changes within the spectral signature of soybean plants among the different treatments can be observed in the visible range around 500 to 650 nm. In soil, the greatest variation was found to be in the 450-900 nm and 2000-2400 nm ranges. As well differences in the leaf structure and soil microbial community were observed.

ABRÉGÉ

Des études ont démontrées qu'il est possible d'identifier des tombeaux clandestins à partir d'images aériennes hyperspectrales (Kalacska 2009; Leblanc, Kalacska et al. 2012). On peut différencier les signatures spectrales provenant d'une tombe de celles des environs pour plusieurs mois (Kalacska 2009). Cette technique de recherche permettrait de découvrir des tombeaux clandestins qui sont tombées dans l'oubli de façon plus sécuritaire et rapide Cette étude vise à améliorer la compréhension des effets de la décomposition d'un cadavre sur les signatures spectrales de la végétation et du sol afin de déterminer s'il est possible de différencier les signatures spectrales de fertilisants comme la farine de sang, la farine d'os et du fumier de celle des environs d'un cadavre en voit de décomposition. Pour approfondir nos connaissances sur ce sujet, des expériences en serres, comprenant 100 plantes de soja et 100 plantes de blé sous différent traitement ont été menées à terme. Les résultats démontrent qu'il est possible de faire la distinction entre les différents traitements, des variations surviennent entre 500-650 nm dans les signatures spectrales des feuilles des plantes de soja. Entre les signatures spectrales du sol et des différents traitements des variations se présentent entre 450-900 nm et de 2000-2400 nm. Il est aussi possible de décelées des différences au niveau de la structure interne des feuilles et dans la composition bactérienne du sol.

ACKNOWLEDGMENTS

During both my graduate and bachelor studies here at McGill, Professor Margaret Kalacska has not ceased to amaze me and help me throughout my scientific endeavor. She has helped me grow as scientist through questioning parts of my research. I was fortunate to work with hi-tech equipment, have funding and assist her along the way with some of her research. Since the beginning from my small independent study to the completion of this thesis, she was always there to support me. I couldn't have done this work without her! Many thanks!

I want to extend my thanks to Tim Moore for being part of my committee and giving me comments on my writing. I have learned a lot from your comments and also learned to love soil over the years. Thanks to Mike Dalva, for helping me at the beginning at Park Safari, it has been great working along your side. I want to extent many thanks to my colleagues, Marc, Julie, Sienna and Eva it was great to discuss things with you and get your insight and to take some pressure off.

Thanks to Dr. Andre Costopoulos, without you this journey might have never started. From being a student in the archaeology field course at Park Safari, meeting Margaret Kalacska, supporting me through my application process to McGill for graduate school.

On a personal level, I want to thank my parents who permitted me to stay at home and supporting me throughout my studies. And finally, thanks to my sister for standing by me when I tried to explain to you what my thesis was all about.

TABLE OF CONTENTS

LIST OF FIGURES

LIST OF TABLES

TABLE OF ABBREVATIONS

Abbreviations	Definitions
Ca	Calcium
C	Carbon
db	Daubechie
DEM	Digital Elevation Model
GIS	Geographical Information System
g	Grams
H	Hydrogen
kg	Kilograms
IR	Infrared
LIDAR	Light detection and ranging
Mg	Magnesium
m	Meters
nm	Nanometers
ROI	Region of interest
NIR	Near-infrared
N	Nitrogen
NDVI	Normalized difference vegetation index
O	Oxygen
P	Phosphorus
K	Potassium
SR	Simple ratio index
ANOVA	Analysis of Variance

CHAPTER 1- INTRODUCTION

1.1 PROJECT OVERVIEW

Clandestine graves and/or unknown grave sites can occur during war, under political instability, genocides or due to natural catastrophes (Bax 1997; Melvern 2006; Ruffell and McKinley 2014). Due to political turmoil, clandestine graves such as mass graves have occurred in many locations such as Bosnia (Jessee and Skinner 2005) , Rwanda and more recently mass graves are being found in Mexico due to drug cartel related violence (Keller and Pipitone 2010). Mass graves can also occur in the aftermath of natural catastrophes such as tsunamis and epidemics for sanitary reasons (Watts 1999; Jessee and Skinner 2005). One of the most common techniques to locate clandestine gravesites relies on witness testimony (Harrison and Donnelly 2009; Larson, Vass et al. 2011). However, witnesses may not come forth or might be uncertain of the location of these graves, thus a lot of time is spent by professionals and volunteers to survey the potential grounds (Harrison and Donnelly 2009).

It has been shown that through hyperspectral data it is possible to identify the location of graves within a tropical moist forest ecosystem (Kalacska 2009) and on grass fields found in a humid continental climate (near Ottawa, Canada) (Leblanc, Kalacska et al. 2012). Spectral signatures are the response (reflectance and absorption) of a material to incoming electromagnetic radiation at varying wavelengths. The use of hyperspectral data, information of incoming electromagnetic radiation at multiple wavelengths, can potentially improve the detection of the location of unknown graves. A better understanding of how cadaver decomposition in different soil types affects the spectral signature of vegetation and soil is needed in order to minimize false positives. The main goal of this research was to test if the spectral signatures of plants grown in soil with fertilizer treatments such as manure, blood meal and bone meal can be differentiated from the spectral signatures of plants grown in soil with a cadaver proxy (swine liver) undergoing decomposition.

1.2 STUDY OBJECTIVE

The main hypothesis of this research is that cadaver decomposition creates distinguishable features in the spectral signature of leaves and soils that are in contact with or in proximity to the remains. The following questions guided this research:

1. Does swine liver (cadaver proxy) decomposition within soil affect the spectral response of the vegetation growing in that soil?
2. Does swine liver (cadaver proxy) decomposition within soil result in distinguishable features in the spectral signature of the soil itself?
3. Are the spectral signatures of fertilized areas (e.g. with bone meal, blood meal or manure) distinguishable from areas affected by cadaveric decomposition?

To address these research questions, greenhouse experiments during the summers of 2011 and 2012 were performed with soybean and wheat plants, swine liver and different fertilizer treatments. Swine liver was used as a cadaver proxy since it is a blood and nutrient-rich organ that is readily available. Hyperspectral measurements were done on the treated soils and plants growing within them. The data were subsequently analyzed.

CHAPTER 2- LITERATURE REVIEW

2.1 CADAVER DECOMPOSITION

Cadaver decomposition occurs in the following stages: autolysis, putrefaction, liquefaction and disintegration and skeletonization (Dent, Forbes et al. 2004; Carter, Yellowlees et al. 2007; Forbes 2008; Tibbett and Carter 2009). Autolysis starts when the heart stops beating and cells, tissues and organs start breaking down due to the lack of oxygen. When cellular respiration stops, the lack of oxygen within the body causes pyruvate acid (CH_3COCOO^-) derived from glucose to be transformed into lactic acid ($C_3H_6O_3$) (Carter, Yellowlees et al. 2007). This causes the pH of the body to decrease; hydrolytic enzymes are stimulated by this drop in pH causing the breakdown of proteins, carbohydrates and lipids (Carter, Yellowlees et al. 2007).

Putrefaction occurs when chemicals within the body interact with each other, causing gases to form; this can be seen as bloating. At this stage, proteins will undergo proteolysis and are transformed through this process into proteoses, peptones, polypeptides and amino acids (Dent, Forbes et al. 2004). Proteoses, peptones, polypeptides and amino acids are subsequently transformed either into phenolic substances such skatole and indole or into gases such as carbon dioxide, hydrogen sulfide, ammonia and methane due to bacteria and enzymes (Dent, Forbes et al. 2004; Carter, Yellowlees et al. 2007). Subsequently, the ammonia (NH_3) from the decomposition of body protein may be converted to ammonium (NH_4^+) in the presence of low soil pH (below 5) and can be subsequently utilized by surrounding plants (Carter, Yellowlees et al. 2007; Forbes 2008; Tibbett and Carter 2009). Under higher pH (>5.5) ammonia (NH_3) can be converted into nitrate, potentially causing denitrification (Carter, Yellowlees et al. 2007; Forbes 2008; Tibbett and Carter 2009). Hence, cadaver decomposition can result in the formation of an enriched environment for vegetative growth, also known as a cadaver decomposition island (Carter, Yellowlees et al. 2007).

It has been observed that in the early stages of decomposition, oxygen is consumed by bacterial activity at a fast rate, giving rise to anaerobic conditions that will create the formation of different gases such as methane (CH_4) (Dalva,

Kalácska et al. 2012). In certain cases, methane emanating from the ground may be a potential indicator of the location of open graves (Dalva, Kalácska et al. 2012). It is proposed that such gas emissions from graves might be governed by the high productivity of microbes that are dependent on anaerobic conditions (Dalva, Kalácska et al. 2012).

The process of decomposition continues with liquefaction, disintegration and skeletonization (Carter, Yellowlees et al. 2007; Forbes 2008). This occurs when bacteria and other processes transform the flesh and organs into different elements which are transferred to the soil (Swann, Forbes et al. 2010). Hydrocarbons are also released throughout the decomposition process such as cadaverine, putrescine, toluene and benzene, among others, until soft tissues start to harden, desiccate or mummify (Dent, Forbes et al. 2004; Forbes 2008; Swann, Forbes et al. 2010). Skeletal remains continue to alter the surrounding soil environment as they decompose by adding minerals such as calcium to the soil (Carter, Yellowlees et al. 2007; Forbes 2008; Tibbett and Carter 2009).

The decomposition rate is affected by four main factors: temperature, moisture, pH and the partial pressure of oxygen (Vass 2008; Vass 2011). Decomposition usually occurs when temperatures are above 2 °C and accelerate when temperatures rise due to increase in bacterial activity (Vass 2011). When soils are dry or waterlogged, the decomposition rate slows down (Ellis and Mellor 1995). The density of the soil has an effect on how decomposition occurs; if oxygen is able to reach the body, decomposition will occur more quickly since aerobic decomposition is more efficient than anaerobic decomposition (Forbes 2008; Vass 2008). Even though decomposition rate is affected by many factors, the body will release nutrients into the soil throughout decomposition.

In sum, during the decomposition process, a cadaver releases many chemicals, elements and nutrients into its surrounding environment. The quantification of different elements found within the body determines the maximum influx of nutrients into the soil that can occur during the decomposition process. The human body is composed of around 64% water, 20% protein, 10% fat, 1% carbohydrates and 5 % minerals (Dent, Forbes et al. 2004). More

specifically, the top five elements that compose the body are: oxygen, carbon, hydrogen, nitrogen and calcium. A human cadaver weighing around 70 kg is composed of around 43 kg of oxygen, 16.1 kg of carbon, 7 kg of hydrogen, 2.1 kg of nitrogen, and 0.7 kg of calcium (Emsley 1998, refer to biological data under each element). These leached elements are expected to affect the surrounding environment as decomposition occurs.

2.2 REMOTE SENSING

There exist many ways to look for clandestine burials; most commonly, it is through witness testimony and search operations that the bodies will be found (Harrison and Donnelly 2009). Other techniques rely on specialized canine units that search for cadavers, or the magnetic response of the ground. LIDAR, digital elevation models (DEMs) and the use of geographical information systems (GIS) have also been proposed as ways to find graves (Carter, Yellowlees et al. 2007; Dorriety 2007; Schultz 2008; Govender, Dye et al. 2009). Using hyperspectral data (Figure 1), ground reflectance of electromagnetic radiation, has shown to be a promising alternative to detect burial sites (Kalacska 2009; Leblanc, Kalacska et al. 2012).

Hyperspectral data can be collected *in-situ* with a spectroradiometer or from a sensor mounted on an airplane or satellite. A hyperspectral data cube is a collection of measurements of the environment that contains information on the reflectance of the target material for multiple or hundred wavelengths (Jones and Vaughan 2010). Figure 1, illustrates a hyperspectral cube composed of multiple pixels. Each pixel contains information on how light is reflected and absorbed, basically indicating the spectral response (also known as the spectral signature) of a given material (Jones and Vaughan 2010).

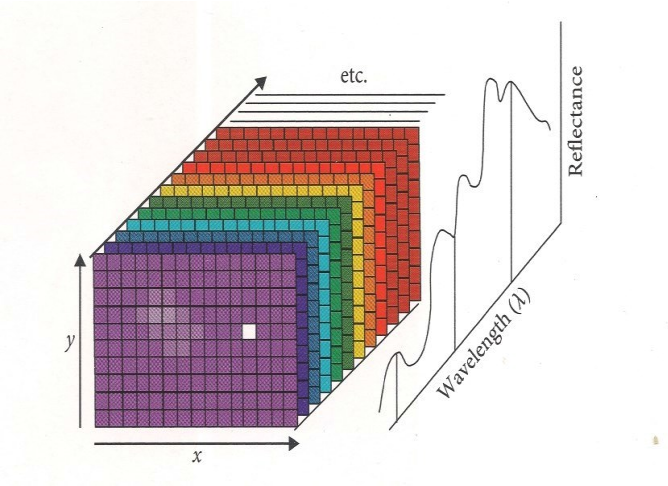

Figure 1: Hyperspectral image cube *(Jones and Vaughan 2010).* Reproduced with permission from the Oxford Press

Electromagnetic radiation interacts with materials in different ways: it can be absorbed, transmitted or reflected (Jones and Vaughan 2010). The amount of radiation that is absorbed, transmitted or reflected at different wavelengths is affected by the texture, chemical composition, structure and water content of the material (Ben-Dor 2002; Govender, Dye et al. 2009; Jones and Vaughan 2010). Hence, we can study the different chemical components that comprise materials by looking at features found in the spectral signatures.

2.2.1 VEGETATION

Different characteristics of plants such as the photosynthetic pigments (e.g. chlorophyll) and leaf structure determine how light interacts with the leaves. For example, in the spectral signature of a leaf, a large change in reflectance between the visible and near infrared range of the spectrum (600-800 nm) is found, this is called the red edge (Jones and Vaughan 2010). Different areas of the spectral signature of vegetation are linked to the plant structure and to pigmentation (Govender, Dye et al. 2009; Jones and Vaughan 2010). At the leaf level, the visible part of the spectrum within the spectral signature of the leaf is linked to pigments found in plants and cell structure is responsible for features found in the near infrared region of the spectrum (Peñuelas and Filella 1998; Govender, Dye et al. 2009) (Figure 2).

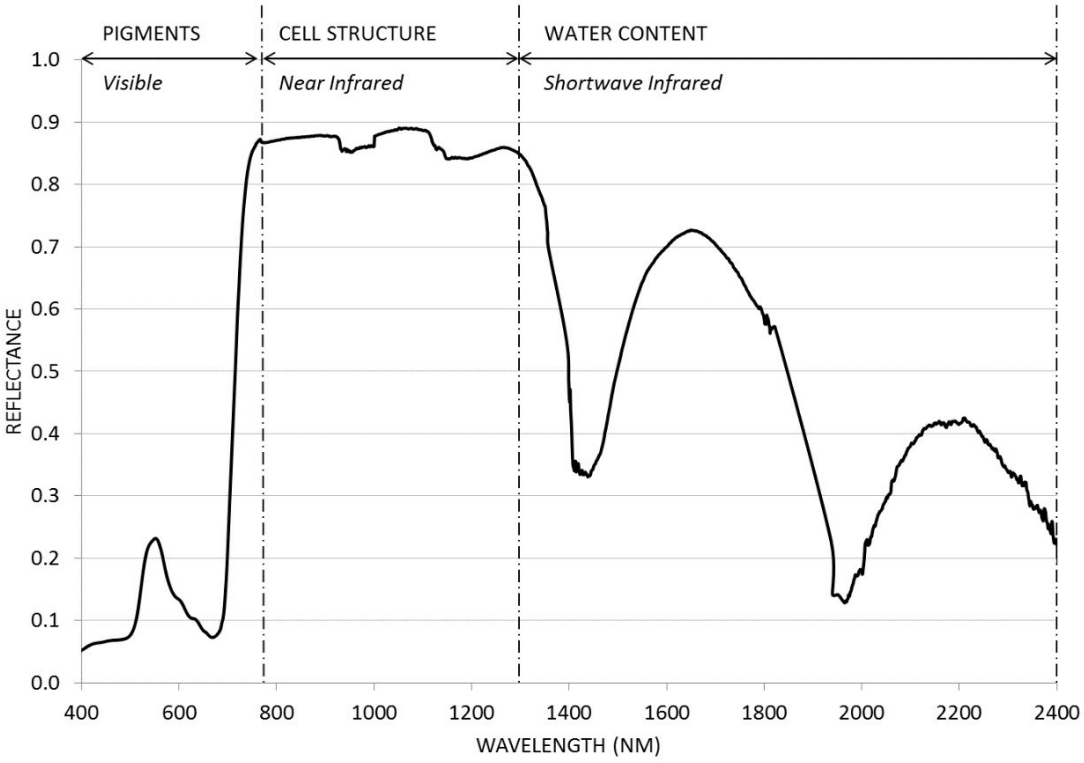

Figure 2: The spectral signature of a soy bean leaf collected with an ASD Fieldspec 3 Spectrometer. The reflectance of light is affected by different components of the leaf. In the visible part of the spectrum the spectral signature is affected by the concentration of pigments such as chlorophyll and carotenoids. The reflectance in the near infrared section in linked to the internal cellular structure of the leaf such as the size of the intercellular space and vacuoles. In the shortwave infrared, the reflectance of light by a leaf is mainly affected by its water content.

Table 1 lists some wavelengths that are related to absorption of energy by certain leaf components such as pigments and protein. Absorption features are defined as the concave shape of the reflectance spectrum at several consecutive wavelengths, where light is absorbed more than reflected. These features that are found in the spectral signature of vegetation are caused by the light interacting with specific leaf components such as the amount of pigments and leaf structure (Knipling 1970; Jones and Vaughan 2010). In the spectral signatures of leaves, the visible portion is highly affected by the chlorophyll and pigment concentrations such as carotenoids, xanthophylls, and anthocyanins (Jones & Vaughan, 2010). The reflectance of a leaf in the infrared portion of the spectrum is affected by its water content and internal cellular structure (Jones & Vaughan, 2010).

Table 1: Main absorption features of a leaf (Jones and Vaughan 2010). Reproduced with permission from Oxford University Press.

Wavelength (nm)	Chemical	Electronic transition or bond vibration
430, 460, 640, 666	Chlorophyll	Electronic transition
970, 1200, 1400, 1940	Water	O-H bond stretching
1510, 2180 (910, 1020,1690, 1940, 2060,2130,2400, 2300,2350)	Protein, Nitrogen	N-H stretching and bending, C-H stretching
2310 (930,1020)	Oil	C-H stretching and bending
1690, (1120, 1420, 1940)	Lignin	C-H stretching
1780	Cellulose and sugar	

The amount of light that is reflected is a function of the cell shape and size and of the amount of intercellular space found within the leaf (Knipling 1970; Jones and Vaughan 2010). For example, when a leaf is infiltrated with water, filling air cavities, there is a reduction in the reflectance of light in the near infrared (Jones and Vaughan 2010). Hence, the internal structure of a leaf is linked to the reflectance of the light in the near-infrared spectrum.

In general, plants uptake nutrients mainly at the root, where the soil solution provides nutrients such as K, N, P, Mg and other elements to the plants (Clemens, Palmgren et al. 2002). Nutrients, metals and toxins absorbed by plants can alter the cell structure of the leaves and the pigmentation (Kabata-Pendias, 2007). Trace elements and heavy metals are often toxic to plants and cause either the plant to have difficulty up taking sufficient water or to photosynthesize (Kabata-Pendias and Mukherjee 2007). Trace element concentrations in plants reflect, in most cases, the abundance of these elements found within the growth media (i.e. soil, nutrient solution, water) (Kabata-Pendias and Mukherjee 2007). The absorption of different trace elements can alter pigmentation or cell structure (Kabata-Pendias and Mukherjee 2007).

Alternation in the pigmentation and in the cell structure of the leaf will be seen in the visible to near infrared portion of the spectral signature .Therefore, it is possible from the basic shape of the spectral signatures to infer whether a plant is under stress.

In general, spectral signatures coming from different plants will be very similar to each other. In order to broadly assess the health of plants through the spectral signature of a leaf, indices have been developed. Indices such as Normalized Difference Vegetation Index (NDVI) (Tucker 1979, Jackson, Slater and Pinter 1983, Sellers 1985) emphasize the differences found in the greenness of plants by looking at the ratio of reflectance at specific wavelengths. Other indices such as the Simple Ratio (SR), Normalized Difference Pigment Index (NDPI), Vogelmann's Red Edge and Photochemical Reflectance Index (PRI) aid to assess the differences in pigments found among plants (refer to Appendix A) or compare the physiological status of different plants. As well, in precision agriculture, indices have been used in order to determine if chlorosis of plants is occurring. Chlorosis is the yellowing or whitening of leaves due to a decrease in chlorophyll (Adams, Philpot et al. 1998). Due to stress changes in the leaf cell structure will often occur, this affects how electromagnetic radiation interacts with the leaf, often resulting in a decrease in the reflectance of light (Adams, Philpot et al. 1998).

In sum, with indices it is possible to infer generalities about the health of the plants simply by looking at specific regions of their spectral signatures. Cadaver decomposition releases many nutrients and hydrocarbons into the soil matrix. This results in the formation of an enriched environment for vegetative growth, also known as a cadaver decomposition island (Carter, Yellowlees et al. 2007). Plants growing under these conditions should have more nutrients available to them, improving their capacity of photosynthesis, thus having an effect on the amount of pigments found within their leaves. This means that indices may help to distinguish between the spectra of plants that are in proximity or in contact with cadaveric decomposition from plants that are not.

2.2.2 SOIL

Vegetation spectral signatures are in part the product of the amount of nutrients available to the plants. This is partially determined by the underling soil. Soils are basically composed of primary minerals, secondary minerals and organic matter (Ellis and Mellor 1995). Primary minerals are minerals, which come from igneous or metamorphic rocks that are chemically and or physically weathered. Secondary minerals are derived from sedimentary rocks, which are found in the soil matrix. These inorganic minerals provide the initial structure of the soil matrix (Campbell, Reece et al. 2003). Organic matter comes from decomposing matter such as leaf litter (Ben-Dor, Inbar et al. 1997). The particle size of the soil determines how a soil absorbs water, how nutrients are transported throughout the soil and its pH. The basic mineralogy determines the ion exchange capacity of soil. The cation exchange is a mechanism that permits roots to take up positively charged ions (cation). Inorganic cations, such as calcium (Ca^{2+}), magnesium (Mg^{2+}) and potassium (K^{+}) can be found on the negatively charged surfaces of the clay particles (Ellis and Mellor 1995). In order to absorb the cations that adhere to the surface of clay particles, roots release hydrogen ions (H^{+}) into the soil solution (Campbell, Reece et al. 2003). Then, the hydrogen ions displace nutrients found on the clay particles, enabling roots to absorb the free cations.

In general, plants utilize the soil solution to extract sufficient nutrients from the ground. When the soil is not dry or waterlogged, plants are able to absorb nutrients adequately which permits them to photosynthesize (Ellis and Mellor 1995; Kabata-Pendias and Mukherjee 2007).

2.2.2.1 SOIL AND SPECTRAL SIGNATURES

The spectral signature of soil is affected by its water content, amount of organic matter contained by the soil and its basic structure. The presence of organic matter darkens the soil's coloration (Bowers and Hanks 1965; Wessman 1991; Ben-Dor 2002; Dematte, Nanni et al. 2010). Soils with high soil organic matter content tend to have a concave spectral shape between 500 and 750 nm (Huete and Escadafal 1991). On the other hand, soils with a low organic matter content have a more convex spectral shape between 500 and 750 nm (Huete and Escadafal 1991). In general, absorption features linked to Fe oxides can be found at 450 nm and 650 nm (Stoner and Baumgardner 1981; Ben-Dor 2002; Dematte, Nanni et al. 2010). Depending on its moisture content, soil will be more or less reflective; wetter soils have lower reflectance than drier soils (Figure 3).

Bands around 1400 and 1900 nm are related to water absorption (Wessman 1991; Ben-Dor 2002; Fidêncio, Poppi et al. 2002), around 2250 nm they are related to hydroxyl being present within the soil. Ben-Dor et al. (2002) studied the reflectance of decomposing organic matter (cow manure and grape mare(grape skins and seeds left over while extracting grape juice to a make wine)) in the visible to short wave infrared region (400-2500 nm). The study found that not only does the reflectance of the two materials differ from one another but also the amplitudes of the reflectance spectra decrease as decomposition advances. The reflectance in the visible to near infrared region of the spectrum is dependent on the amount of organic matter that is present within the soil. Soils with larger amounts of organic matter tend to be darker in coloration thus less reflective. The near infrared to shortwave infrared region of the spectrum contains information relating to hydroxide bonds and the structure of the soil (Ben-Dor, Inbar et al. 1997; Ben-Dor 2002). Nevertheless, it is important to note that soil reflectivity is very sensitive to water; drier soils will generally be more reflective than wet soils (Bowers and Hanks 1965) (See Figure 3).

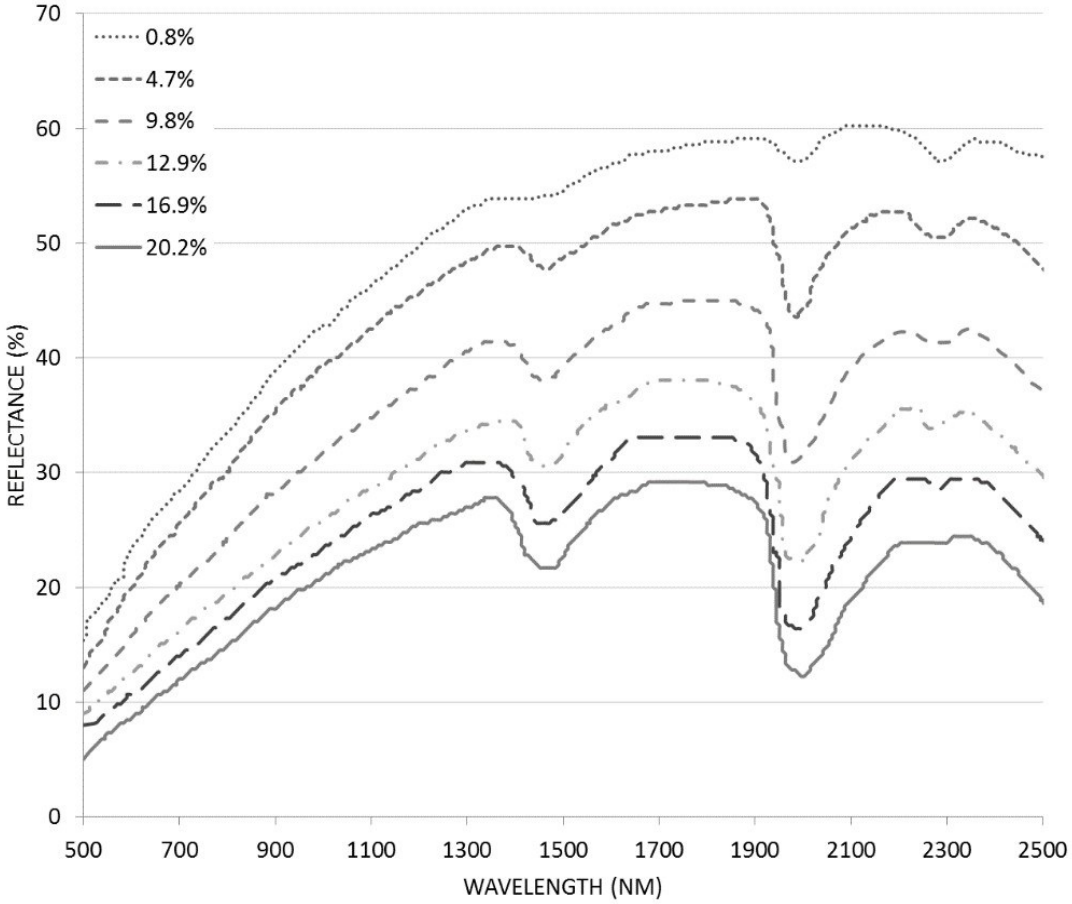

Figure 3: Soil reflectance at different moisture levels (0.8 %, 4.7%, 9.8%, 12.9% 16.9% and 20.3%) (Bowers and Hanks, 1965), Reproduced with permission of Wolter Kluwer Health publishers. The reflectance of the soil is affected by its moisture level, wetter soils are less reflective than soils that have little moisture.

2.2.3 FERTILIZERS

As mentioned previously, the decomposition of a cadaver releases nutrients into the ground promoting plant growth (Dent, Forbes et al. 2004; Forbes 2008; Tibbett and Carter 2009; Larizza 2010; Swann, Forbes et al. 2010). When looking for cadavers through the use of hyperspectral data it is important to understand how different fertilizers such as bone meal, blood meal and manure are from each other and from grave soil. Literature on how to monitor animal feed provides valuable information on how spectrally different blood meal is from different types of feed. Garrido-Varo (2008) showed that the spectral difference between the types of meals occur mainly from 1560 to 1800 nm. As decomposition increases, the amount of organic matter within the soil increases; presence of organic matter in the soil darkens the soil's

coloration; this is observable in the spectral signature from 500 to 750 nm (Huete and Escadafal 1991; Bartholomeus, Schaepman et al. 2008; Dematte, Nanni et al. 2010).

Other studies have focused on identifying the nitrogen and carbon content of soils, trying to determine if indices can be created in order to assess these differences within soil (Filella, Serrano et al. 1995; Stone, Solie et al. 1996). Features along the 1600 to 1800 nm range can be attributed to the O-H bonds that occur within the soil (Ben-Dor 2002). Some studies have found that it is possible to attribute specific features found along the spectra of organic matter to certain functional groups: aliphatic C-H (1414 nm), water O-H (1440 nm), which also shows absorbance in the region of 1800–1900 nm, aliphatic C-H (1760 nm), phenolic O-H (1500 to 1800 nm), amide N-H (1980 nm) (Ben-Dor, Inbar et al. 1997). In the region of 2000 to 2400 nm there are groups such as phenolic O-H (2000 to 2200 nm), amine N-H (2000 to 2100 nm), aliphatic C-H (2308 nm) and amide N-H (2050 and 2180 nm) (Huete and Escadafal 1991; Ben-Dor, Inbar et al. 1997; Ben-Dor 2002).

Since there are particular features that are linked to organic matter and the amount of nitrogen present within the soil, it is most likely that similar features can be found to differentiate fertilized soils, non-fertilized soils and grave soils from one another; as a result these features can be observed in the spectral signatures of soil.

CHAPTER 3- METHODS

This study was conducted over summer 2011 and 2012; the first consisted of a preliminary experiment during summer of 2011 in the Phytotron facility at McGill University, and the second experiment was conducted during summer 2012 within a greenhouse located in Vaudreuil-Dorion, QC.

The main objective was to determine the degree to which treatments applied to soil would influence the spectral signature of the soil and plants grown within them. Two plant species were utilized for both experiments: wheat (*Triticum durum*) and soybean (*Glycine max*). These plants are physically different; the soybean is considered a N_2 fixer and is a crop that is widely utilized by farmers in the region. The second is wheat, a grass type and a common crop. Different experiments were conducted in order to determine the influence of decomposing animal tissue (swine liver) on soil and vegetation spectra. The following will initially describe the set-up of each experiment and then go over the analysis that was performed on the spectral signatures.

3.1 SET UP AND DATA COLLECTION

3.1.1 VEGETATION EXPERIMENTS

3.1.1.1 PHYTOTRON

The main objective of this experiment was to determine if it is possible to distinguish the spectral signatures of soil and vegetation affected by different fertilizer treatments (blood meal, bone meal and manure) from the spectral signature of plants and soil that are in contact with a cadaver proxy (swine liver).

The experiment took place from June to August 2011 at the Phytotron facilities at McGill University's downtown campus in Montreal, Canada (Figure 4). A greenhouse room that was equipped with a bench measuring 305 x 550 cm, a hose with running water and ventilation system was used for this experiment. The temperature within the greenhouse can be maintained around 4°C below ambient but during the summer temperatures may rise up to 40°C.

Two types of soil were used; the first soil that was collected came from a control area at Parc Safari animal graveyard. The control area is believed to be free of animal remains and was verified by test pits approximately every 5 m

along 3 transects. The park is situated in Hemmingford QC (45°02' 44N, 73°31'58 W). St-Bernard series soil dominates the area: it is well drained, stony, gravelly clay loam. The soil is Eutric Brunisol derived from calcareous and dolomitic till (Mailloux and Godbout 1954). The second soil was purchased at the Phytotron facility. It was Fafard brand black organic soil. The fertilizers: blood meal and bone meal were purchased at the local gardening center. These fertilizers are easily obtained and are used by local gardeners. The manure was obtained from McGill's MacDonald campus farm from cows that were given a grass diet.

The soil and manure were autoclaved prior to the experiments to follow the Phytotron safety and bio-hazard regulations. This process removed any living organism and bacteria found in the soil that would promote decomposition. The decomposition rate may be altered due to the removal of existing microbial community. At the end of the experiment the soil and liver were disposed following bio-hazard waste disposal guidelines.

A total of 108 ,1.1 liter, pots (48 containing wheat, 60 containing soy) with one of the following treatments applied: liver (150 g), manure, blood meal, bone meal or nothing mixed into the soil (see Appendix B for Phytotron treatment breakdown) was used. For the fertilizer mixture, 15 g of fertilizer was applied to each pot requiring the treatment. Half of the pots for each type of plants contained soil collected from the control area at Parc Safari and the other half contained Fafard black organic soil. Plants were watered on a daily basis allowing for the soil to become completely wet, water then drained through the holes at the bottom of the pots. Ladybugs were purchased to prevent and to lessen aphids proliferating on the plants being grown at the facility. Aphids feed on the plant's sap causing damage to the plants (Dixon 1998), so it is important to use a method that has little impact on the spectra signature on the plant to get rid of these pests.

Each pot contained roughly 1.1 liters of soil with their respective treatment. Pots with wheat plants were placed on the right bench and soybean on the left bench. Then, the pots were randomly distributed throughout the work bench (Figure 4).

Figure 4: Photograph taken at the Phytotron facility (end of July 2011). The samples were randomly distributed on each bench (left bench= soybean, right bench =wheat).

The plants were planted on June 21st 2011. The first height measurements were recorded two weeks later once the plants emerged from the pots. This was done with a measuring tape, extending it from the top of the soil to the uppermost leaf.

The hyperspectral data of the leaves were collected three times (8th of July, 3rd of August, 12th of August of 2011) during this experiment with an Analytical Spectral Devices Hand Held spectrometer. This instrument measures reflected radiation in the 350-1200 nm range. The measurements were taken by using a leaf clip, which allowed for contact measurements of the leaves. The measurements were done on grown leaves to avoid damaging the plant during the initial growth stages. Between each leaf measurement a white reference measurement with a 99% reflective Spectralon panel was done. The spectral measurements were then truncated to 450-950 nm range in order to remove noise.

On the same days as collection of spectral data, leaf samples from ten randomly selected plants were collected. These leaves were frozen for chlorophyll extraction. Additional soil mixtures were kept for analysis to compare with soil previously collected at the animal cemetery of Parc Safari. The soil that was collected was sieved, oven dried and ground in order to homogenize texture and moisture levels throughout the samples.

3.1.2 VAUDREUIL-DORION

The second part of the experiment took place in a greenhouse in Vaudreuil-Dorion, QC, (45°21'29 N, 74°01'55 W) during the summer of 2012 from May to September. A total of 200 plants were planted in pots, half were soybean and the rest were wheat. The experiment used liver, fertilizer and control treatments (Table 2). Table 2 shows the different combination of treatments that were applied to the soil. Treatments numbered from 1-10 are pots planted with soybean and treatments from 11-20 were wheat. Each treatment had 10 replicates. A total of 100 pots contained wheat plants and 100 pots contained soybean plants under the different treatments. Figure 5 illustrates the setup. The swine liver was purchased at a local butcher shop. Soybean seeds were obtained from a local farmer and the wheat at the agricultural co-op.

Table 2: Treatments applied in the Vaudreuil-Dorion experiment. Soybean and Wheat ID identify the treatments that were applied within different pots. These ID numbers were used in the random block design.

Soybean ID	*Wheat ID*	*Fertilizer Treatment*	*Amount of Swine Liver (in grams)*
1	11	0	0
2	12	15 g of Manure	0
3	13	15g of Bone meal	0
4	14	15g of Blood meal	0
5	15	0	50
6	16	0	100
7	17	0	200
8	18	15 g of Manure	50
9	19	15g of Bone meal	50
10	20	15g of Blood meal	50

The pots were placed in the greenhouse using a random block design (Figure 5A). The random block design was utilized instead of a Latin square design due to space limitation (the benches are rectangular within the greenhouse with a total space of 5.8 m^2). The first bench measured 4'x 6' (1.22 m x 1.83 m), the second bench measured 3'x 13' (0.91 m x 3.96 m). The blocks consisted of trays that are only capable of holding 8 pots (Figures 5B). There were a total of 25

trays (blocks), 10 trays contained only non-liver treatments and the 15 others contained liver treatments (Table 2). For more detailed breakdown refer to Appendix B. The treatments were randomly distributed within the blocks (Figure 5 B). This design was utilized in order to limit the effects of lighting and air circulation as possible factors in the experiment (Potvin 1993).

Pest control was done biologically, for example, when aphids, were found. Praying mantises were bought to control the problem, they were chosen since they eat a larger array of insects that can be harmful to plants than ladybugs. These insects do not influence the plant or soil spectra since they are predatory.

Plant height was recorded on a weekly basis. Photographs were taken with the measurements to visualize the growth of the plants over time. On a monthly basis, leaf reflectance was recorded with an Analytical Spectral Devices Handheld Spectrometer from 325 nm to 1025 nm using a leaf-clip with an integrated halogen light source. The signal was reduced to a 450 nm - 950 nm range in order to reduce the amount of noise found in the data.

A

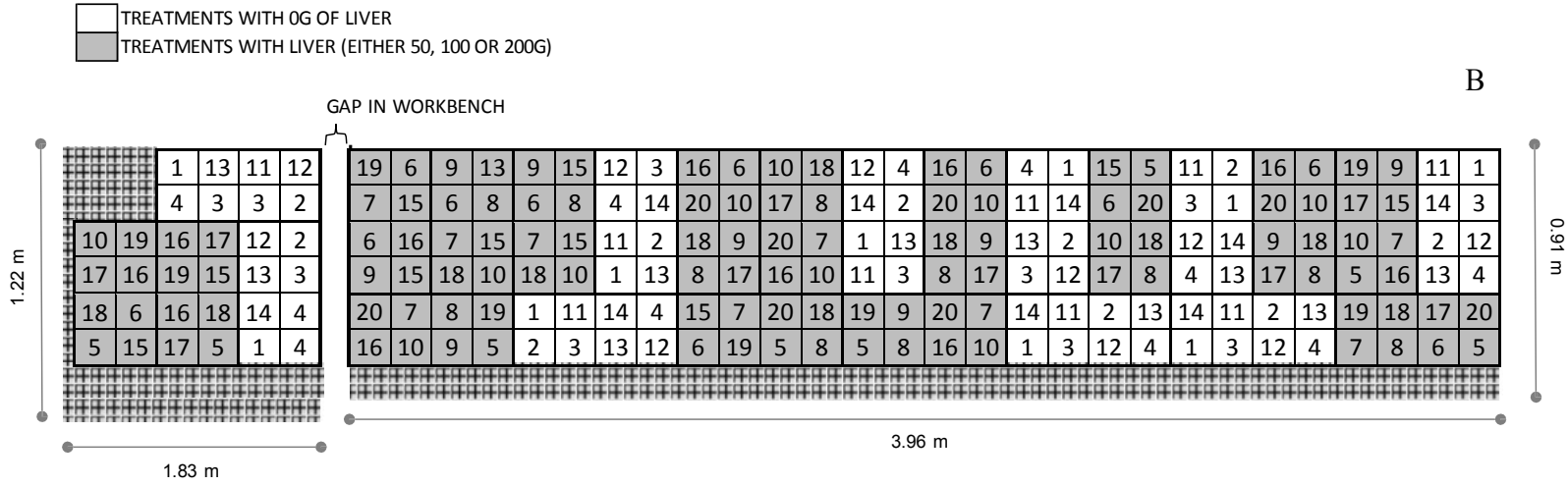

Figure 5: Vaudreuil-Dorion Experiment Set-up. Panel A shows the setup of the plants within the greenhouse during summer 2012. B illustrates the random block design; trays seen in panel A were used to separate liver treatments (containing 50 g, 100 g, and 200 g) from non-liver treatments (0 g of liver). The numbers within the cells are the treatment IDs (refer to Table 2). The greenhouse had two benches, the first bench measured 4'x 6' (1.22 m x 1.83 m), the second bench measured 3'x 13' (0.91 m x 3.96 m), they were separated by a gap. Trays were placed on the benches and then the treatments were distributed randomly respecting the blocking (liver (15 trays) and non-liver (10 trays)).

3.2.1 SOIL EXPERIMENTS

A key objective of this research was to determine where in the spectral signature identifying features may occur due to cadaveric decomposition. The following questions guided this research:

1. Are there variations found between the spectral signature of grave soil and non-treated soil?
2. Are certain chemicals leached by the body responsible for the changes along the spectral signature of grave soils?
3. Is it possible to distinguish fertilized soil spectral signatures from grave soil spectral signatures?

In order to answer the questions above, three experiments were performed. The main goal of the first experiment with soil was to determine if it is possible through parametric classification to distinguish between different fertilizer treatments and grave soil. This was initially done with soil from the animal cemetery of Parc Safari. This experiment was repeated with soil collected in Vaudreuil-Dorion, to test whether different treatments were still separable when mixed with a different soil type.

The second experiment tested whether different amounts of swine liver within the soil would affect the spectral signature of the soil differently. For this experiment, 0, 50, 100 and 200 g of swine liver were placed into pots for a two month period, the soil spectral signature was collected biweekly. The spectral signatures were measured in the lab at McGill. This was done in a dark room under constant viewing and lighting angles, the halogen light was placed at 30 cm above the surface of a table with an angle of 45 degrees. This set up was kept throughout the experiment.

The final experiment examined the effects of certain chemicals that are produced by the decomposition of the body on the spectral signature of the soil. This consisted of mixing chemicals with soil at 1 part chemical to 5 parts soil ratio. This experiment was repeated twice, once with soil coming from the reference area at Parc Safari and second with soil collected in proximity to the greenhouse in Vaudreuil-Dorion. This experiment studied the spectral signatures

of soil from 450 to 2200 nm with an Analytical Spectral Devices (ASD) FieldSpec3 spectrometer.

3.2.2 SOIL COLLECTION

As mentioned above, soil for the experiments were collected at two different sites. The first site, situated in Hemmingford, Quebec, is an African animal zoo graveyard. The animals were buried there over the past 50 years. Some graves have been located by the McGill archeological field course. The age of these graves remains unknown. The archeological field course's objectives were to teach students archaeological methods such as test pitting and excavation. For the first soil experiment, soils from three graves and an area known to not contain animal remains were used (reference/control soil). The reference area was verified through test pits dug by students participating in McGill's archeological field class; no animal remains were found. Only the top layer of the soil (0-15 cm) was collected. The area is dominated by St-Bernard series soil; it is well drained, stony, gravelly clay loam Eutric Brunisol derived from calcareous and dolomitic till (Mailloux and Godbout 1954).

Prior to the spectral measurements, these soils were sieved, dried and ground to assure homogeneity of texture and moisture levels between samples. The reference soil was mixed in equal parts with each of the fertilizers. Reflectance of the reference area soil, grave soil, fertilized soil (manure, compost, bone meal and blood meal) and pure fertilizer was measured with an Analytical Spectral Devices Handheld Spectrometer (from 400-950 nm) in a darkroom with a high intensity halogen light source for illumination. Lighting and viewing geometries were kept constant for each set of measurements; the light source was placed on a tripod at 30 cm from the table angled by 45 degrees towards the sensor that was placed 5 cm above from the sample.

Soil from near the greenhouse in Vaudreuil -Dorion was also collected, and only the top soil was kept (top 15 cm). The greenhouse is situated in Vaudreuil-Dorion in the political administrative county of Soulanges and Vaudreuil. The region is mostly underlain by Potsdam sandstone (Lajoie and Stobbe 1951). Through glaciation the region received silt and alluvial deposits.

The soil around the greenhouse is of Rideau series, which contains clay. The Rideau series soils are normally acidic (around 5.4 pH) but in some instance they can become almost neutral depending on drainage conditions (Lajoie and Stobbe 1951). Two cups of the untreated Vaudreuil soil were sent for microbial count and soil chemistry analysis at the start and the end of the experiment to the Soil Foodweb Canada Laboratories situated in Vulcan, AB, Canada. At the end of the experiment two cups of soil treated with liver were also sent for the same analysis.

The second experiment was done to test whether different amounts of swine liver decomposing within the soil would have a similar or different impact on the soil spectral signature. A set of 1.1 liter pots filled with Vaudreuil soil with 0, 50, 100 or 200 g of swine liver (each treatment had 3 replicates) were placed in the greenhouse. This experiment ran from September to December 2012. On a biweekly basis, 15 mL of soil was taken from the pots, ground, sieved and the reflectance was measured in a darkroom, keeping the same lighting and viewing geometry that was previously used for the first experiment. The reflectance measurements from 350 to 2500 nm were also performed with the Analytical Spectral Devices FieldSpec3. Samples were placed in small black trays (made of black cardboard). Ten spectra were collected per sample. These ten spectra were later averaged for analysis. Between each sample, a white reference was taken with a 99% reflective Spectralon panel.

The main focus of the third experiment was to examine how chemicals produced by cadaveric decomposition affect the spectral signature of the soil. The purpose was to determine whether the chemical compounds mixed with soil produce distinct features in the spectral signatures, thus enabling a better identification of graves through soil spectroscopy.

The following chemicals were used in the experiment: toluene, styrene, benzene, xylene, ethyl benzene, 1, 1, 2, 2-tetrachloroethane and carbon tetrachloride. These chemicals were chosen because they are described in the literature as being present in large amounts through the decomposition process (Vass 2008). To determine the effect of the compounds on the spectra, mixtures of 1 mL of chemical to 5 mL of non-grave soil were made. These soil mixtures were

measured with an Analytical Spectral Devices Fieldspec 3 Spectrometer (350-2500 nm) in a darkroom under a high intensity halogen light source for illumination. The lighting and viewing geometries were kept constant for each measurement.

3.3 ANALYSIS

The hyperspectral data collected throughout the different experiments were analyzed in the same way. The following explains the analysis of the hyperspectral data.

3.3.1 HYPERSPECTRAL DATA

Spectral measurements were taken from leaves and soil throughout the various experiments. These data were initially looked at for inconsistencies; measurements which contained negative values were discarded. Due to instrumental or measurement error there are often small variations in each spectral signal. To account for this noise, signals collected with the ASD handheld spectrometer were initially truncated; 450-950 nm range was kept. For the signals collected with the ASD Field Spec3 the spectral signature ranging from 450-2400 nm was kept. Then, to attenuate small variations, the spectral signatures were smoothed out using a Savitzky-Golay smoothing filter in MATLAB. The 3rd order filter with a window of 15 nm was used in order to attenuate small-scale variations.

Saviztky Golay can be understood as a moving average filter which attenuates small variations found along the spectral signature (Bromba and Ziegler 1981). This is often done in order to smooth out inconsistency and noise found within data.

To explore the data, a continuous wavelet transform was performed on the smoothed spectral signatures. This technique compares the signal (spectral signature) to a shifted and compressed or stretched version of a mother wavelet (Daubechies 1990; Daubechies 1992). The compression or the stretching of the wavelet is done through the use of a scale factor. A low scale factor will show small variation compared to a large scale factor which will highlight broader changes (Grossmann, Kronland-Martinet et al. 1989). The results are dependent on the wavelet that is used. The wavelet is a specific waveform, such as Mexican hat or a wave from the Daubechies (db) family (Grossmann, Kronland-Martinet et al. 1989).

The transform calculates the similarity found between the mother wavelet and the spectral signature. This method results in a scalogram, which helps to visualize the variation found along a given spectral signature at all scales. The scale chosen was the maximum scale (maximum scale= 127) allowed for the spectral signature. This was done in order to visualize large variations that occur in the spectral signatures due to the different treatments. It is possible to compare the different scalograms to visually identify differences found between the different spectral signatures. Through this method, Cheng, Rivard et al. (2010) were able to determine which trees were damaged by the pine beetle in a portion of boreal forest. By focusing on bands in the spectral signature that are affected by water deficiency and chlorophyll, it was determined that the features between 950- 1390 nm helped to distinguish healthy trees from trees affected by the northern pine beetle. This indicates that it is possible through the use of scalograms to differentiate healthy plants from ones experiencing stress.

Spectral fingerprints were generated to help visualize the difference found between the treatments. The conversion of spectral signatures to spectral fingerprints consists of using derivatives to emphasis the variation; Fingerprints were generated within Matlab from coefficients obtained through the continuous wavelet transform and then by generating a contour map. This method only allows visualization in order to gain a better understanding of where most variations occur within the spectral signatures.

The reflectance data were subsequently classified through the use of different classifiers. A supervised classification requires prior knowledge of objects found in the different classes (Duin, Juszczak et al. 2007). Initially, the data needed to be partitioned into training and testing subsets. A training dataset consists of defining classes in a subset of your data. A classifier is defined as an algorithm that is used to implement classification, in other word separate classes. A parametric classifier assumes some statistical properties of the data, such as normal distribution (Duin, Juszczak et al. 2007). A non-parametric classifier such as knnc (nearest neighbour) does not assume a particular distribution of the data.

In Matlab, when using the PrTools toolbox (Duin, Juszczak et al. 2007) it is possible to train several types of classifiers such as linear (ldc) orquadratic (qdc), to separate the dataset. By applying the trained classifier to the testing data subsets a validation error is calculated.

Initially, the data were partitioned into halves (training and testing subsets). Then, a forward feature selection was performed on the data, in order to rank the best bands to separate the data. Only the top five bands were used to separate the data since using more bands did not improve the separability of the classes

The following classifiers were used to separate the data: ldc, qdc, parzenc, knnc. Finally by applying the trained classifier to the testing data subsets a validation error is calculated.

3.3.2 HYPERSPECTRAL DATA CUBE

Creating an image with the different spectra facilitated the implementation of a broader range of analyses implemented in remote sensing software such as ENVI Classic. The spectral signatures that were collected during this experiment were subsequently placed into a data cube in order to replicate an image (Figure 6). This process was done in Matlab, the script can be found in Appendix D. In this case, each pixel represents a spectrum of a leaf (Figure 6). Since the matrix is constructed from the different spectra, each treatment can be pinpointed within the image. This allows for a straightforward selection of regions of interest (ROIs) that are specific to each treatment (Figure 6, B). Window B of figure 6

depicts ROIs, green represents the average June soybean spectral signature of treatments containing no liver (control, blood meal, bone meal and manure), red is soybean grown on a mix of soil and liver (150g), blue shows the non-liver treatments for wheat plants, yellow indicates treatments with wheat and 150g of liver in soil.

From these ROIs it is possible to calculate basic statistics and to perform some classifications. Once the different statistics are computed it is also possible to gain a better knowledge of how to reduce the dataset to specific bands in order to get a better separation of the different classes when performing.

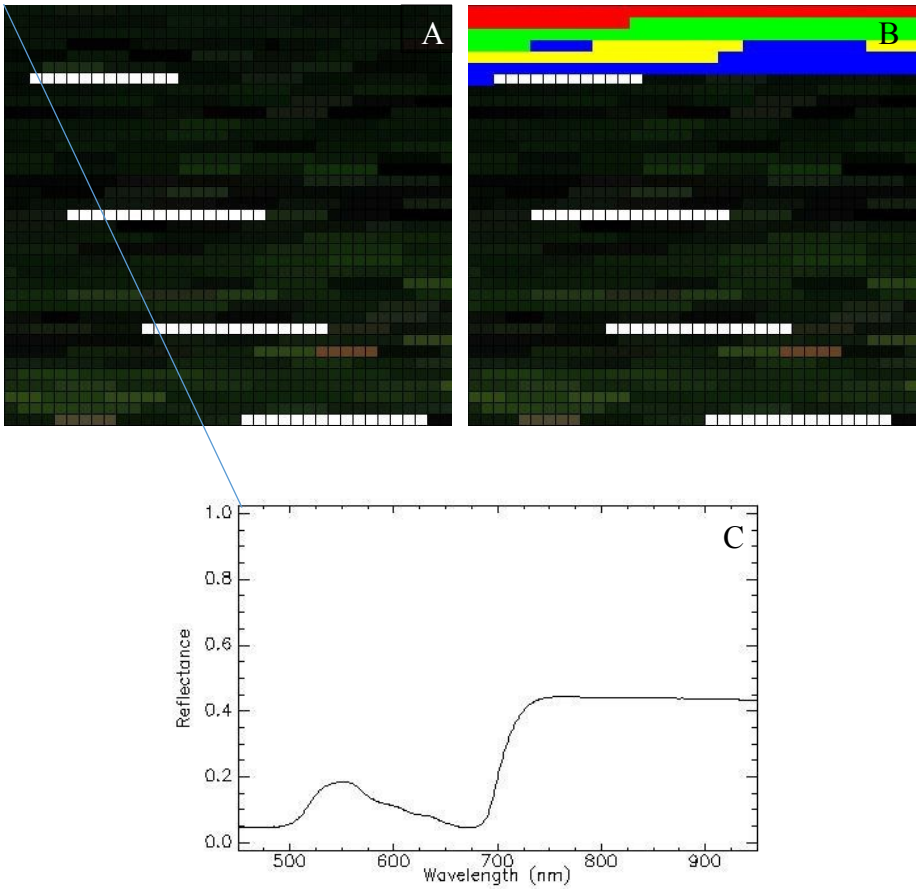

Figure 6: Summer 2012 leaf spectra hypercube. Window A illustrates the resulting hyperspectral data cube that was generated from leaf spectra collected during summer 2012 and window B depicts ROIs. The green ROI represents the average June soybean spectral signature of treatments containing no liver (control, blood meal, bone meal and manure), red is soy bean grown on a mix of soil and liver (150g), blue shows the non-liver treatments for wheat plants, yellow indicates treatments with wheat and 150g of liver in soil. Window C indicates that a pixel of the hypercube contain spectral signature of leaf.

3.3.3 TEM IMAGES

During the summer 2012 experiments it was noticed that spectral reflectance in the near infrared was different among treatments. These differences were thought to be associated with changes occurring in the structure of the leaves.

A comparison between two soybean leaves was performed in order to see the structural difference found between leaves grown on liver and soil from the ones grown on only soil and fertilizer. The leaves were initially frozen for chlorophyll extraction. From these leaves, two soybean leaves were selected for a comparison under an electron microscope. When the leaves were placed in the freezer, the leaves were wrapped in foil to prevent degradation. After inspection of the leaf it was determined that little damage was done by the freezing of the leaves, no change in coloration of the leaf was seen and little to no signs of freezing were seen under a microscope. These leaves were thawed and then placed in a polymer to fixate the leaves (see Appendix C for detailed procedure), thinly sliced and imaged with a transmission electron microscope at various magnifications. This process was done at the FEMR facilities at McGill University.

Once the images were obtained, they were viewed and analyzed using Image J software (Rasband 2012). Image J 1.47v is an open-source software that allows one to visualize and measure images. In Image J, the scale can be set to correspond to the image size (Figure 7). After obtaining the size of the cells for the treated leaf and control leaf, an ANOVA was performed to determine whether the average cell size was significantly different.

A B

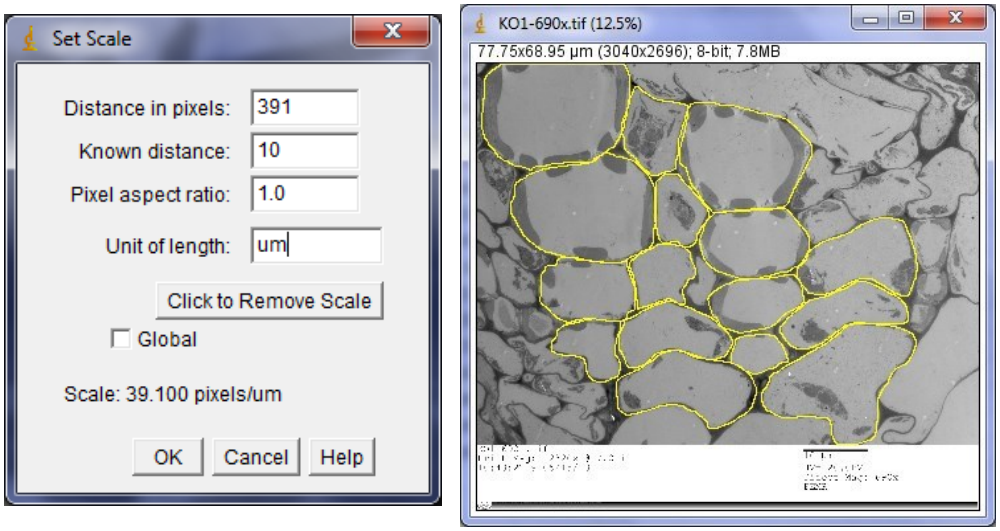

Figure 7: Using Image j, Panel A shows the setting up of scale, initially a measurement with the straight line tool is made and then the scale is set up. Panel B shows the outlines of the measured cells in the control leaf. Image J reports the area of each area that was drawn out.

3.3.4 CHLOROPHYLL EXTRACTION

To further investigate differences found between the treatments, chlorophyll extraction was performed on sampled leaves. The chlorophyll and carotenoids of these leaves were extracted using the Dimethyl sulfoxide (DMSO) digestion method (Aron 1949; Hiscox and Israelstam 1979). This method consists of using a specific amount of leaf material (e.g. 1 cm^2) that is digested in 5 mL of DMSO (Hiscox and Israelstam 1979). The absorbance of the solution was measured with the Thermoelectron Corporation GeneSys 10uv spectrophotometer at 470, 650, and 666 nm. The equations from Arnon (1949) and Lichtenthaler (1987), were calibrated to the spectrophotometer and used to determine chlorophyll and carotenoid concentrations respectively:

$$ChlA\left(\frac{g}{l}\right) = (0.0127 * Abs\ 666) - (0.00269 * Abs\ 650)$$

$$ChlB\left(\frac{g}{l}\right) = (0.0229 * Abs\ 650) - (0.00468 * Abs\ 666)$$

$$ChlTotal\left(\frac{g}{l}\right) = (0.0202 * Abs\ 650) + (0.00802 * Abs\ 666)$$

$$Cartenoids\left(\frac{g}{l}\right) = \frac{\left((1000 * Abs\ 450) - (1.82 * ChlA) - \left(\frac{(85.02 * ChlB)}{198}\right)\right)}{1000}$$

CHAPTER 4- RESULTS

4.1. VEGETATION - PHYTOTRON

4.1.1. GROWTH

On average four soybean plants emerged from non-liver treatments compared to two plants from pots which had liver inside them. Similar observations were seen for wheat, fewer plants emerged in pots that contained liver but this was harder to quantify since some plants grew closer together.

It is noticeable that for the initial growth stages (July 5th to 19th, 2011), plants seem to be hindered by decomposition, and remain shorter than plants under treatments that did not contain liver (Figure 8) (refer to Appendix D for measurements). Later in the growth stages plants under liver treatments reach the same height as plants that were only treated with fertilizers. The decrease in plant height from July 19th to Aug 2nd, 2011 (Figure 8) corresponds to plants dying off; during the period between the 19-26th of July 2011, Montreal experienced a heat wave. Even though the experiment was conducted within a greenhouse, temperatures increased to around 35°C. It is probable that some plants died due to the heat stress and lack of water.

A two way ANOVA test of the plant height at a given time period was done in order to test the difference found between groups and time. On figure 7, the group labeled as 'soy with liver,' is an average of all treatments containing liver (including manure, blood meal and bone meal mix); the ones without liver also include the different mixes of fertilizers. This was done to take into account whether differences occurred depending on the addition of liver within the treatments. The error bars on figure 8 correspond to 1 standard deviation.

The results of the two way ANOVA indicates that both through time and treatments, the plant heights show a significant difference with p=0.0012. This indicates that at different time periods, plant height was different and that between treatments there is a significant level of difference found with a p-value of less than 0.05.

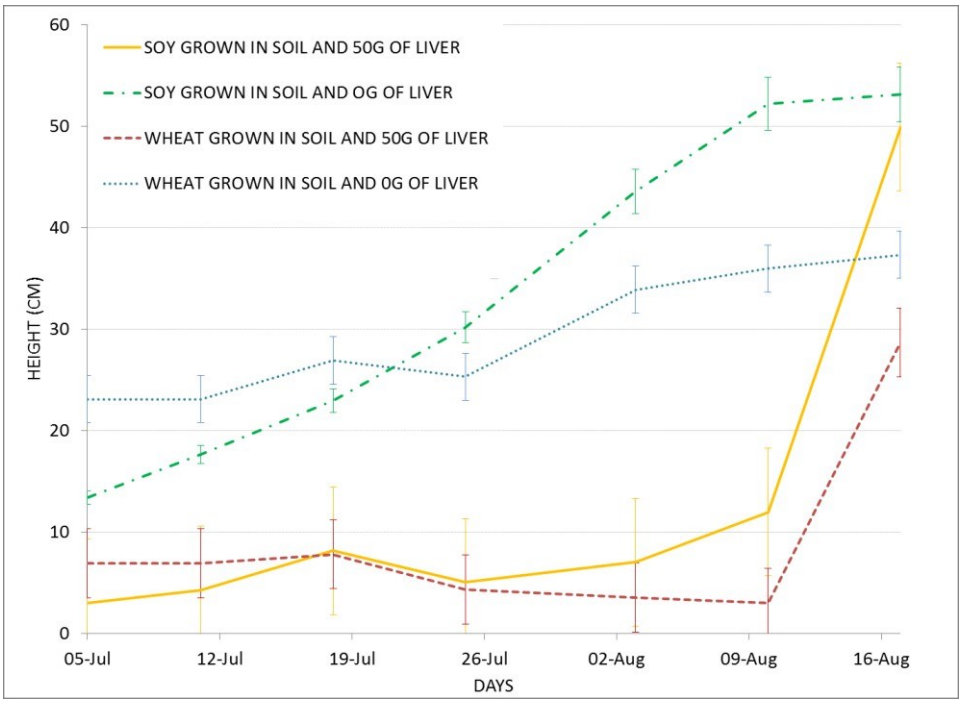

Figure 8: Average plant growth from July to August 2011. Error bars represent 1 standard deviation. The lines show the growth pattern of plant under 0g of liver and 50g of liver.

4.1.1.2 SPECTRAL SIGNATURES

Figure 9 illustrates the average spectral signatures collected from the soy control treatment (no fertilizer treatments), the soy with liver (150 g), wheat with liver (150 g) and wheat control. The reflectance of the plants grown with the liver treatments is generally lower than those grown in soil without liver (Figure 9). The average spectra show differences in amplitude, the slope along 500- 600 nm and 680-750 nm respectively (Figures 9). For both soybean and wheat, leaves from the control pots are more reflective than the ones planted in a substrate of soil and 150 g of liver; this might be due to differences in the leaf's internal structure.

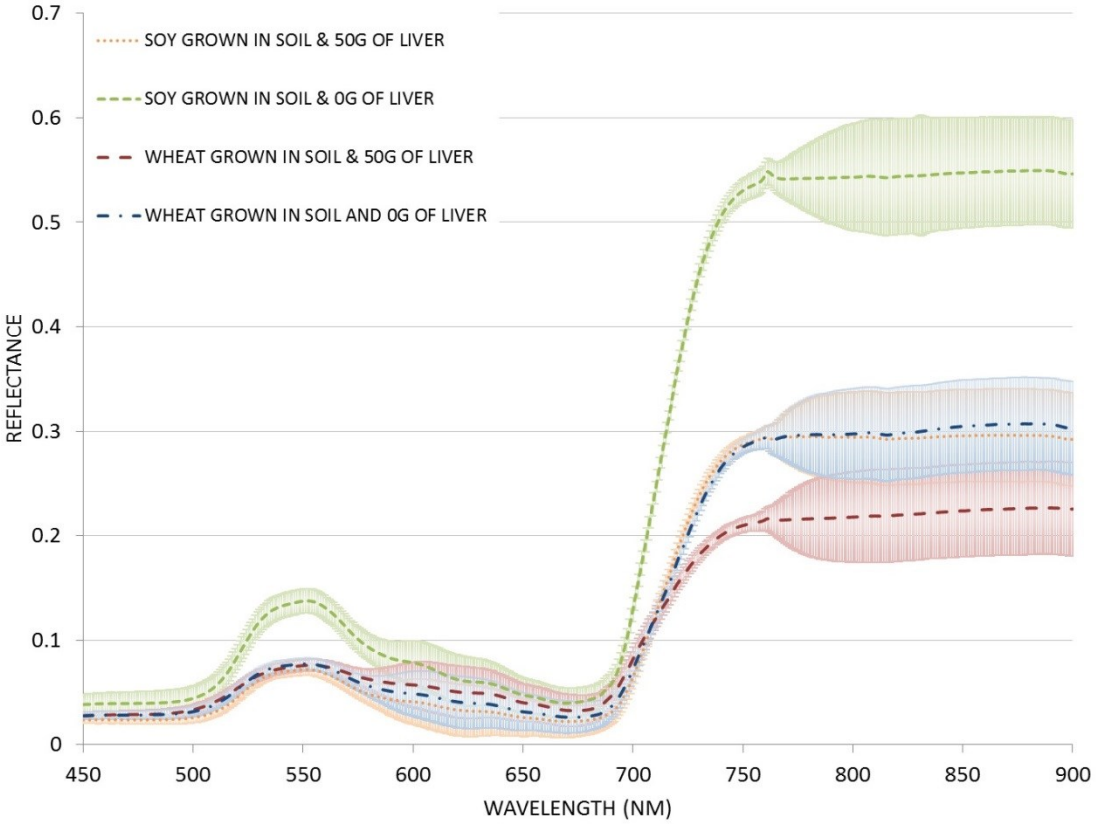

Figure 9: Average Soy and Wheat Spectra Collected on July 8th, 2011. The error bars indicate 1 standard deviation

Figure 10 illustrates soybean leaf reflectance from different fertilizer treatments taken on July 8th, 2011. In general, plants from treatments containing liver have a lower reflectance than plants grown only in soil or a mix of fertilizer and soil. The liver decomposition had an effect on the reflectance of the plants that is different from the common types of fertilizers tested here (blood meal, bone meal and manure). This is also observed in the growth pattern of the plants; plants affected by the liver decomposition are generally smaller in size (Figure 8).

Similar patterns were observed for wheat; however wheat plants have overall a lower reflectance compared to soybean plants (Figure 9). In August, when the plant attained maturity, the spectral signature from plants grown on treatments with liver become more similar to the plants grown without liver (see Figure 8). From the spectral signatures it becomes more difficult to assess visually where most of the variations between the signatures occur.

In order to visualize differences found between the different spectral signatures, a continuous wavelet transform was used (Figure 12). The continuous wavelet transform scalogram represents the similarity between the chosen wavelet and the data. This was applied to the spectra that were collected in July2011 and August 2011 at the Phytotron.

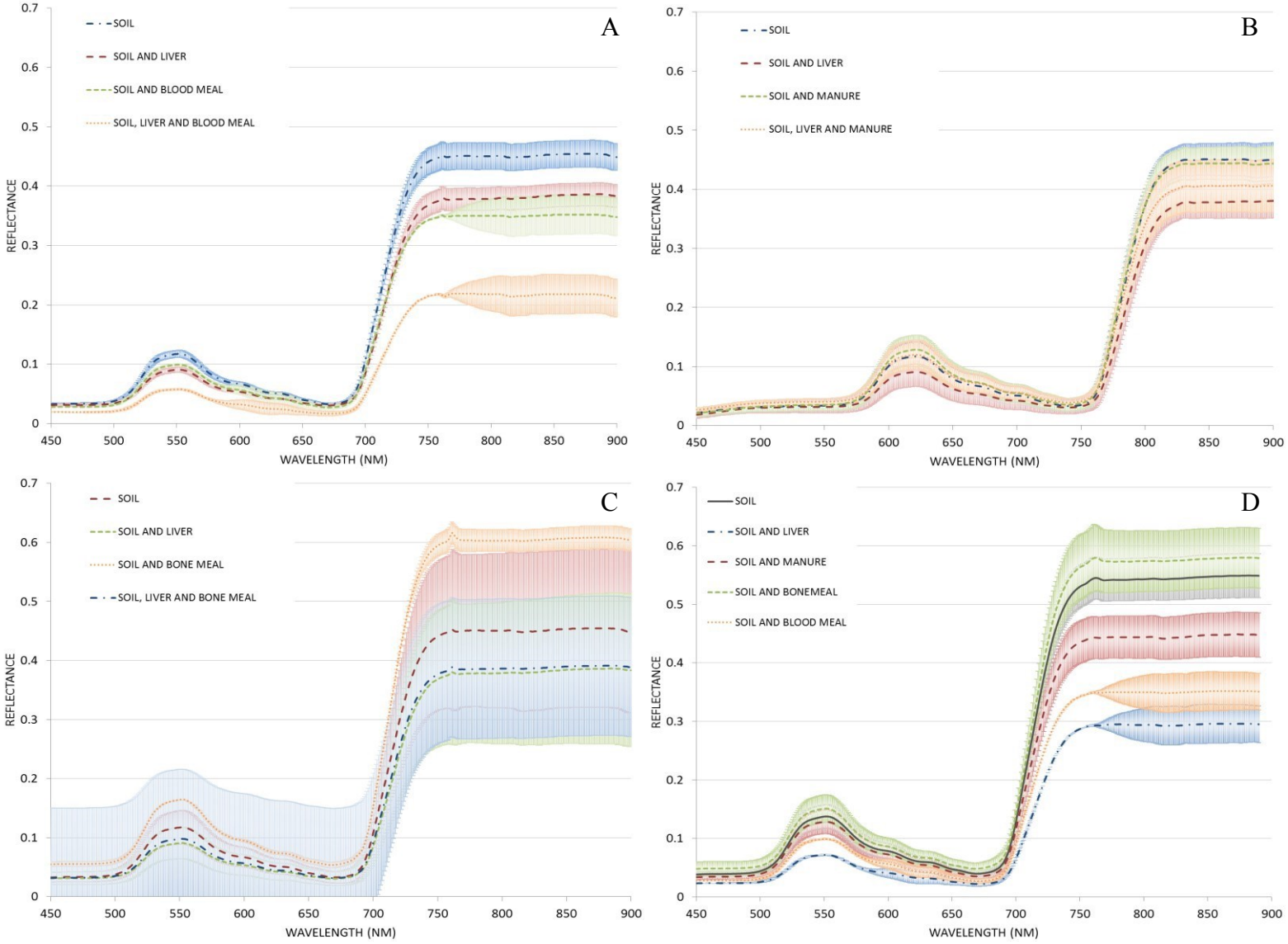

Figure 10: Spectral Signature of Soybean plants affected by treatments, A- Soil, Soil and Liver and blood meal treatments, B- Soil, Soil and Liver and manure treatments, C- Soil, Soil and Liver and bone meal treatment, D- Soil, Soil with different fertilizers (Manure, bone meal and blood meal)

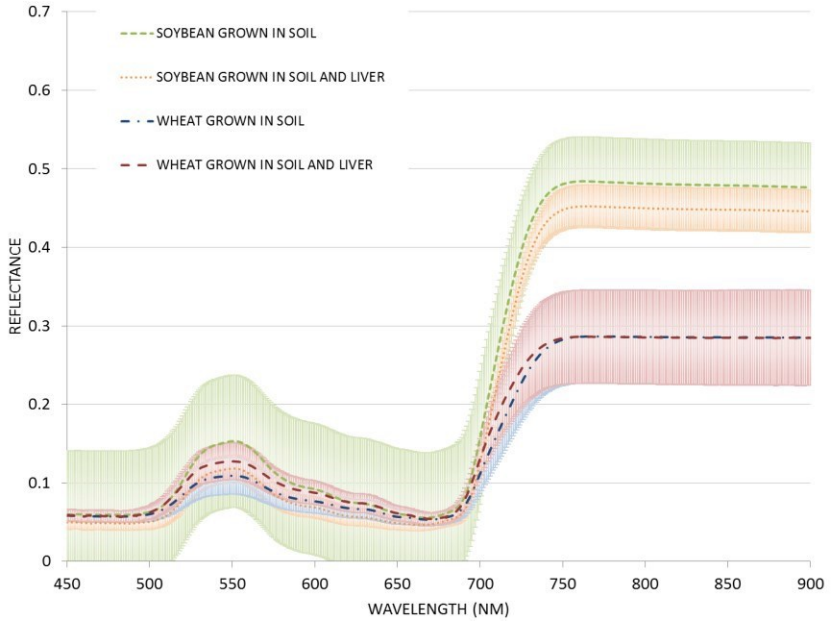

Figure 11: Average Soy and wheat blade spectra collected on August 12, 2011. The error bars represent 1 standard deviation.

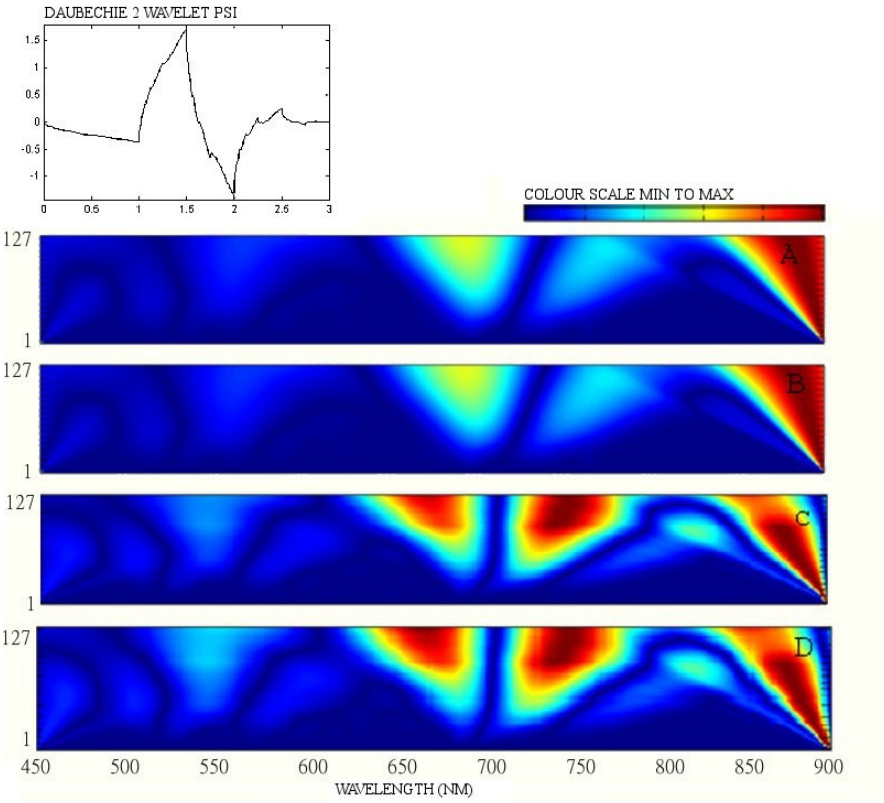

Figure 12: Wavelet and Scalograms for Soybean Leaf Spectral Signatures. The continuous wavelet transform indicate the intensity of variation found between the data and the mother wavelet, in this case a Daubauchie 2 Wavelet was used. Window A shows the scalogram for the average of non-liver treatments for soybean leaves spectral signatures measured in July, window B shows the average spectral signature for liver treatments in July 2011, window C shows the scalogram of liver treatments for August 2011 and finally window D shows the average non liver treatments taken in August 2011.

The scalograms (Figure 12) from the continuous wavelet transform indicate the similarity found between the data and the mother wavelet at different scales. Figure 12A and 12D illustrates the scalogram for the average non liver treatments that were measured in July and August 2011 for soy. The scalograms indicate how similar a particular area of the spectrum is to the mother wavelet. The scale maximum scale of decomposition was 127. When looking at the scalogram it is possible to distinguish that there is a greater similarity between plants collected at same time. Figures 12A and B are more similar to each other than treatments collected in August, Figures C and D.

Similar to a scalogram, spectral fingerprints can help visualize the variation that is found along the spectral signature at different scales (Figure 13). When comparing the July 2011 spectral fingerprints to each other, it is possible to distinguish that differences are present between the non-liver treatments and the liver treatments are found between 750-850 nm regions. From the spectral fingerprint of the August 2011 data it is possible to see that there is variation present from 600 nm to 650 nm (Figure 13). These regions have often been linked to changes in pigments and changes that occur within the leaf internal structure.

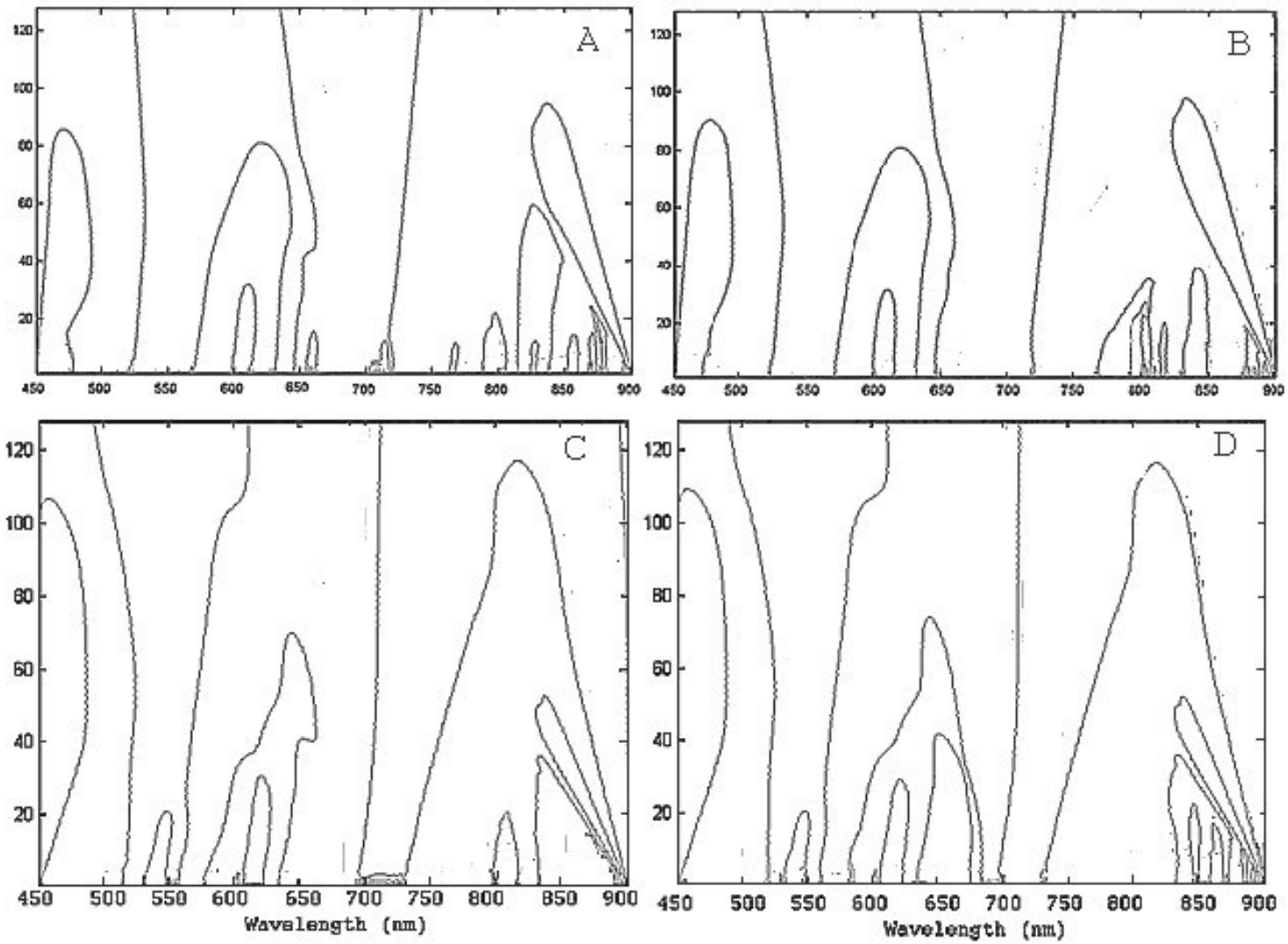

Figure 13: Spectral fingerprint of soybean treatments. A indicates Soybean Leaf Fingerprint for July 2011, figure 12 B shows Soybean Leaf Spectral Fingerprint on Liver Treatment for July 2011, C indicates Soybean No-Liver Fingerprint for August 2011 and D Liver Treatment Fingerprint for August 2011.

4.1.1.3 PIGMENTS: CHLOROPHYLL AND CARTENOIDS

A t-test was performed between total chlorophyll content of leaves grown on soil with blood meal, blood meal and liver treatments; this resulted in a slightly significant difference with a p value of 0.046. For the bone meal vs. bone meal with liver treatments the results were non-significant (p= 0.20) (Figure 14).

For chlorophyll A, similar results were obtained. The difference between Chl A from blood meal and blood meal treatments are significantly different (p= 0.046) compared to the blood meal and liver treatment (Figure 14). However, the difference between bone meal and the bone meal with liver treatment is non-significant (p= 0.20). Differences in chlorophyll b concentration are non-significant with a p value of 0.06 (See Figure 14). As for the carotenoids, between the treatments, they have an overall significant difference with a p-value of 0.043 (See Figure 15). In this case it is observable that treatments containing liver have lower concentrations of pigments than their non-liver treatment counterparts.

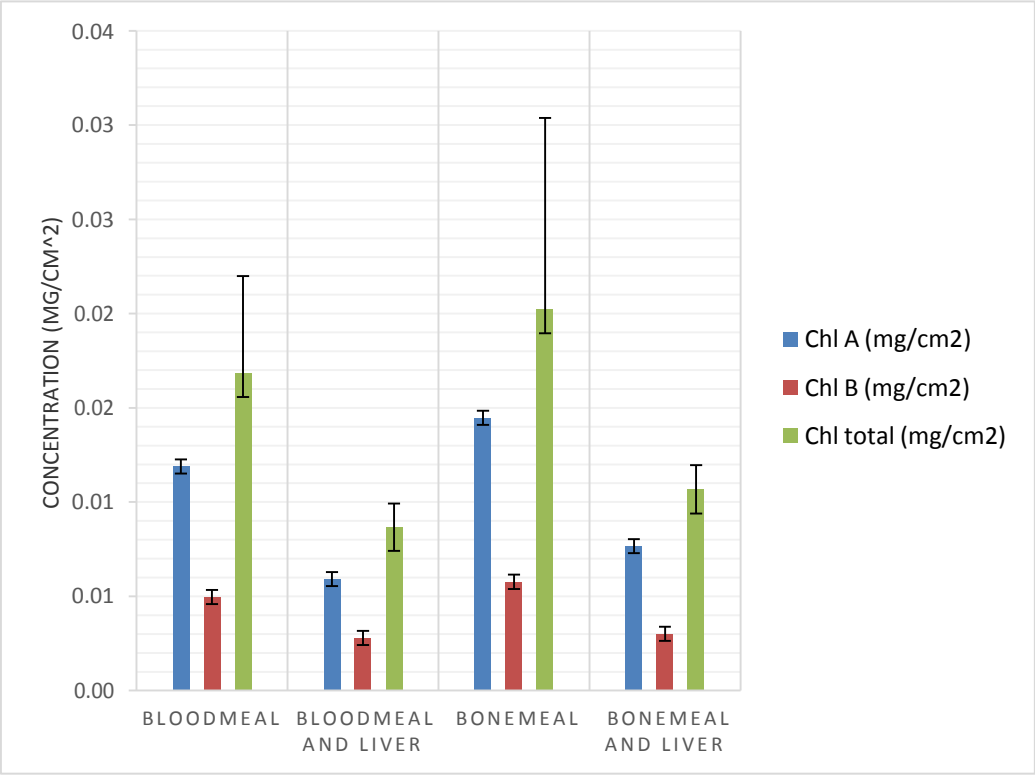

Figure 14: Chlorophyll Concentration in Wheat, August 2011. Compares the different levels of Chl A, Chl B and Chl total for wheat leaves collected during August 2011 at the Phytotron. The error bars represent an error of 1 standard deviation. Treatments with soil, blood meal or bone meal and liver have lower concentration of leaves than their non-liver treatment counterpart.

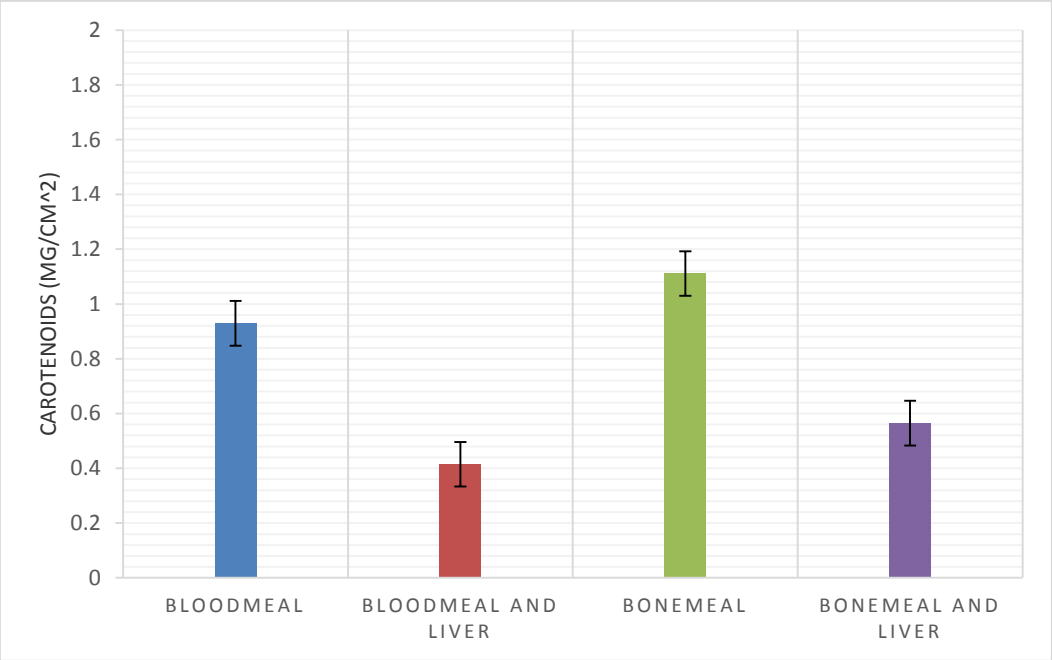

Figure 15: Carotenoid Concentration in Wheat, August 2011. The error bars represent an error of 1 standard deviation.

4.1.1.4 CLASSIFICATION

A forward feature selection was performed using the PrTools toolbox (Duin, Juszczak et al. 2007) in Matlab on the spectra of the leaves of the soybean at the Phytotron. The forward feature selection essentially selects the best bands for the groups to be classified. The top five bands were used to separate the data since including more bands did not seem to improve the separation of the data into different classes. The top five bands that were used to separate the data into two separate classes for soy in July 2011 are situated at 709, 809, 935, 644 and 450 nm. For wheat, in July, it was 713, 465, 574, 629 and 639 nm. The five top bands to separate the data into the two separate classes for soy in August are situated at 515, 514, 516, 506 and 517. For wheat, in August they are 615, 468, 604, 600 and 612 nm. Table 3 shows the classification error associated with classifying the soybean spectral signatures into two classes: soybean control and soybean with 150 g of liver. For the data from July, the validation errors (soybean) for the ldc, qdc, parzenc and knnc classifiers ranged from 10% to 20%. In August, the following classifiers separated the soybean spectra into the two classes without

error: ldc, qdc, knnc, and udc. This means that it is possible to separate the spectral signature of soybean liver and non-liver treatments from another.

Table 3: Parametric Classification Error for soy bean leaf spectra signature and soybean grown on 150 g Liver of soil July 2011 and August 2011

Parametric Classification – Soybean Control vs. 150g Liver, Phytotron , July 2011		
Classifiers	*Training Error*	*Testing Error*
Ldc	0	0.2
Qdc	0	0.2
Parzenc	0	0.1
Knnc	0	0.1
Parametric Classification – Soybean Control vs. 150g Liver, Phytotron , August 2011		
Classifiers	*Training Error*	*Testing Error*
Ldc	0	0.0
Qdc	0	0.0
Parzenc	0	0.5
Knnc	0	0.0
Udc	0	0.0

In terms of wheat's spectral signature, the classification becomes more difficult over time between the liver and non-liver treatments (Table 4). LDC, Parzenc and Knnc show the most promise for getting clear separation between non-liver and liver classes in July for the wheat treatments with a validation error less than 20%. However, this falls apart in August, where none of the classifiers tested showed very good results (40-70% error). The best classifier in August for separating the wheat spectral signature into non liver and liver classes was the qdc classifier with 40% testing error. This means that for wheat it is not possible to identify the liver treatments from the non-liver in August using this classification method. Furthermore, the training errors of 10-30% (Table 4) also indicate that either a different band set would need to be chosen or the sample size increased in order to potentially improve the classification.

Table 4: Parametric Classification – Wheat grown on 0g of liver vs. wheat grown on 150g Liver, Phytotron, July 2011 and August 2011

Parametric Classification – Wheat Control vs. 150g Liver, Phytotron , July 2011		
Classifiers	*Training*	*Testing*
Ldc	0.06	0.20
Qdc	0.83	0.83
Parzenc	0.16	0.16
Knnc	0.06	0.06
Udc	0.40	0.46
Parametric Classification – Wheat Control vs. 150g Liver, Phytotron , August 2011		
Classifiers	*Training*	*Testing*
Ldc	0.10	0.50
Qdc	0.20	0.40
Parzenc	0.20	0.60
Knnc	0.30	0.70
Udc	0.30	0.50

4.1.2 VAUDREUIL-DORION

4.1.2.1 GROWTH

Figure 16A shows the measured plant height under different fertilizer treatments, and Figure 16B shows the height of plants grown with different amounts of liver at various dates during the experiment that took place during the summer 2012 in Vaudreuil.

It is possible to observe that in general, plants grown in pots containing liver are shorter than those grown without liver. In order to determine the amount of variance between the plants grown on liver versus the different treatments a two-way analysis of variance was performed.

The results from the different fertilizer treatments show that the treatments are statistically significant with $p<0.05$, 9 degrees of freedom and F value of 62.99.

When comparing the difference in plant height between the varying amounts of liver (50, 100, and 200 g) there is a significant difference found between the different treatments for the plants grown in Vaudreuil. The results indicate that the difference found between the different fertilizer treatments are statistically significant with $p<0.05$, 12 degrees of freedom and an F value of

37.59. It is interesting to notice that plants grown with 50 and 200 g of liver were in general shorter than plants grown with 100 g of liver and the control (no liver).

For wheat plants, the differences between plant heights at different time periods was non-significant, this is probably due to the large variability that was found in the plant height of wheat, and to some difficulties encountered in measuring the height consistently throughout the experiment. Wheat will grow new tillers as it matures which made it difficult to get consist measurements.

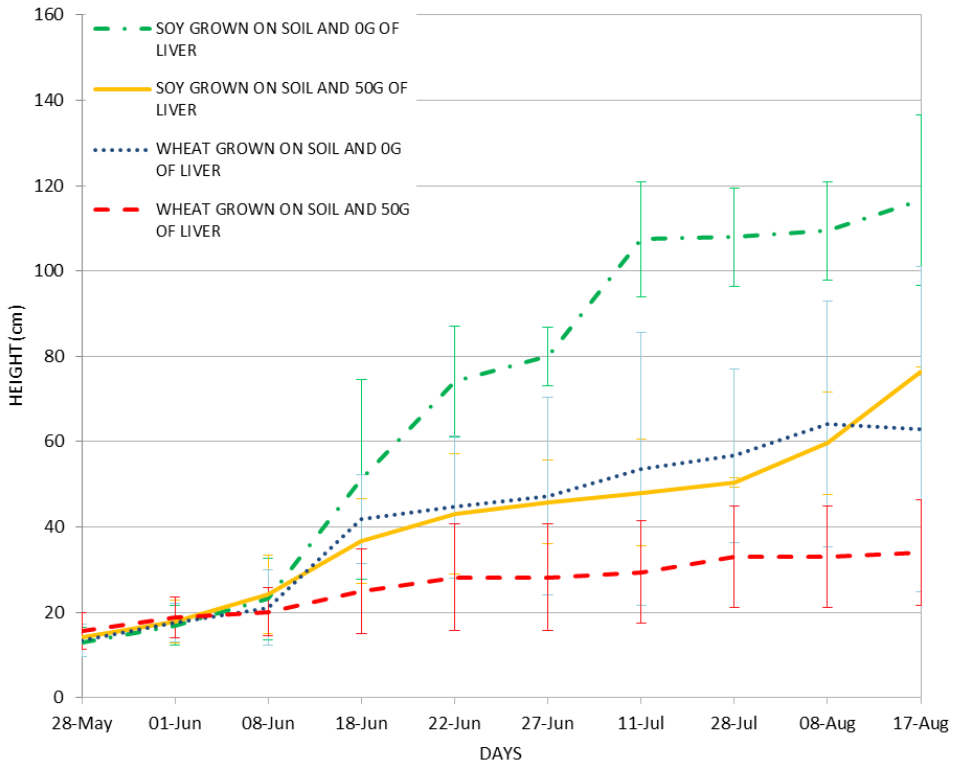

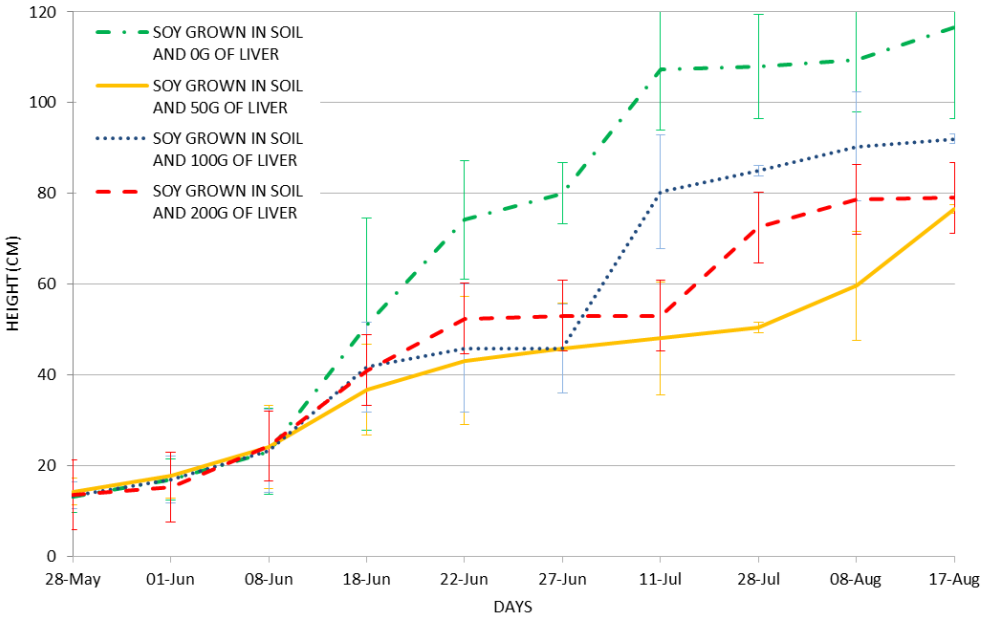

Figure 16: Average Plant Height (cm) in Vaudreuil, Figure A represents the average plants height grown on 50g of liver treatment for both soybean and wheat plants. Figure B illustrates growth of soybean affected by different amounts of swine liver (0g, 50g, 100g and 200g).

The difference in size between the plants grown in 2011 and 2012 may be attributed to the amount of time allowed for the growth of the plants. The experiment that took place during summer 2012 in Vaudreuil started in May and ended in September. The experiment at the Phytotron started at the end of June 2011 and ended at the end of August 2011. This means that plants grown during summer 2012 had a five month growing period compared to a 3 month growing period for plant grown during summer 2011.

4.1.2.2 SPECTRAL SIGNATURE

The spectral signature of both the wheat plants and soybean plants show a similar pattern at the beginning of their growth, the treatments differ mostly along the 500-600 nm range (Figure 17).

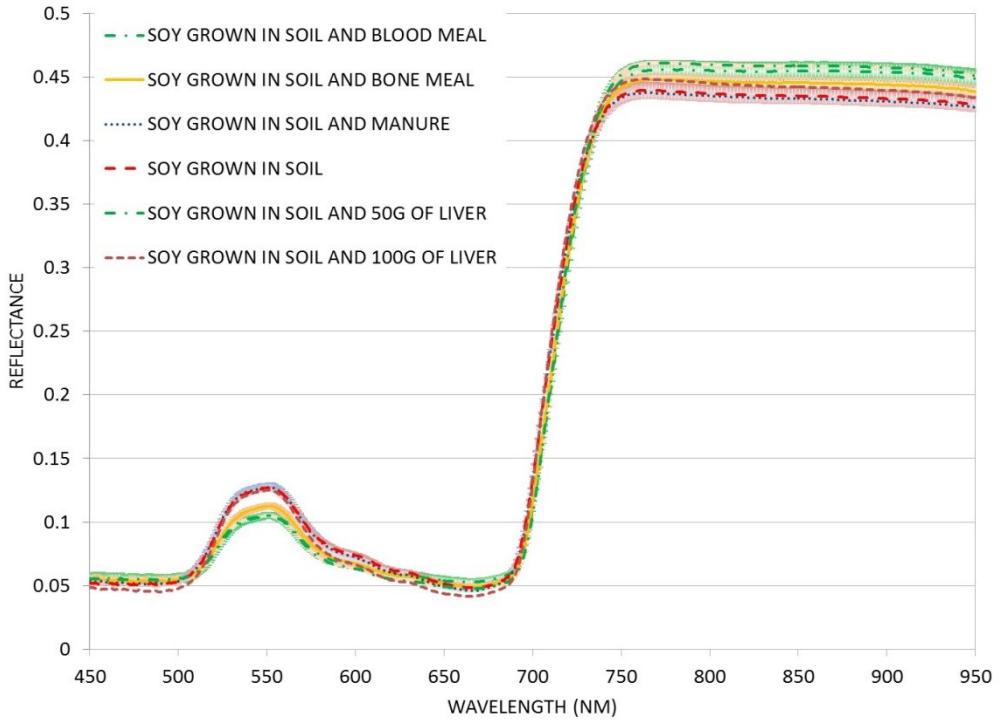

Figure 17: June 2012 Soy Treatments Leaf Spectra collected in Vaudreuil. Error bars represent one standard deviation error.

The most striking difference can be seen in the 500 to 600 nm range for the different treatments applied to soybeans in June 2012. When observing the results for the soy 100 g of liver treatment, it is noticeable that the overall shape is different from other treatments. Fertilizer treatments show the most variation around the 500 nm to 600 nm range.

4.1.2.3 CLASSIFICATION

The results from the classification show that the differences found between spectra of the plants grown in pots containing liver versus those not containing liver change over time. The forward feature selection indicates that in June, the differences are mostly found in the infrared; however, in July, the differences are found within the green region of the visible spectrum. Through forward feature selection, the bands with the greatest separability in June are found at 795, 729, 796, 793 and 728 nm, for July at 515, 506, 512, 517 and 677 nm and for August at 690, 648, 691, 651 and 689 nm.

The results indicate that with the June data it is possible to separate the two classes (Liver vs. Non Liver) with a 17% error rate by using either the ldc, qdc, parzenc or loglc classifier.

Using this same method to separate the liver from non-liver treatments in August, higher error rates are obtained. With the Ldc and Qdc classifiers an error rate of 29% is obtained. For the loglc classifier, a slightly better performance is achieved with an error of 21%. Finally, the parzenc classifier performed poorly with a classification error of 50%. The results of the forward feature classification correspond well to what is observable on the spectral signatures (Figure 18 and 19).

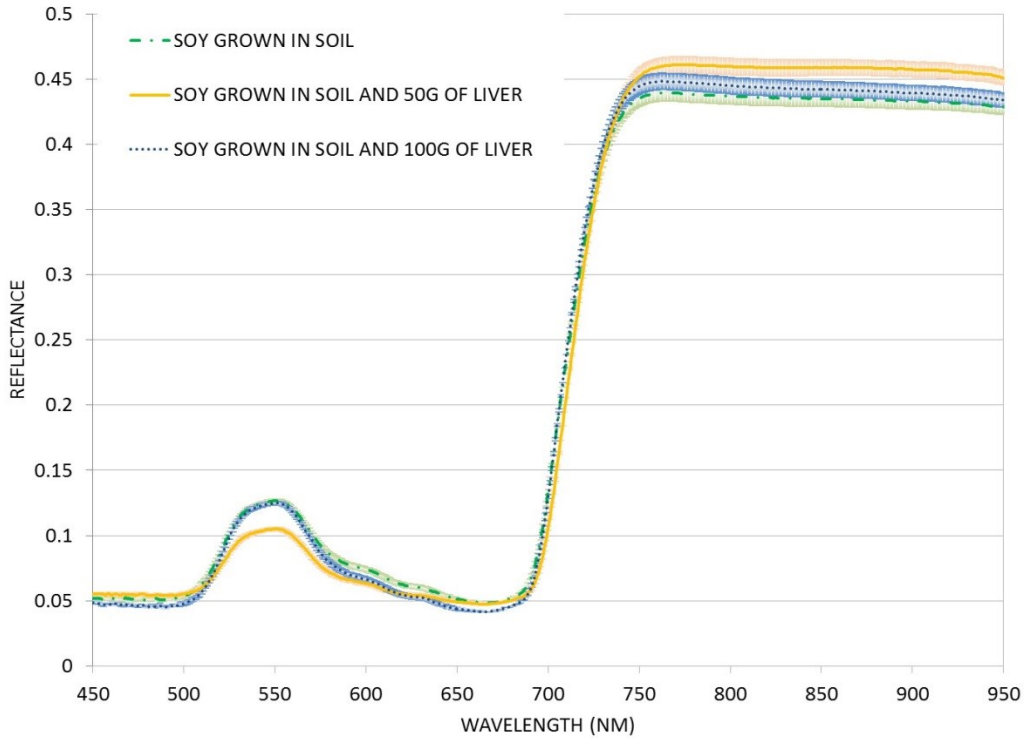

Figure 18: Soybean Spectral Signatures of treatments grown in soil vs treatments grown in 50g and 100g of liver and soil, June 2012.

From the soybean spectral signature it is possible to see that differences between the treatments occur mostly in June at wavelengths of 500 nm to 600 nm and some after 750 nm.

In July 2012, it is around the visible area of the spectrum that variations occur; differences can be observed from around 500 nm to 600 nm and from 720 nm onwards.

In August 2012, the most striking differences seen between soybean spectral signatures are around 600 nm to 700 nm and from 750 nm to 950 nm. From the spectra it is possible to infer that differences are found between the soy control treatment and liver 50 g treatment from 750 nm to 950 nm. It is possible to infer that differences in the internal structure of the leaf are likely to exist. The changes in the visible range of the spectra can be attributed to the variation of pigment production such as chlorophyll within the leaves.

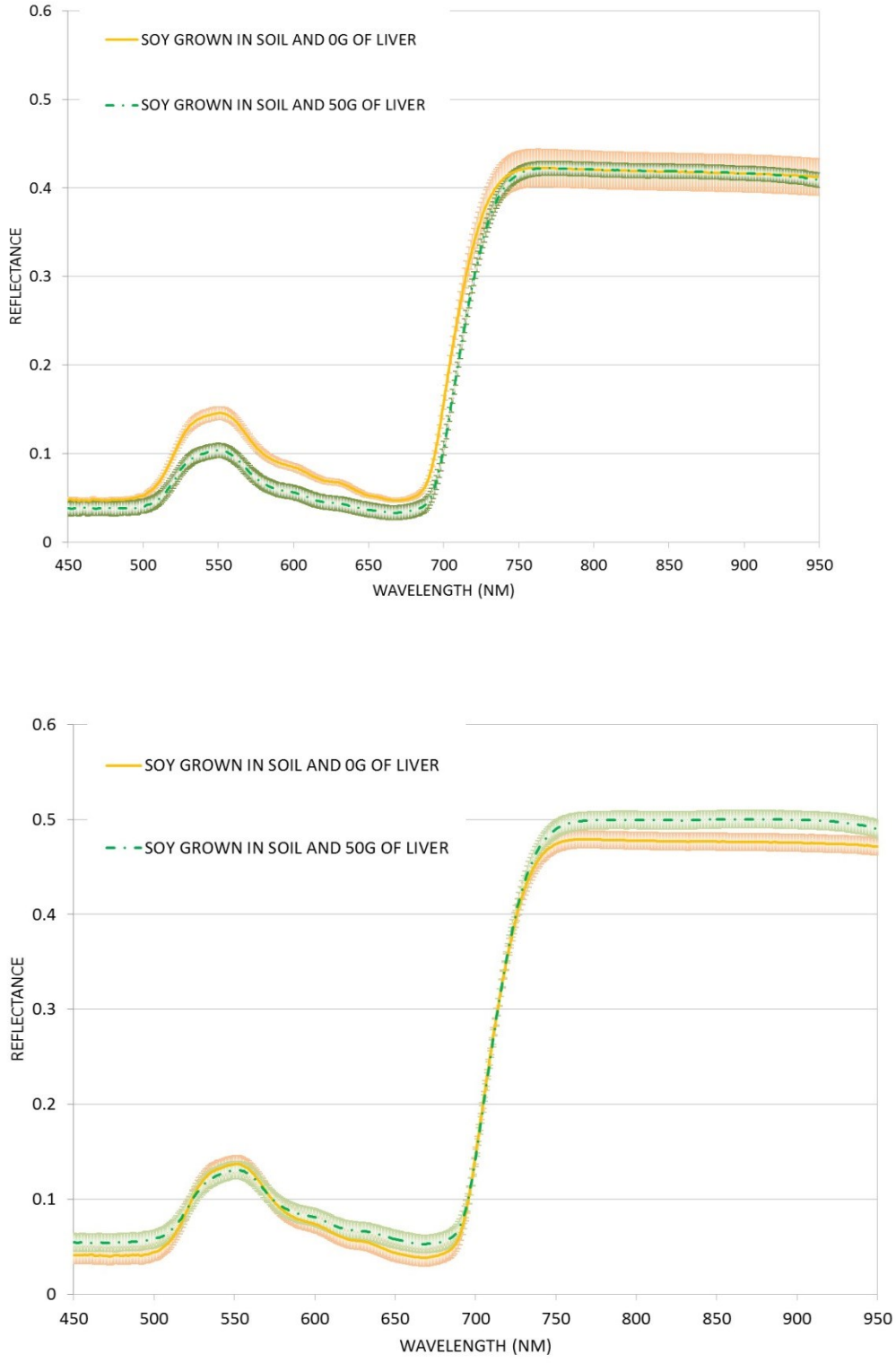

Figure 19: Spectral Signature of Soybean leaves for July (A) and August (B) 2012

4.1.2.4 PIGMENTS: CHLOROPHYLL AND CAROTENOIDS

The shapes of spectral signatures of leaves in the visible area are dependent on the amount of chlorophyll and carotenoids found within them. In terms of the concentration of chlorophyll, no significant difference was found between the treatments for soybean during June or August 2012, this is shown in Figures 20A and 20B.

However, there is a large difference found between the carotenoid concentration for soy bean leaves in June 2012 and in August 2012. This is most likely due to the natural cycle of plants; in June, plants are in their initial growing stages while in August, the plants have attained maturity and are soon going into senescence. Similar results were previously found by a colleague when studying vegetation at Parc Safari (Degea 2011).

In terms of carotenoids, there is no significant difference ($p=0.5$) when considering all the treatments for carotenoids concentration levels collected in June 2012 (Figure 21).

In August 2012 (Figure 21), there is less variation present between the treatments for chlorophyll and carotenoids concentrations within soybean leaves than observed in than observed in the month of June.

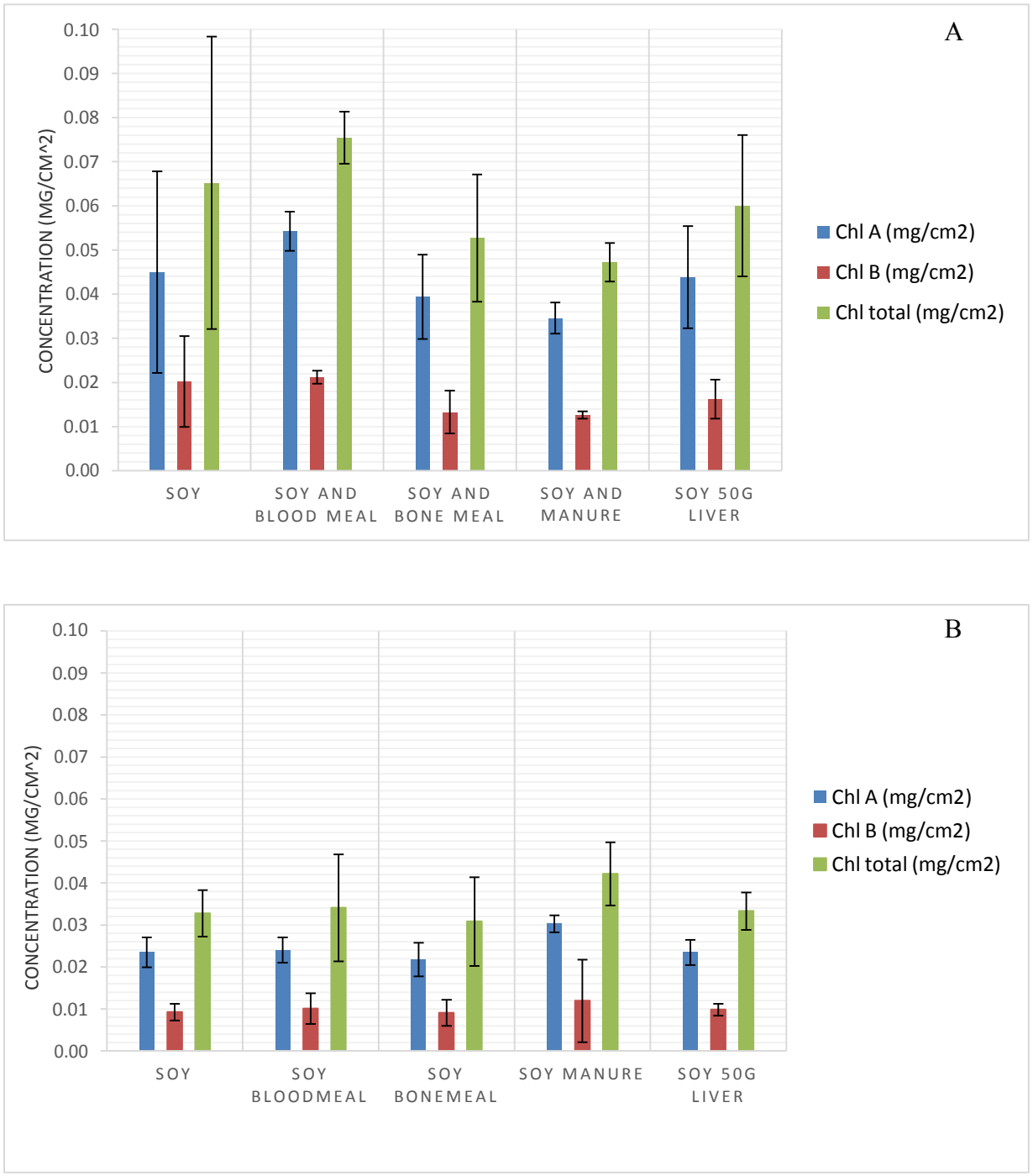

Figure 20: Chlorophyll Concentration for Soybean plants in June (A) and August (B) 2012

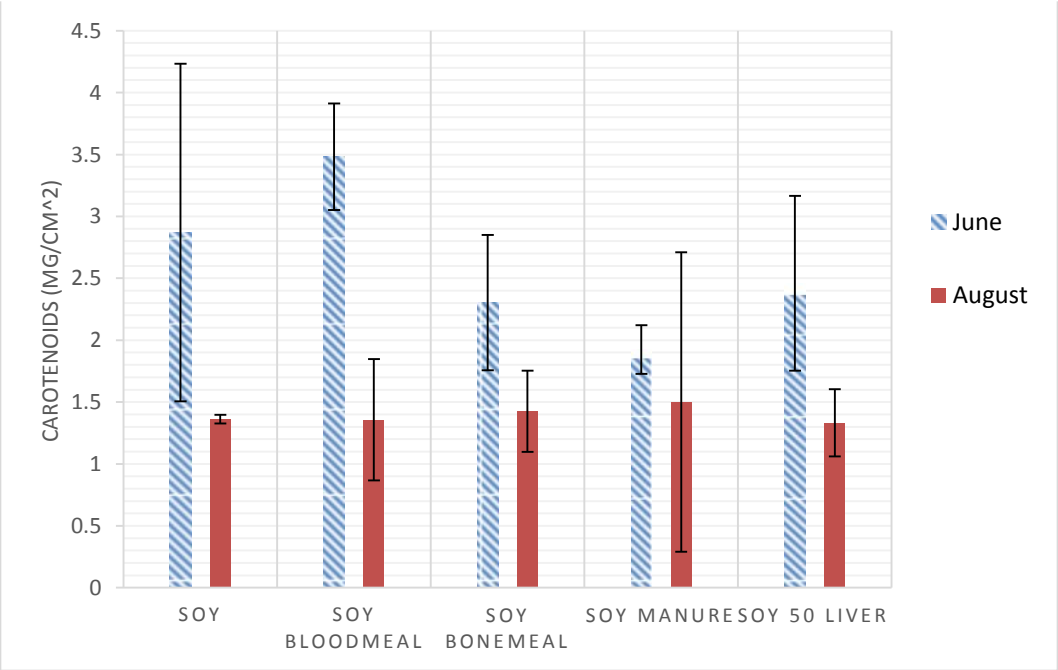

Figure 21: Carotenoids concentration for soybean for June and August 2012, the blue bars represent the carotenoid concentration for soy bean leaves collected in June 2012, the red bars indicate the average carotenoids concentration found in August. The error bars represent on standard deviation. There is a significant difference between the levels of carotenoids in June than in August.

The different treated wheat blades also went through chlorophyll and carotenoid extraction. In June, for both chlorophyll and carotenoid concentration, the wheat grown on bone meal and soil has higher concentration levels (Figure 22 and 23).

In August, the bone meal and soil treatment no longer show a contrasting difference with other treatments. The concentration of the pigments remains relatively constant with no significant difference between the different treatments. This agrees with the observation that the spectral signatures of the leaves that were treated become more similar to each other over time.

These changes in concentration can account for the differences seen between treatments along the visible range of the spectra.

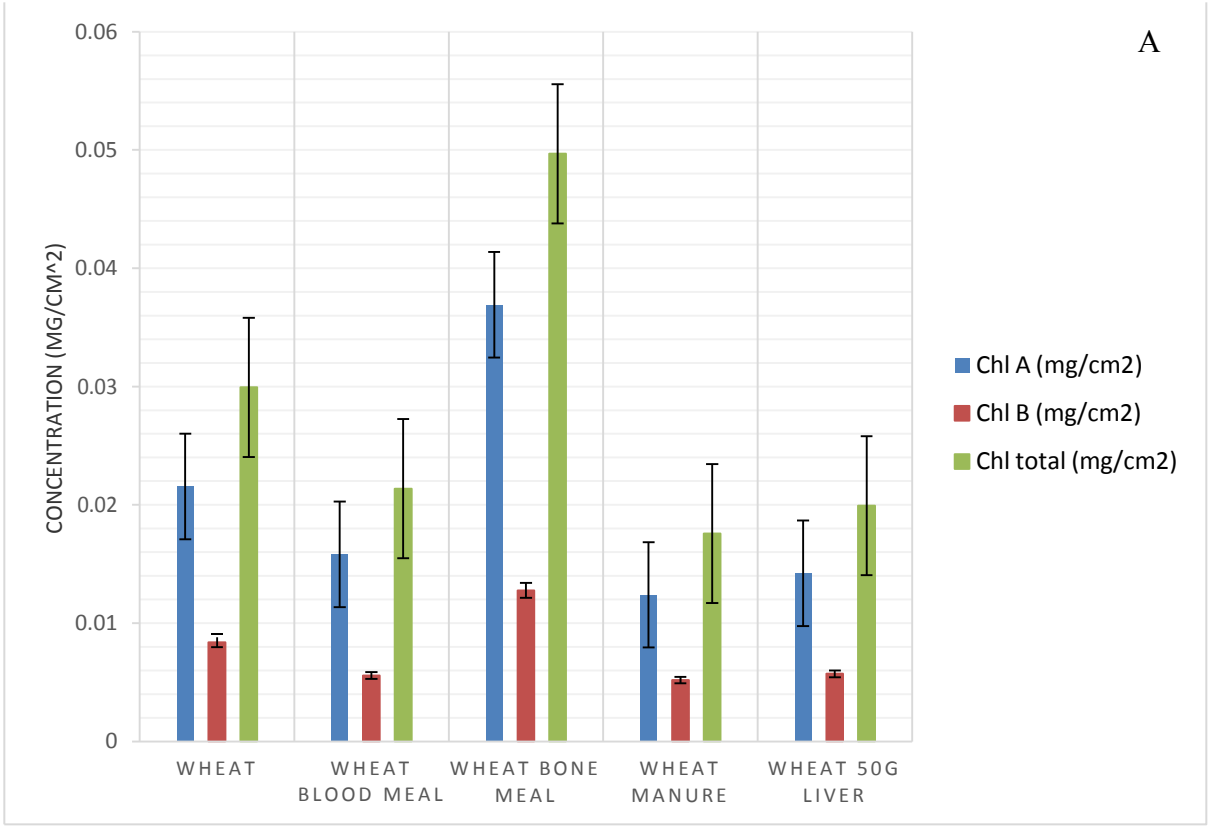

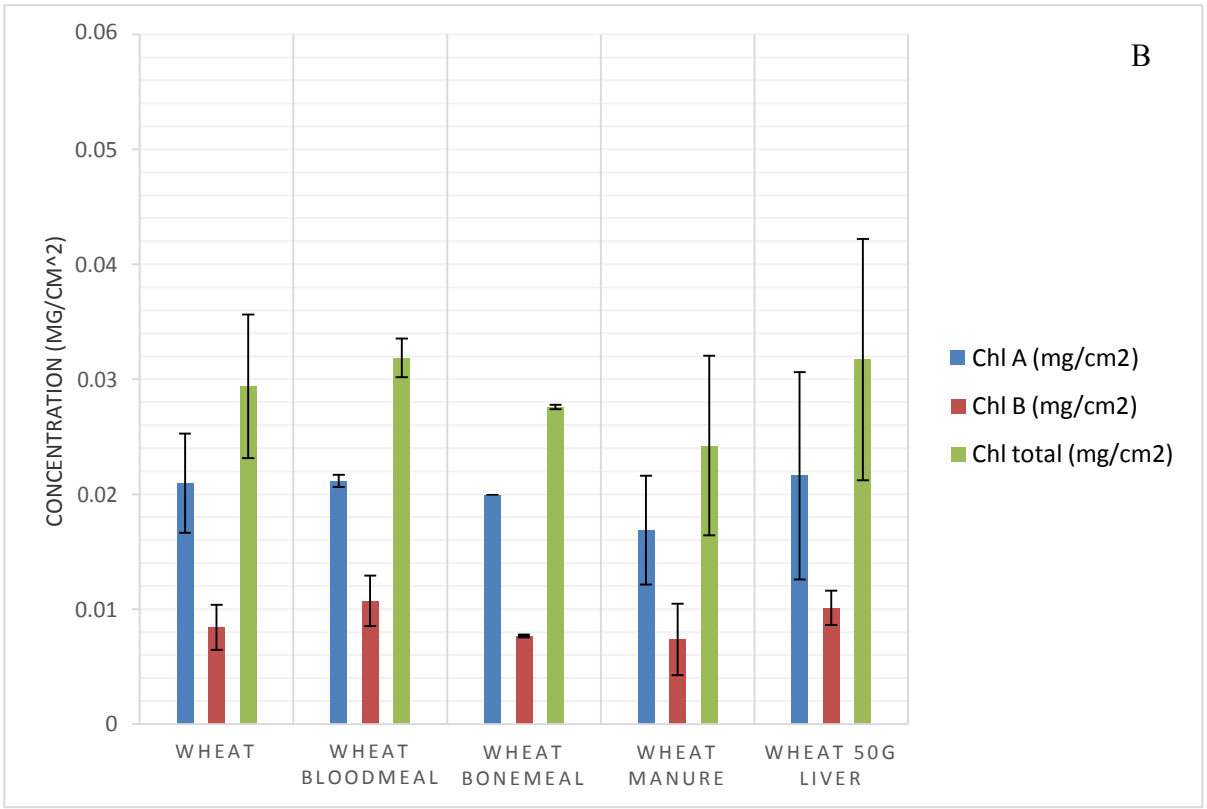

Figure 22: Chlorophyll concentration A, B and total in Wheat leaves, June and August 2012, the error bars represent one standard deviation.

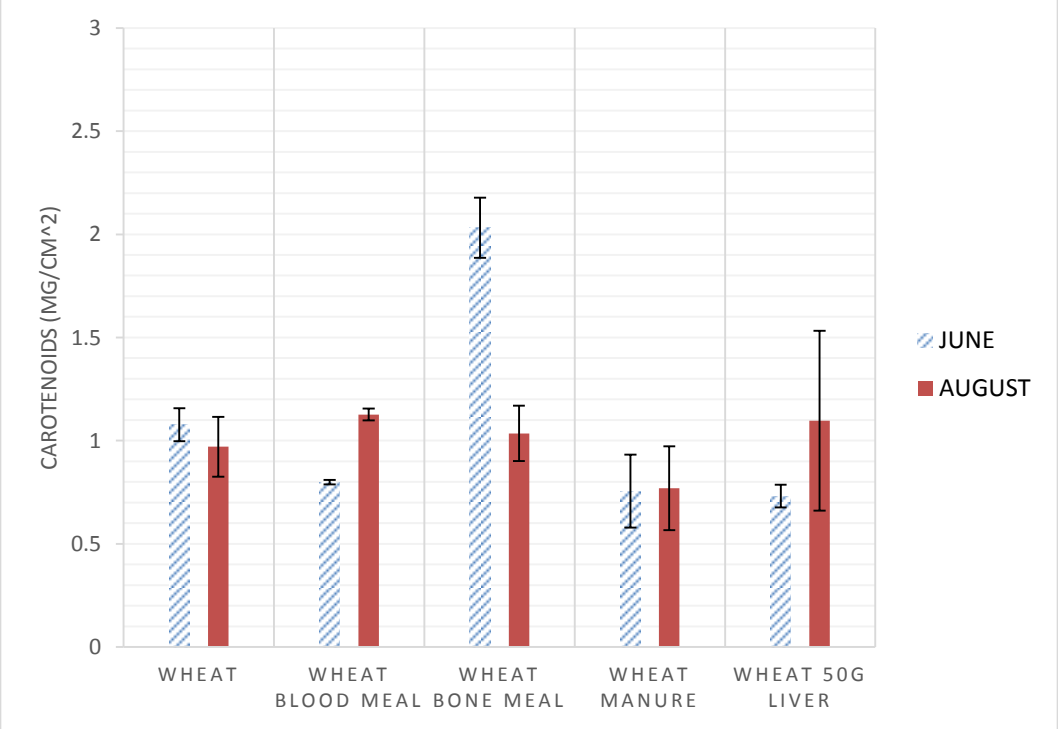

Figure 23: Carotenoids concentration for Wheat leaves for June and August 2012. The blue hatched bars represent the carotenoid concentration found in wheat in June. Red bars are indicative of wheat blades carotenoid concentration in August.

4.1.2.5 TRANSMISSION ELECTRON MICROSCOPE

To determine if differences are seen within the structure of the leaf, a pair of leaves (liver vs. non liver) was imaged with a transmission electron microscope. The images (Figure 23 a control, b, liver) illustrate differences in the amount and size of the vacuoles. The general size of the vacuoles differs. The average size for the control leaf was 102 um ± 82um and for the treated leaf of 34um± 22um (See Appendix E).

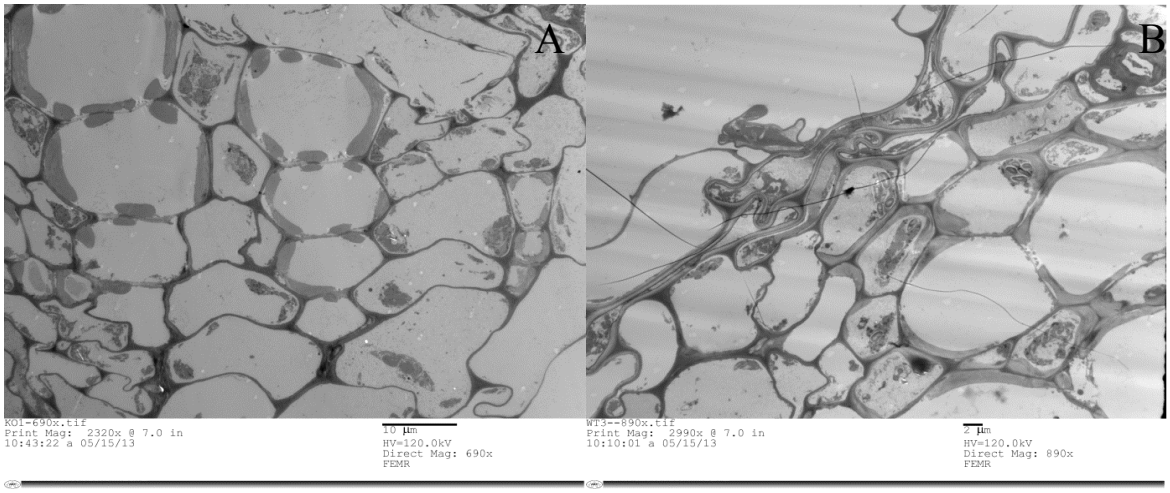

Figure 24: Control Soybean Leaf structure (A), 690x, Liver Treatment Soybean Leaf Structure (B) July 2012, 890x magnification.

As seen previously, the spectral signature of leaves of the treatments that contain no liver have generally higher reflectance in the near infrared than those that contain liver. The vacuoles in the control leaf are larger and seem more structured than the treated leaf. It is important to notice that the magnification is different for both images; the one control is magnified at 690x and the leaf with liver at 890x. The images are in different magnification because I wanted the same amount of vacuoles to show up on the images. The vacuoles were measured with Image J, an open source biological image processing software (Rasband 2012). The size of the vacuoles was compared against one another by performing an ANOVA. A total of 30 vacuoles were compared against each other. The results indicate that there exists a significant difference with a p value of 0.00005 with a degree of freedom of 1 and an F value of 9.09 between the sizes of the vacuoles of the control soybean treatment vs. soybean grown with the liver.

4.1.2.6 VISUALIZING MULTIPLE BANDS

The image shown in Figure 22 corresponds to the leaf spectra collected throughout the summer 2012 from June to September. White cells (Figure 23) are white reference measurements with a reflectance of 1 across the wavelength range. These cells were included in the image in order to serve as markers between different months of data. From the image it is possible to compute different statistics.

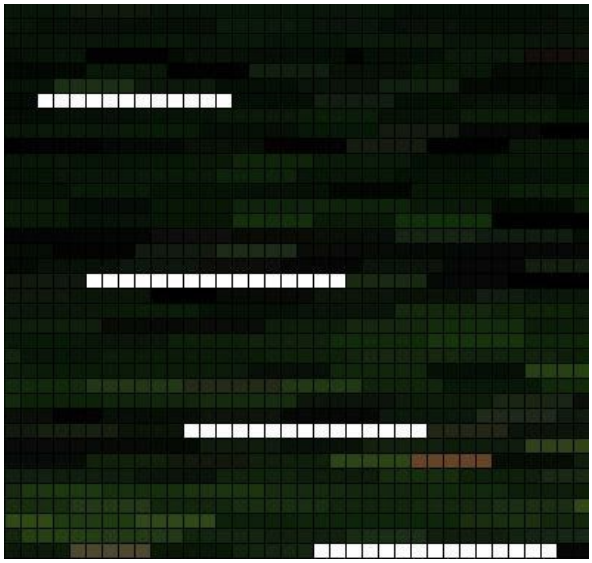

Figure 25: Hyperspectral cube, summer 2012 data. This figure illustrates the resulting hyperspectral data cube that was generated from leaf spectra collected during summer 2012

A ratio between the bands was made in order to determine if clusters could be seen between different classes. The following ratio was tested: ρ750/ρ550 (Figure 26). The resulting scatter plot shows that with the different treatments it is possible to see a distinction between species.

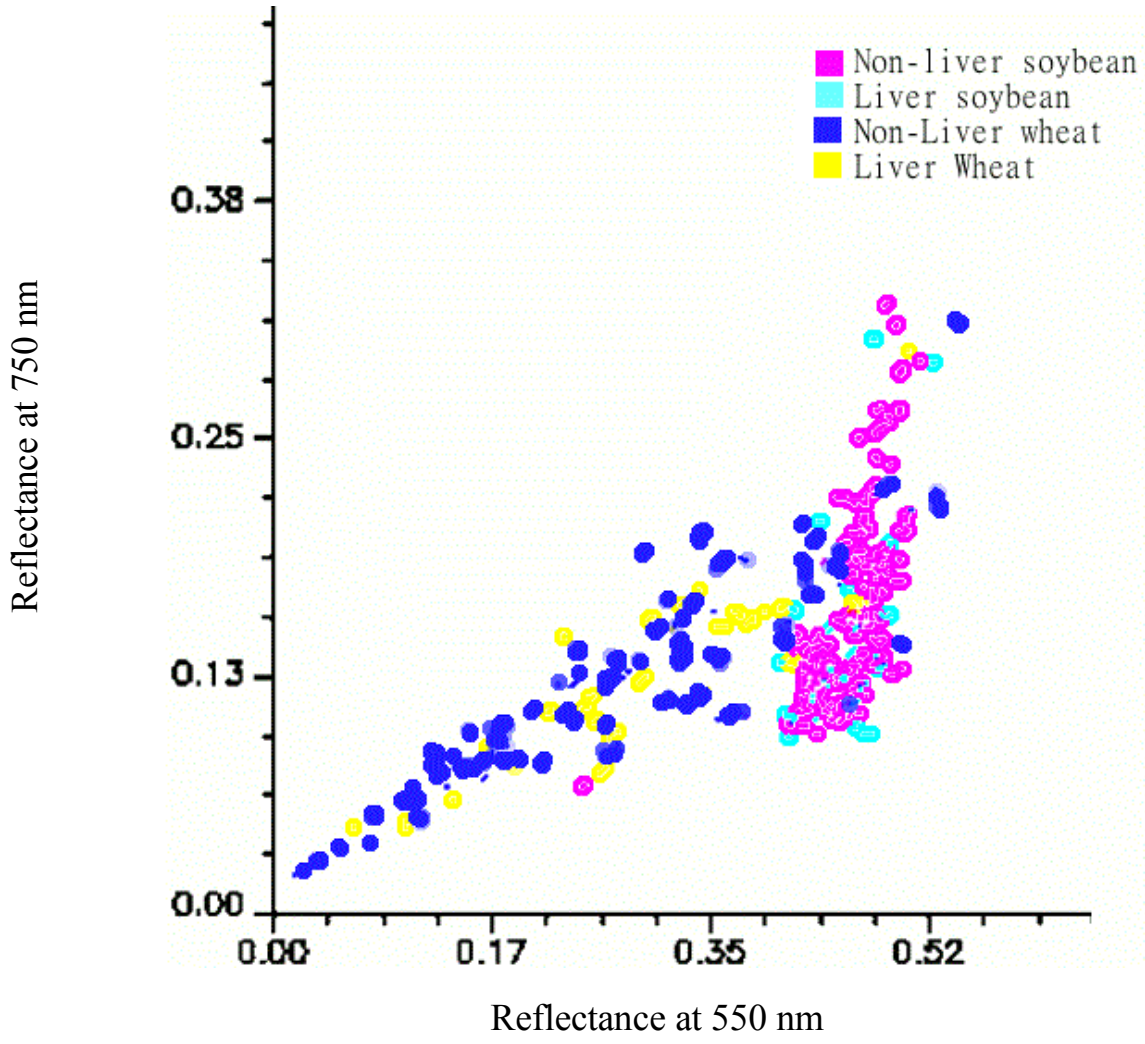

Figure 26: 2D scattered plot of the reflectance at 750 / 500 nm. The figure indicates that soybean treatments cluster more closely together than wheat. However no significant difference between liver treatments (soy vs liver) exist. The same is observable for wheat treatments. All of this should go in the text.

The following indices: NDVI, Simple Ratio, Vogelmann Red Edge index 1 were tested on the June and August 2012 data. There is no significant difference between the liver treatment and non-liver treatments using these indices. However, in general it is possible to observe that wheat plants have a lower value than soybean plants. Values for the PRI in August are lower than the ones collected in June (Table 5). This could be due to normal biological change in the plants as the plants mature.

Table 5: Average value and standard deviation of results obtained for selected indices.

	JUNE		AUGUST	
NDVI	**Average**	**Standard deviation**	**Average**	**Standard deviation**
Soy Liver	0.81	0.02	0.76	0.08
Soy Control	0.79	0.01	0.77	0.04
Wheat Liver	0.70	0.13	0.61	0.06
Wheat Control	0.75	0.06	0.61	0.10
SR	**Average**	**Standard deviation**	**Average**	**Standard deviation**
Soy Liver	9.81	1.20	7.83	1.87
Soy Control	8.76	0.99	8.00	1.68
Wheat Liver	6.66	2.61	4.25	0.83
Wheat Control	7.58	2.06	4.54	1.52
VOG1	**Average**	**Standard deviation**	**Average**	**Standard deviation**
Soy Liver	1.55	0.14	1.45	0.16
Soy Control	1.59	0.08	1.37	0.12
Wheat Liver	1.50	0.12	1.28	0.04
Wheat Control	1.47	0.12	1.28	0.08
PRI	**Average**	**Standard deviation**	**Average**	**Standard deviation**
Soy Liver	0.06	0.02	0.03	0.02
Soy Control	0.06	0.01	0.03	0.02
Wheat Liver	0.04	0.04	0.02	0.01
Wheat Control	0.06	0.01	0.02	0.02

The indices that were applied were not helpful in terms of separating the data. Other indices that use different bands could be investigated to separate the treatments (See Appendix A for more information). By looking at the data derived from the whole image using ROIs as a class image, it is possible to derive statistics on the spectral signature of the treatments. From this it is possible to visualize that variations are mostly found within the 500 nm to 600 nm range than in the regions. Figure 27 shows the separation of the data using five bands. In this case bands 278 (728 nm), 280 (730 nm), 344 (793 nm), 346 (795 nm) and 347 (796 nm) were used since they were identified as the best bands for separability for the June spectra through a forward feature selection.

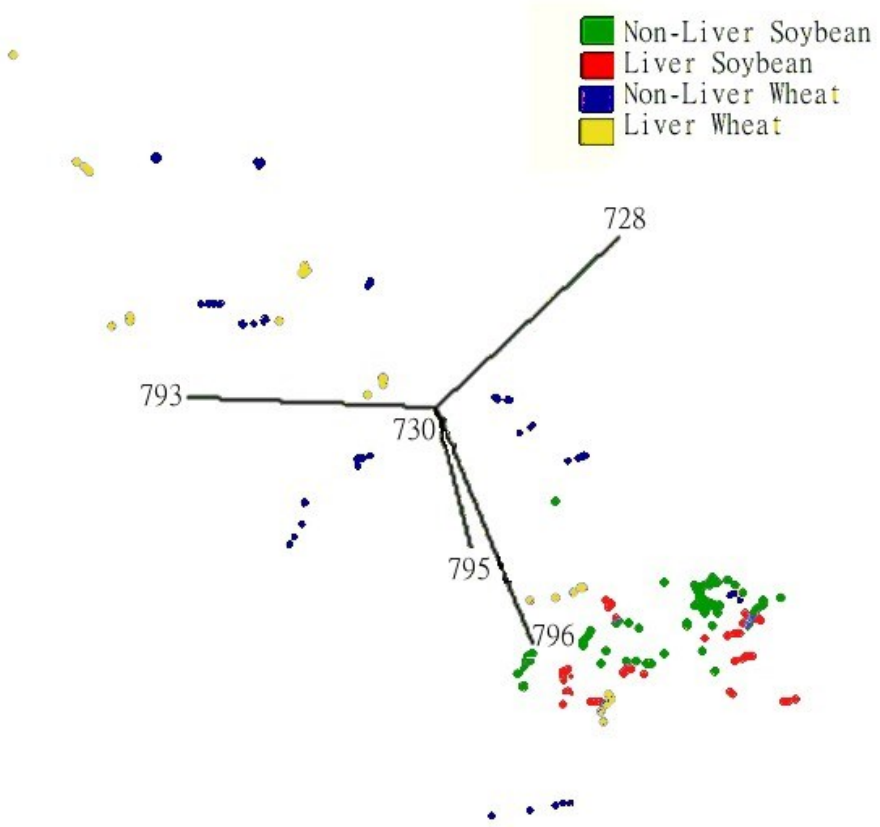

Figure 27: 5-D visualization using Bands at 728 nm, 730 nm, 793 nm, 795 nm and 796 nm. , Green represents the average June soybean spectral signature of treatments containing no liver (control, blood meal, bone meal and manure), Red is soy bean grown on a mix of soil and liver (150 g), blue shows the non-liver treatments for wheat plants, yellow indicates treatments with wheat and 150 g of liver in soil.

From Figure 27, it is possible to see that different ROIs cluster together, showing promise for separability. To gain a better understanding of the separation of the different region of interest, a Jeffries Matusita test of separability was performed using bands 728 nm, 730 nm, 793 nm, 795 nm and 796 nm. Jeffries-Matusita values range from 0 to 2.0 and indicate how well the selected ROI pairs are statistically separable. A value greater than 1.9 indicates that the ROI pairs have good separability. For the June data, the results indicate that it is easier to separate wheat from soybean plants spectrally with a Jeffries Matusita test of 1.92 (Table 5). Lower values are seen for separating liver from non-liver treatments. This is well reflected by the 5D-visualization figure (Figure 26). The yellow and the blue that represent wheat are separable from the red and green, which cluster more closely together.

Overall, results show that differences exist between the spectral signature of vegetation for treatment with liver, non-liver and different fertilizers. Plants grown on liver treatments remain generally smaller and most probably show differences in their internal structure.

Table 6: Separability of ROI using 728nm, 730nm, 793nm, 795nm and 796nm. Jeffries-Matusita values range from 0 to 2.0 and indicate how well the selected ROI pairs are statistically separable. A value greater than 1.9 indicates that the ROI pairs have good separability. The results indicate that it is easier to separate wheat from soybean spectral signatures using the five bands that were selected. This should be in the text (some of it is)

Pair Separation	Jeffries-Matusita
Wheat Non-Liver and Wheat Liver	1.07
Soy Liver and Soy Non-Liver	1.23
Soy Liver and Wheat Non-Liver	1.71
Soy Liver and Wheat Liver	1.77
Soy Non-Liver and Wheat Liver	1.87
Soy Non-Liver and Wheat Non-Liver	1.92

4.2 SOIL

In terms of grave detection it is also important to assess the difference that occurs within the soil as decomposition occurs. During the initial stages, a grave is often left bare, without vegetation cover (Tibbett and Carter 2009). This section will go over two experiments aimed to assess what variations occur in soil spectral signatures that are in contact with swine liver decomposition and test if it is possible to separate fertilizer treatments from the ones affected by swine liver.

4.2.1 FERTILIZER EXPERIMENT

The goal of this experiment was to test whether different fertilizer treatments could be distinguished from grave soil. Pure fertilizers are very different from one another prior to being mixed with the soil (Figure 26). The differences are mostly found in the visible range and around the 1750 nm to 1900 nm range. Bone meal and blood meal are similar after 1900 nm but at lower wavelengths they are different from one another (Figure 26). When performing a classification on the pure fertilizers it is possible to separate them adequately through the use of different classifiers ldc, qdc, parzenc, knnc, udc. The associated testing error is of 5% for the linear (ldc) classifier and of 0% for the qdc, parzenc, knnc, udc. According to the forward feature selection the best bands are situated along the 470 nm to 500 nm range.

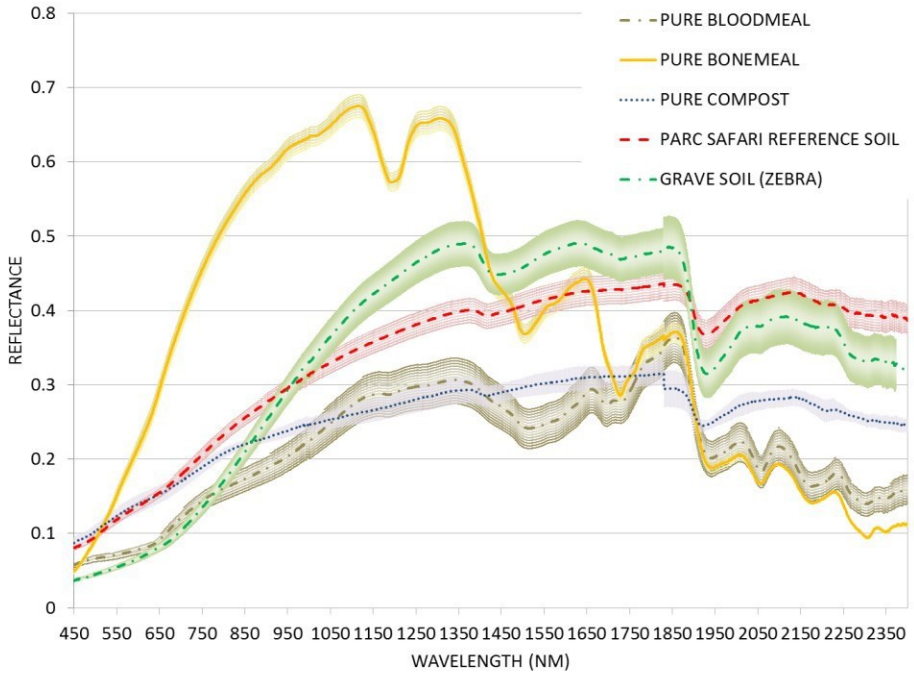

Figure 28: Pure Fertilizers vs. Soil collected at Park Safari, bars surrounding the spectral signatures represent an error of one standard deviation.

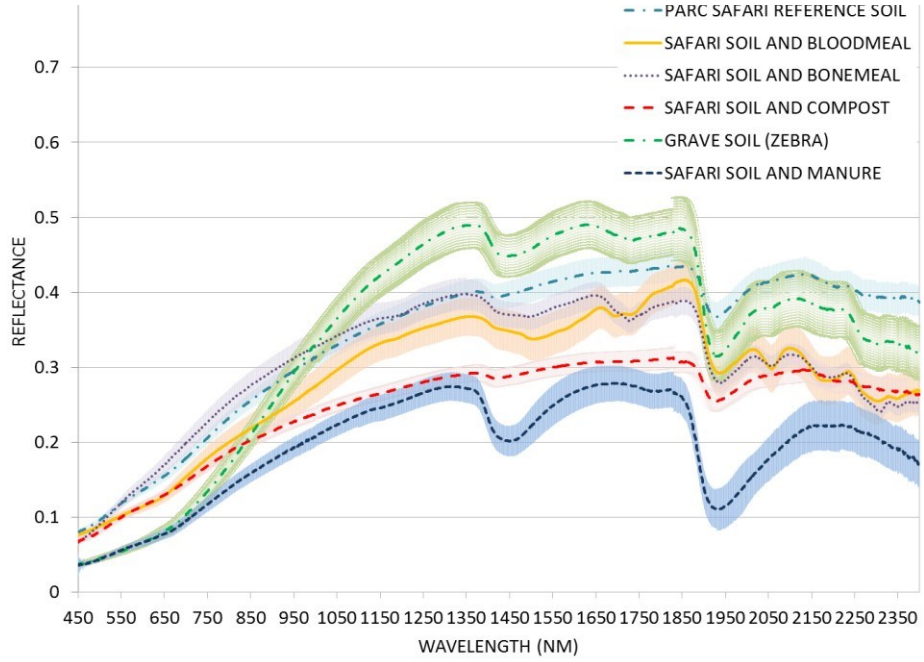

Figure 29: Spectral signature of 1:1 fertilizer to soil mix; Bars surrounding line represents one standard deviation.

In their pure form, not mixed with soil, fertilizers diverge spectrally to a large extent (See Figure 28). Once the fertilizers are mixed with the same amount of soil the difference between the treatments is less obvious (Figure 29 and 30). A classification using PrTools was performed on the soil mixture spectral signatures. Through a forward feature selection, it was determined that only 3 bands were needed to separate the dataset; more features did not improve separability of the results. The three best bands for best separability between the different treatments are 726 nm, 1889 nm and 2058 nm. The classification performs well; the ldc separates perfectly the different treatments with a 0% classification error, parzenc and knnc separate the data with an error of 3%, udc with a 20% error followed by the qdc parameter which has a testing error of around 40%.

The results indicate that it is possible through the use of a linear (ldc) classifier to separate the different types of treatments from each other. This experiment was also performed on soil coming from Vaudreuil-Dorion with different amounts of liver to replicate cadavers of different sizes (Figure 30).

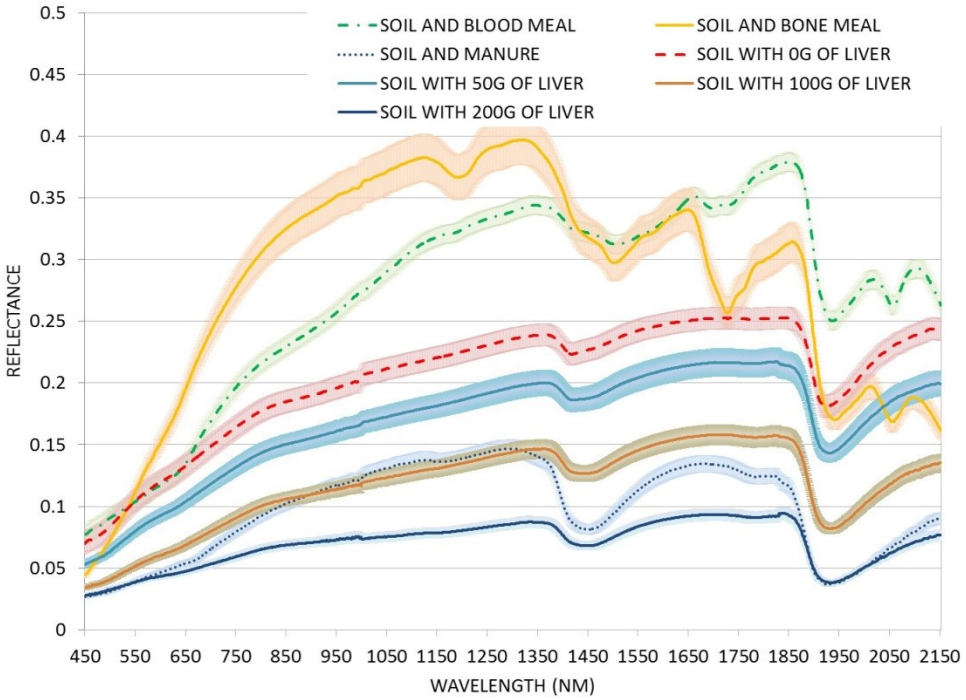

Figure 30: 1 to 1 Fertilizer to Vaudreuil Soil Spectral Signatures, The graph illustrates the spectral signature soil with different treatments and its error of one standard deviation.

The soil mixture spectral signatures of fertilized soils diverge from the control and the liver treatments. The soils treated with fertilizers have generally a

slightly more concave shape in the visible than the control soil and the soil affected by liver, this difference can be attributed to the presence of organic matter (Figure 30). This is well demonstrated by the manure and soil mixture.

After 1200 nm, the soils treated with blood meal and bone meal differ greatly from the non-fertilized soils and soil with liver. The soil affected by liver has a feature around the 1800 nm to 1850 nm range, which might be linked to phenolic O-H bonding (Ben-Dor 2002) that is occurring within the soil. The spectral signatures show that the 1:1 mixtures are highly distinguishable from the non-fertilizer soil. Although the amount is greater than the ratio used by farmers, the near infrared and shortwave infrared regions (after 1200 nm) should be considered in order to distinguish the fertilizer from non–fertilizer soil and grave soil.

In order to gain a better understanding of the differences between soils, it is possible to convert spectral signatures into spectral fingerprints. The spectral fingerprints in Figure 30 illustrate visually the difference found between the spectral signature of reference soil and grave soil. When visualizing the spectral fingerprints, it is noticeable that the grave and reference soils present differences.

From the fingerprints generated from the different soils (control and commingled grave soil) collected at Parc Safari it is possible to see variations between the reference soil and grave soils around the 450 nm - 900 nm and from 2000 nm - 2400 nm range (Figure 31).

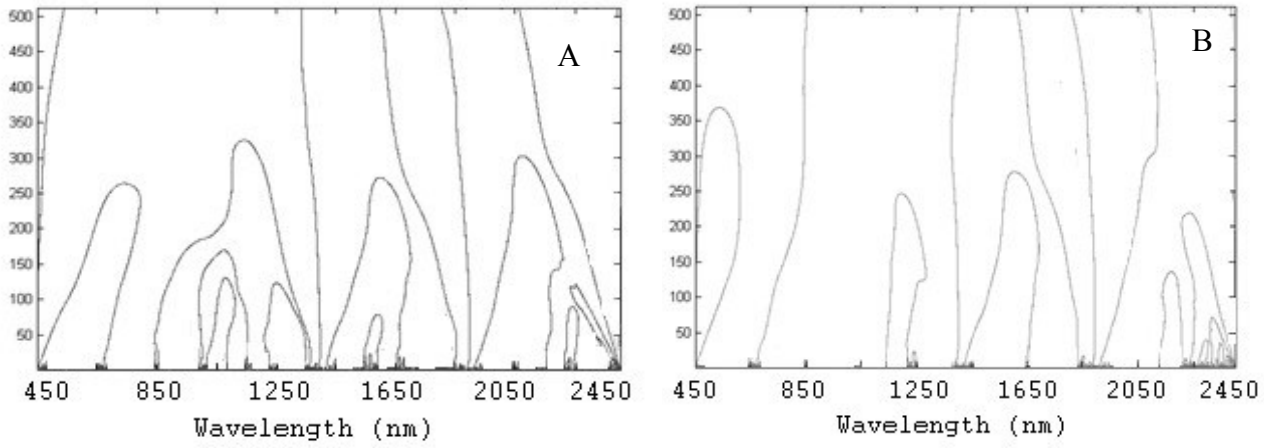

Figure 31: Spectral Fingerprints of control soil (A) and comingled grave soil B. Difference between both charts indicate where the treatments' spectral signature differs.

. However, certain features are similar to the reference soil. Nevertheless, the soils fertilized spectral signature (manure, bone meal, blood meal or compost) remain distinct from grave soil (Figure 32). This limits the possibility of false-positives when identifying grave though soil spectrometry.

The fingerprints indicate that there is difference between grave and reference soils in the 700 nm - 950 nm range. Some of the variation in the graphs can be due to noise, especially at the lower scales. When looking at the fingerprints (Figure 32), it is noticeable that the bone meal and soil mix spectral fingerprints are the most different from the grave and reference soil. Similarly manure, compost and blood meal treated soil differ from the graves soil and have a greater resemblance to the reference soil (Figure 32).

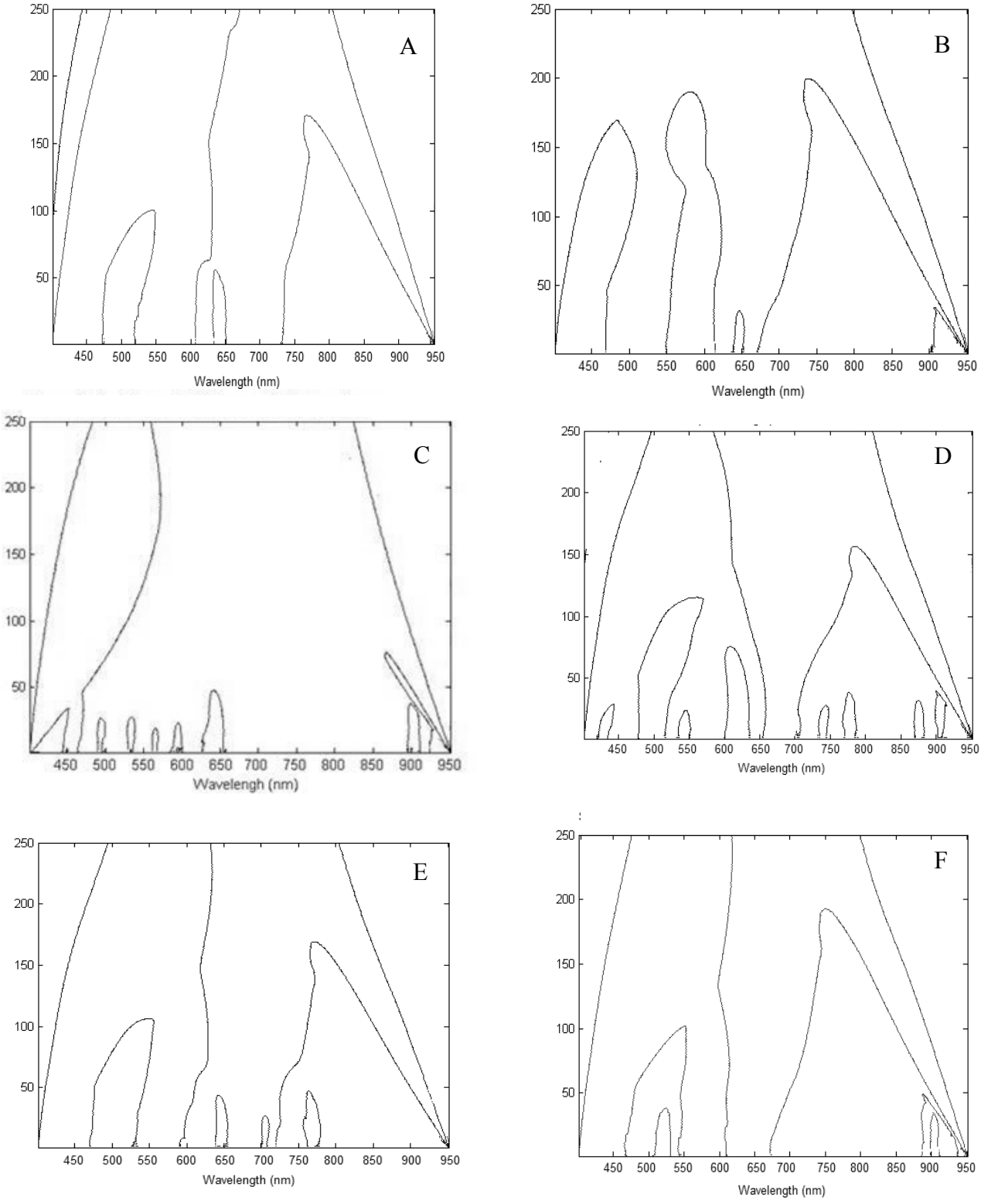

Figure 32: Spectral fingerprint of soil with no treatment (A), Bone meal and Soil (B), Grave Soil (C), Manure Treated Soil (D), Compost and Soil (E) and Blood meal and Soil (F). The grave fingerprint (C) remains distinctive from soils treated with fertilizer treatments.

The bone meal and soil treatments show specific features compared to the rest of the fingerprints from 550 nm to 600 nm (Figure 32). It is possible to quantify the differences found between the signatures through classification.

From the four chosen classifiers (ldc, qdc, lmnc and knnc) three of the classifiers can be considered as candidates well suited to demonstrate the difference between grave and reference soil. The nearest neighbour (knnc) seems to separate both soils into their respective classes with 0 % error. Ldc and qdc are also good candidates to describe the difference obtained between grave and reference soils (Table 7) whereas Qdc has a 23% error when classifying the data.

As well, the results indicate that the blood meal mixed with soil differs from grave soil (Table 7). The qdc classifier indicates an 11% of error between reference and blood meal indicating that there is some similarity between the blood meal mix and the reference soil. The error shown for the grave versus blood meal comparison for the ldc classifier is 30% and 7% for the qdc classifier. Thus, the quadratic classifier (qdc) seems to be better suited for differentiating these spectral signatures.

For the compost mix, the errors are similar between all classifiers used in this experiment. Compost resembles more the reference spectra, although with 7% error, the classification is still possible.

The error that the classifiers present for manure varies from around 4% to 12%. Nearest neighbour and linear classifiers are well suited to separate manure treated soils from reference soil and grave soil.

Table 7: Classification Errors for Parc safari Soil and Fertilizers

Testing Spectral datasets		**Classifiers**			
Dataset A	*Dataset B*	*Ldc*	*qdc*	*lmnc*	*knnc*
Reference Soil	Buffalo	0.00	0.00	0.04	0.00
Commingled Grave Soil	Buffalo	0.15	0.23	0.08	0.00
Reference Soil Spectra	Blood meal and soil	0.08	0.12	0.00	0.00
Commingled Grave Soil	Blood meal and soil	0.31	0.08	0.50	0.00
Reference Soil	Bone meal and soil	0.00	0.00	0.00	0.00
Commingled Grave Soil	Bone meal and soil	0.22	0.10	0.05	0.00
Reference Soil	Compost and Soil	0.08	0.08	0.08	0.08
Commingled Grave Soil	Compost and Soil	0.00	0.00	0.00	0.00
Reference	Manure and Soil	0.00	0.00	0.00	0.00
Grave	Manure and Soil	0.04	0.12	0.12	0.04

In sum, it is possible to separate with reasonable error (< 10%) the different treatments from one another using spectral fingerprints and knnc classification.

4.2.2 IMPACT OF LIVER TREATMENTS ON SOIL

In this case, the spectral response of fresh liver was measured in order to gain some knowledge on its impact on the spectral signatures when introducing it to soil (Figure 31). It is important to look at the reflectance in the red bands because they are linked to the high reflectance of red by hemoglobin (Bremmer, Nadort et al. 2011). This is why we perceive that liver is a reddish brown color. My hypothesis was that addition of this substance on soil will create some spectral features within the soil signature that are directly related to the spectral signature of liver. When examining the spectral signature of the soil collected on October 27th 2012, a week after the experiment started, no significant changes are observed between the treatments containing different amounts of decomposing liver.

Even though variations do occur around the 1800 nm, the spectral signatures remain difficult to classify when using top three bands: overall error of 63% to 88% using the ldc, qdc, parzenc, knnc and udc classifiers (Table 8). Adding more bands to the classification did not improve separation between the classes.

Table 8: Classification soil 0g, 50g, 100g and 200g liver October 27

	Ldc	Qdc	Parzenc	Knnc	Udc
Train	0.32	0.17	0.43	0.00	0.55
Test	0.88	0.63	0.73	0.67	0.77

The soil affected by various quantities of liver remains difficult to separate from one another.

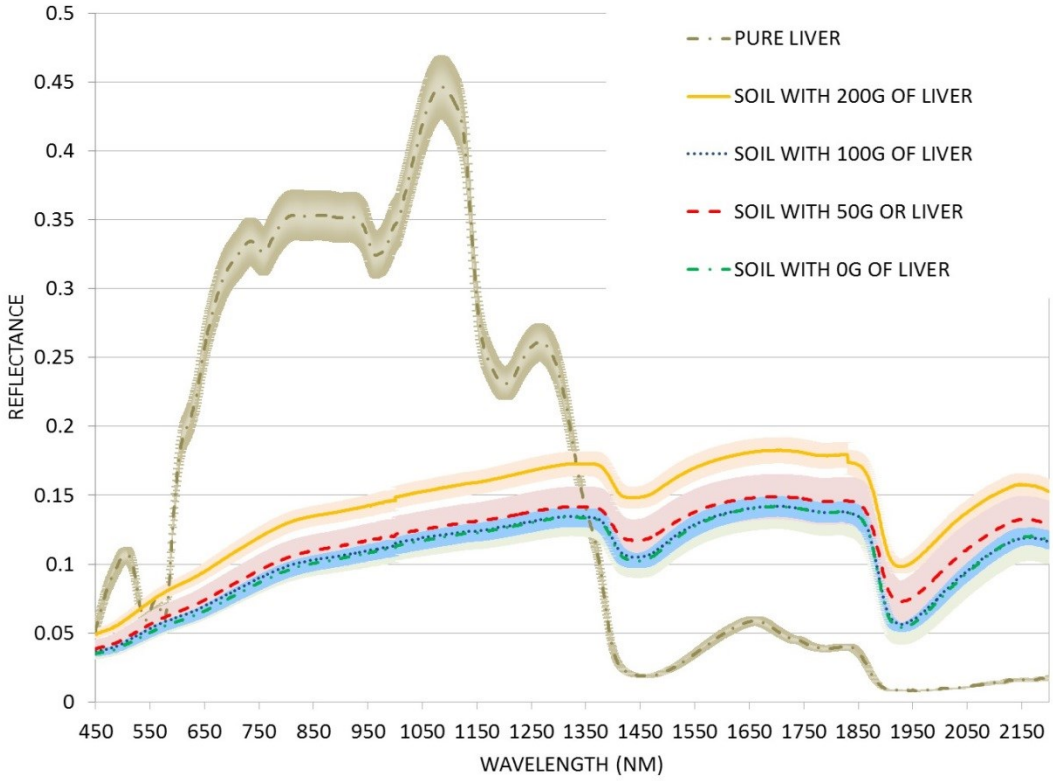

Figure 33: Soil Spectral Signature on Oct 27th, 0g, 50g, 100g and 200g of Liver and Pure Liver. The bars surrounding the spectra represent one standard deviation.

The next measurement took place on November 1st 2012. According to the feature forward selection, the best top 3 bands to separate soil with different amounts of swine liver into their respective classes are around bands 1100 nm to 1160 nm. Through the knnc and udc classifiers it is still possible to classify the data into the different groups with 8% to 14% error. However, other classifiers become ill suited in order to separate the different classes having a testing error of 85% (Table 9).

Table 9: Classification error of spectral signature measured on November 1st 2012. The classification used the top3 bands with different amounts of liver 0g, 50g, 100g and 200g. .

Classification of Soil Treatments		
Classifier	Training error	Testing Error
Ldc	0.85	0.85
Qdc	0.85	0.85
Parzenc	0.85	0.85
Knnc	0.00	0.08
Udc	0.00	0.14

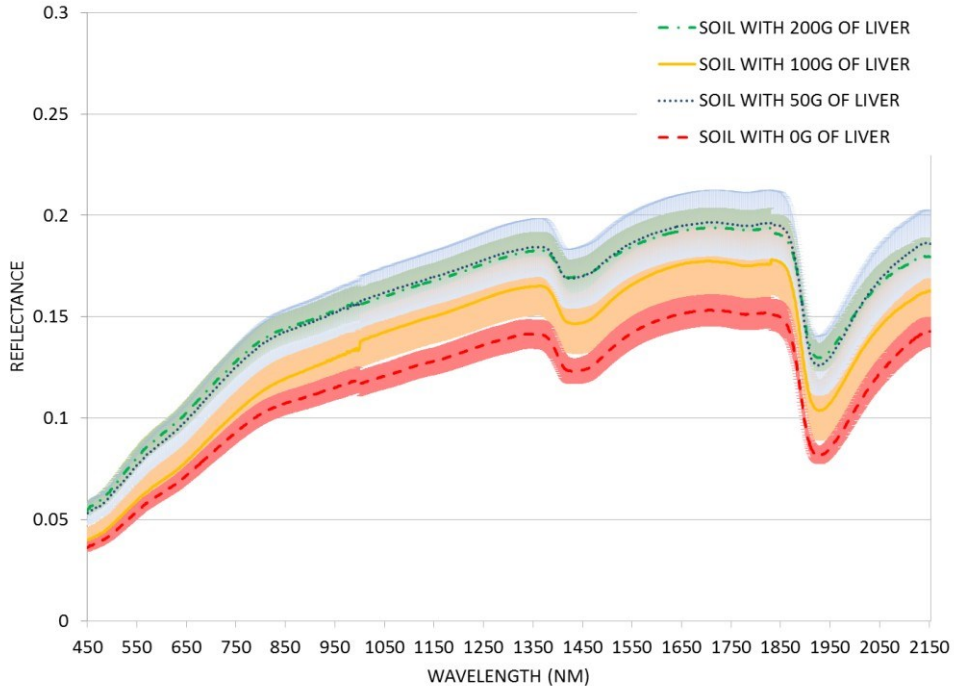

Figure 34: Soil Spectral Signature on Nov 1st, 0g, 50g, 100g and 200g of Liver. Error bars represent one standard deviation.

The following measurement of the soil was taken on November 15th,2012. The classification was performed with the same parameters that were used previously. The bands around 1800 nm seem the most appropriate in order to separate the spectral signature of the different treatments. The Ldc, Qdc, Parzenc classifiers performed better on the November 15th data than on the previously recorded data.

The differences might be linked to the amount of liver that is in the different treatments. It remains difficult to distinguish between different amounts of liver, but it is possible to separate non-liver treatment from a mean of the liver treatment (50, 100 and 200 g).

Table 10: Classification error of spectral signature measured on November 15th 2012. The classification used the top3 bands with different amounts of liver 0g, 50g, 100g and 200g.

Classification of Soil Treatments		
Classifier	Training error	Testing Error
Ldc	0.00	0.55
Qdc	0.00	0.73
Parzenc	0.00	0.47
Knnc	0.00	0.57
Udc	0.12	0.53

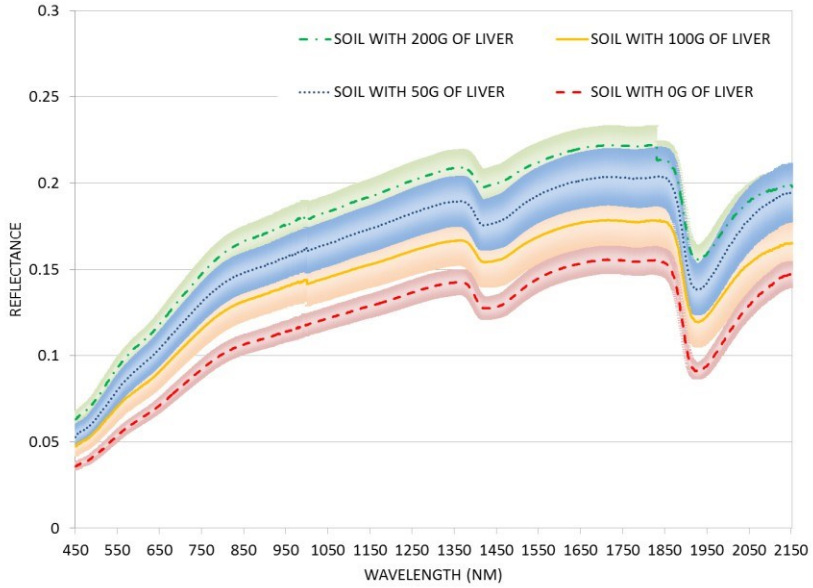

Figure 35: Soil Spectral Signature on Nov 15th 2012, 0g, 50g, 100g and 200g of Liver. Error bars represents one standard deviation.

It is expected that as time progresses, it would become easier to separate the different liver amounts. Further investigation must be done to confirm this.

4.2.3 CHEMICAL COMPOUND MIXTURES WITH SOIL

A decomposing body releases different compounds into the ground (Vass 2008). The goal of this experiment was to determine whether certain key hydrocarbons identified in the literature as important components of decomposition affected the soil in a similar way as cadaver decomposition. By observing the graph of the spectral signatures of the soils treated with a 1:5 ratio of chemical to soil the following compounds diverge from the rest of the chemicals: Ethyl benzene, Styrene, and 1,1,2,2 Tetrachloroethane (Figure 36,A). The spectral signature of the soil affected by xylene and ethyl benzene tends to be less reflective than the control and soil affected by liver (Figure 36, B). This demonstrated that these cyclical hydrocarbons do have an influence on soil spectral signatures.

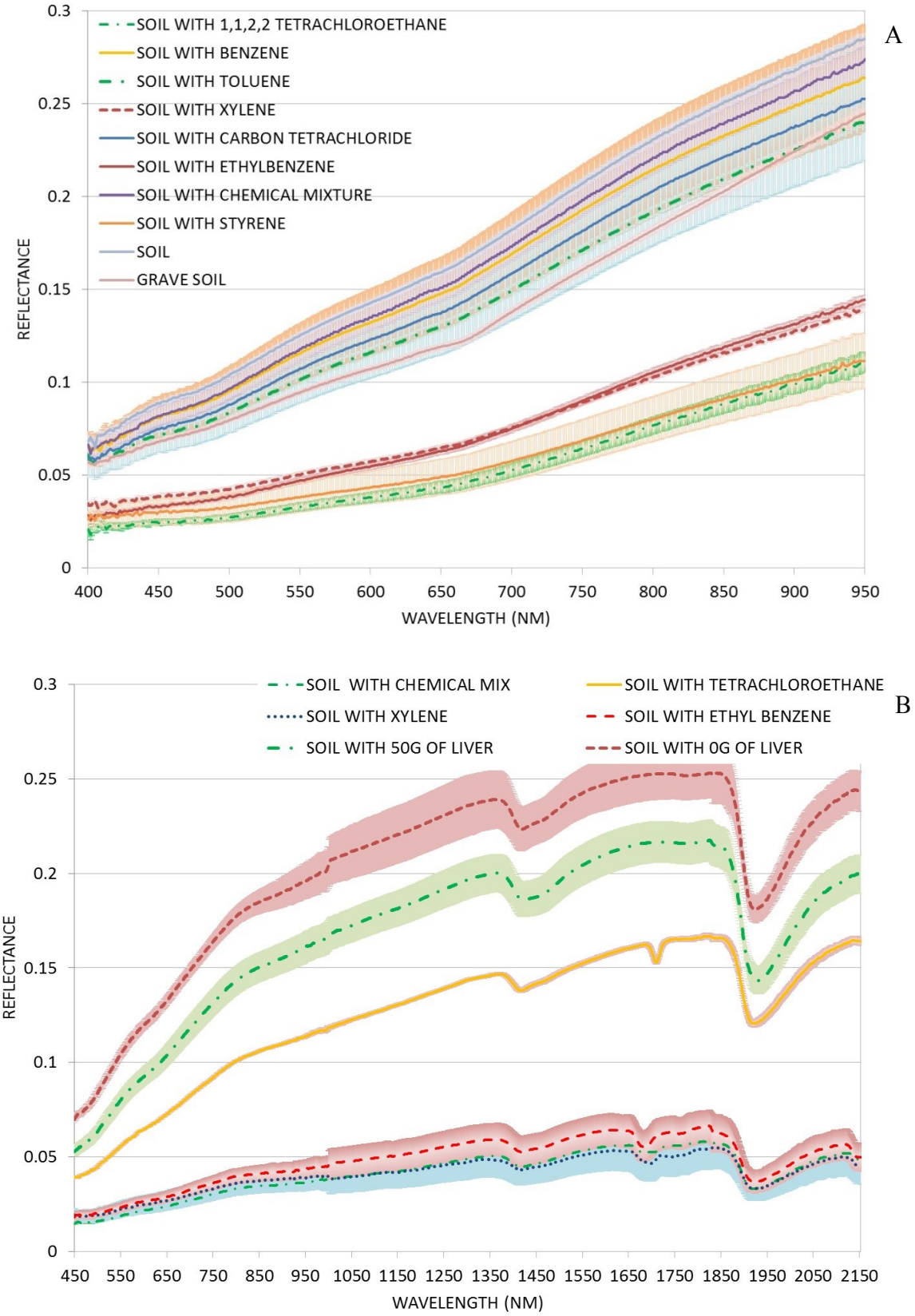

Figure 36: Chemical Mixture and Parc Safari Soil (A). Chemical mixture and Vaudreuil Soil Spectral Signatures (B)

The spectral signatures were then transformed into spectral fingerprints in order to gain a better visualization of the changes caused by the chemicals. Styrene (Figure 37, D), 1,1,2,2 tetrachloroethane (Figure 37, G) and xylene (Figure 37, J) present a feature that starts to resemble a grave signature within the 400 nm – 500 nm range, yet they are still different from a grave. Nevertheless, this indicates that these chemicals do influence the spectra and may cause the reference soil to become more similar to a grave. This is also the case for chemicals added to Vaudreuil Soil. When the same chemicals are added to Vaudreuil soil, features start to appear in the spectral fingerprint of the mix that is similar to grave soil. As for the rest of the chemicals tested in this experiment, they seem to have little effect on the spectra of the reference soil in regards to the spectral fingerprints obtained from the spectral signature of the mixtures (See Figure 37).

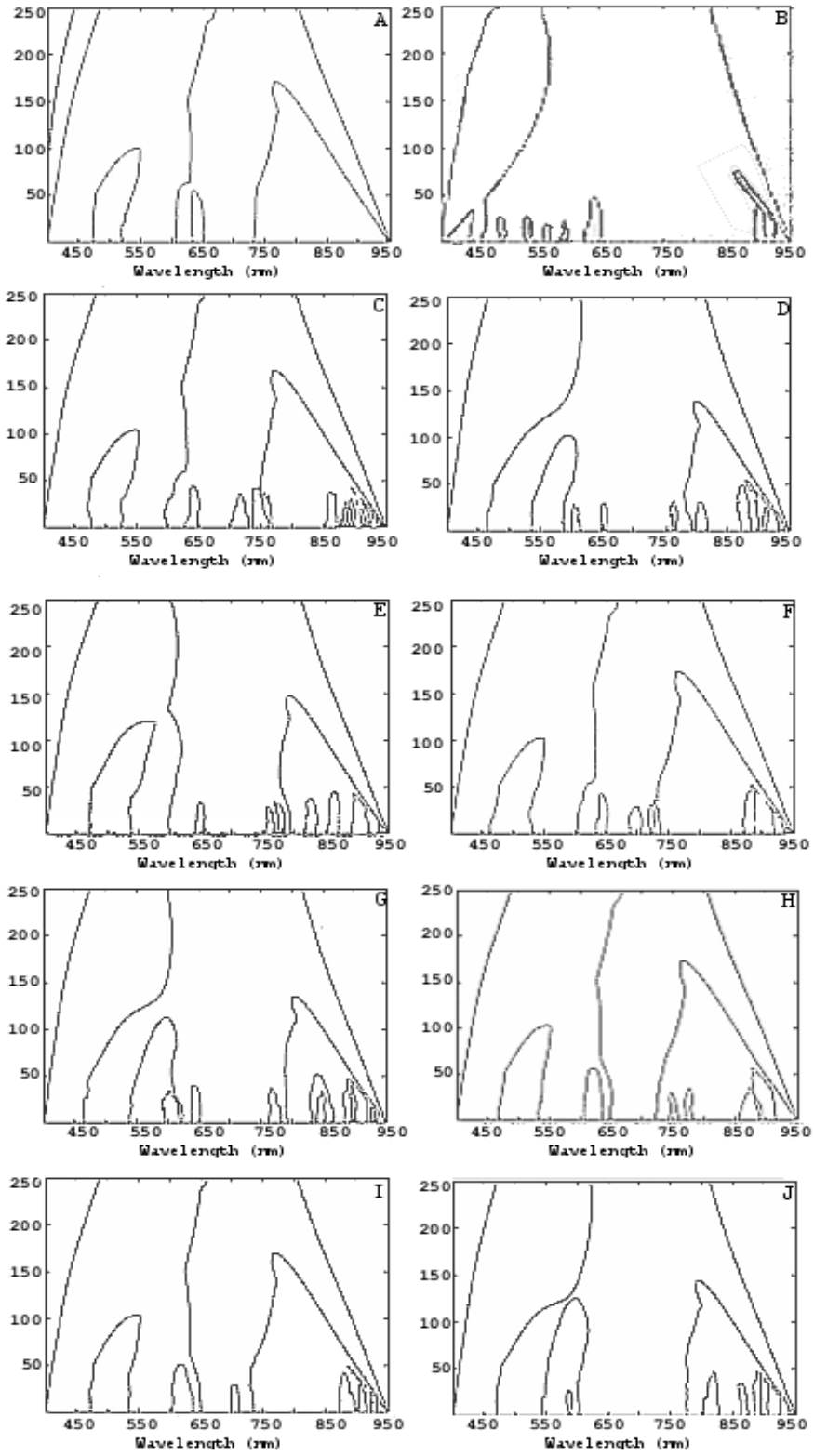

Figure 37: Spectral Fingerprints of Chemicals with Parc safari soil. A-Reference Soil, B-Grave Soil, C-Toluene and soil, D-Styrene and Soil, E- Ethyl Benzene and Soil, F-Benzene and Soil, G- 1,1,2,2, Tetratchloroethane and soil, H-Carbon Tetrachloride and soil, I-Mixture of chemicals (Toluene, Styrene, Ethyl Benzene, Benzene, 1,1,2,2 Tetrachloroethane, Carbon tetrachloride) and soil, J-Xylene and soil.

A classification was performed to see if classes were separable from one another. In this case, the reference soil spectral signature was compared against the spectral signature of the soil mixed with the different chemicals. The soil chemical mixtures were also compared to the spectral signature of soil coming from a commingled grave (zebra, bird). The classification resulted in tetrachloroethane, ethyl benzene and xylene being highly different from the reference soil (1 chemical: 5 soil mixture) (Tables 10 - 11).

Table 11: Testing Error for Classification between chemical treated soil vs. reference soil

Testing datasets		ldc	qdc	Lmnc	knnc
Reference	Tetrachloroethane	0.00	0.00	0.00	0.00
Reference	Ethyl Benzene	0.00	0.00	0.00	0.00
Reference	Xylene	0.00	0.00	0.00	0.00

Table 12: Testing Error for Classification between grave soil and chemical mix

	Testing datasets	ldc	qdc	Lmnc	knnc
Commingled Grave	Tetrachloroethane	0.00	0.00	0.00	0.00
Commingled Grave	Ethyl Benzene	0.12	0.23	0.31	0.19
Commingled Grave	Xylene	0.00	0.00	0.00	0.08

For 1,1,2,2 Tetrachloroethane and xylene, their differences can be seen in the fingerprints of these spectral signatures. However, when comparing these chemicals to the commingled grave spectra, only ethyl benzene comes closer to a grave. Thus ethyl benzene as a chemical affects the reference soil spectra to appear closer to the grave soil (Table 11).

This experiment although small in scope provides valuable information that it is possible to observe the effect of chemicals on soil spectra. Ethyl benzene (C_8H_{10}) is a hydrocarbon, which according to Vass (2008) is a chemical that is found at the surface of gravesites (Vass 2008) during decomposition. Thus, it is important to consider this chemical in further analysis.

In sum, hydrocarbons such as xylene and ethyl benzene have a tendency to lower the overall reflectance of the soil immediately after application. As well, it is possible to easily distinguish between different types of fertilizers, the control soil and grave (liver treatment) soils. The results have shown that features around

1800 nm are important in order to distinguish between treatments. Further study on the effects of chemicals on soil spectroscopy is highly recommended.

4.2.4 BACTERIA AND CHEMICAL CHANGES

The results thus far have shown that it is possible to see major differences between plants that have been treated with liver from plants only treated with fertilizers. The changes seen in the plants such as height differences and leaf structure can be attributed to the different treatments applied to the soil. In order to assess changes within the soil, soils were sent to the Soil Food Web Canada Laboratories in order to determine the composition of the microbial communities.

Table 12 illustrates the variation in concentration of different elements found within the soil as well as pH and conductivity.

Table 13: Chemistry composition of the soil

Component	Control - May (ppm)	Control with Wheat - Aug (ppm)	Wheat with 50 g of liver - Aug (ppm)	Control with soy - Aug (ppm)	Soy with 50g of liver – Aug (ppm)
Calcium	2064	3220	3426	3013	3508
Phosphorus	66	1	136	6	82
Potassium	311	230	795	140	702
Magnesium	508	718	669	669	1015
Nitrate nitrogen	4	<1	314	5	166
Ammonia nitrogen	2	<1	12	<1	34
Sulfur	24	108	112	76	100
Copper	9	<1	<1	<1	<1
Iron	<1	25	<1	<1	15.50
Manganese	<1	<1	<1	<1	<1
pH	7.11	7.17	6.71	6.97	7.89
Conductivity	0.55	0.42	0.30	0.20	1.10

It is important to note that levels in calcium increase in all soils in August 2012. Potassium shows a difference between the levels of treatments containing liver versus treatments that do not contain liver. Higher concentrations of nitrate nitrogen are found in the liver treated soils than the control (Table 12).

Not only does the chemistry between treatments change but so does the microbial community (Tables 14-16).

Table 14: Bacterial and Fungal Community Changes

	Control (May)	Control Wheat (Aug)	Wheat 50g liver (Aug)	Control soy (Aug)	Soy 50g of Liver (Aug)
Active Bacterial (ug/g)	13.50	7.35	4.92	42.90	10.60
Total Bacterial (ug/g)	712.00	267.00	326.00	130.00	168.00
Active Fungal (ug/g)	0.00	20.70	39.30	16.00	0.00
Total Fungal (ug/g)	687.00	656.00	1,207.00	407.00	521.00

Table 15: Protozoa and Nematodes in soil

	Control (May)	Control Wheat (Aug)	Wheat liver (Aug)	Control soy (Aug)	Soy 50g of Liver (Aug)
Total Protozoa (#/g)	7,631	43,620	405,598	46,715	80,341
Flagellates	5,680	6,203	380,268	21,234	78,198
Amoebae	1,880	37,339	19,013	21,234	1,779
Ciliates	71	78	6,317	4,247	364
Total Nematodes (#/g)	3.74	2.78	2.59	1.67	3.33
Plant Nitrogen N Supply	50-75	100-150	300+	100-150	100-150

The available amount of nitrogen within the treatments increases with time, however, there is a difference found between the level of control soy and soy liver in the soils sampled at the end of the experiment. It is noticeable that in both cases for soy and wheat plants there are more protozoa in the liver treatments than the non-liver treatments. The basic message to take from these results is that differences in nutrients and bacterial activity are found between non-liver and liver treatments. These differences influence the decomposition rate of material within the ground, influencing the amount of nitrogen in the soil.

Table 16: Nematodes by species in soil

Nematodes per gram of soil	Control (May)	Control Wheat (Aug)	Wheat liver (Aug)	Control soy (Aug)	Soy 50g of Liver (Aug)
Bacterial Feeders					
Acrobeloides	0.69	0.00	0.00	0.00	0.00
Chronogaster	0.5	0.00	0.00	0.00	0.00
Eucephalobus	0.75	0.00	0.00	0.00	0.00
Plectus	0.56	0.00	0.00	0.00	0.00
Diplogaster	0.00	0.34	0.50	0.31	0.76
Rhabditidae	0.00	0.06	0.42	0.08	0.00
Cutilaria	0.00	0.3	0.55	0.70	0.71
Panagrolaimus	0.00	0.000	0.17	0.00	0.00
Predatory					
Monochoides	0.00	0.00	0.25	0.00	0.18
Fungal Feeders/Root Feeders					
Dorylamidae	0.37	0.00	0.00	0.00	0.00
Aphelenchoides	0.00	0.00	0.00	0.00	0.59
Tylenchus	0.00	0.00	0.00	0.00	0.29

The results (Tables 14-6) also indicate that the type of microbe community changes over time. For example, no bacterial feeders were present at the beginning of the experiment but were found to be present at the end. Only in the soil affected by liver are monochoides present. Monochoides are predatory nematodes that eat other nematodes. The amount of bacterial feeder in the ground is related to the amount of bacteria present in the soil. Diplogaster and Monochoides feed on bacteria and smaller nematodes (Khan and Kim 2007); they are more present depending on the amount of prey that is present within the soil (Freckman 1982). The changes of the soils can be linked to the changes of environment; many nematodes are present when certain environmental condition are met and then might no longer live if the conditions change. Liver treatments might attract more bacteria, therefore, increasing the amount of predatory nematodes such as monochoides.

CHAPTER 5-DISCUSSION AND CONCLUSIONS

The results indicate that the decomposition of the liver (cadaver proxy) alters plant growth. Plants grown on liver are generally shorter than plants grown on soil or a fertilizer soil mix. It is important to note that the spectral signature of leaves is affected by both the decomposition of liver, and changes throughout the seasons. The height of plants grown during the summer of 2012 in Vaudreuil-Dorion are higher than the plants grown in 2011, this is likely due to the longer growth period, a five month growth vs. three months in the prior experiment. In the beginning both experiments, liver decomposition negatively affected the growth of plants resulting in a delay in height of the plants compared to the plants that were not in contact with swine liver. From the analysis of the soil mineral and nutrients done by Soil Foodweb Canada, it is clear that nitrate nitrogen is higher in the liver treated soil than the control at the end of the experiment. It is known that plant growth can be hindered by high level concentration of ammonium nitrate and nitrate nitrogen (Kabata-Pendias and Mukherjee 2007). Therefore, it is most likely that the liver decomposition releases large amounts of nitrate nitrogen and ammonia nitrogen into the ground in the early stage of decomposition hindering the growth of the plants. In future studies, more sampling and chemical analysis at the beginning of the experiment would help to obtain a clearer picture of the processes that are occurring.

Furthermore, analysis under the electron microscope demonstrates that differences between the internal structure of plants on liver and non-liver treatments exist. The soybean leaf from the non-liver treatment is more structured and shows more vacuoles than its counterpart. This confirms the differences seen in the spectra in the near-infrared. This is based on a very small sample and should be investigated in future studies.

As for changes between types of fertilizers in vegetation spectra, there is almost no difference found in the near infrared in their spectral signature. However, changes can be observed in the visible range of the spectra around 500 nm to 650 nm. According to the literature, this portion of the spectra is linked to the pigments present within the leaves (Gerendás, Zhu et al. 1997; Penuelas and

Filela 1998). The chlorophyll extraction of the summer 2012 leaves showed that significant differences between the amounts of chlorophyll are already present in June, after only one month of growth of the plants. By using bands from the NIR and the green regions of the spectrum it is possible to assess the physiological status of the plants. From the chlorophyll information collected at the Phytotron it is possible to affirm that differences are observable between fertilizer treatments and liver treatments as there are statistically significant differences found between the amounts of chlorophyll within their leaves.

By using Parametric and Non-parametric classifications of the spectra it is possible to distinguish between plants affected by liver (cadaveric decomposition) vs. plants grown under normal conditions. One of the strengths of this method is that it allows for a reduction of the dataset to a more manageable size and provides information on the accuracy of the classification.

The bands that should be considered in order to differentiate liver treatment from non-liver treatments in vegetation spectra should include bands in the 700 nm to 800 nm region. However, if only fertilizer treatments should be separated from one another (*ie:* bone meal from manure) then bands in the 500 nm - 600 nm range should be considered.

As a leaf matures the best bands to separate the different treatments changes as well; in July 2012 they are situated at 709, 809, 935, 644 and 450 nm. For wheat in July 2012 the best bands are 713,465,574,629 and 639 nm. For soy in August the best bads are situated at 515, 514, 516, 506 and 517 nm. For the wheat in August they are 615, 468, 604, 600 and 612 nm. These bands were found for both the collections during summer 2011 and summer 2012.

The soil sent for analysis at the food web lab has shown that soils containing liver have higher levels of nitrate nitrogen. It has been found that soils under liver treatments contain also more predatory nematodes. However, the active bacteria count remains different between the different treatments. Further investigation on the bacterial count and nematodes could be useful in order to gain a better insight of the differences found between soils affected by cadaveric decomposition from those only treated with fertilizer.

Soils affected by different treatments are also distinguishable between one another through classification. It remains difficult to separate the different amounts of liver contained in the soil from one another. Nevertheless, features unique to liver treatments can be found around 1800 nm. The presence of certain chemicals compounds created during decomposition could explain the formation of these features. A mixture of hydrocarbons, such as tetrachloroethane and ethyl benzene, seems responsible for some of the features found along the spectral signature of grave soil.

This study has shown that it is possible to separate fertilizer from liver treated soils. The results of this study can be related to soft tissue decomposition where skin, muscle and organs are presents. However, it is possible that the difference found between cadaveric soil and non-affected soil might be more pronounced and longer lived since cadavers have bones that will continue to decompose and affect the soil matrix over time, thus affecting the nutrient availability of plants. Plants such as wheat and soybean are not likely to occur on a grave site, nevertheless all plant species can be affected by the presence of decomposing animal tissue. Therefore, changes occurring within the soil and plants may be longer lived than shown in this research.

Due to nutrients migrating within the soil overtime it is expected that spectral differences seen between the different treatments will become more evident. Hence, a study over a longer time period could be beneficial to evaluate the potential of separating the different fertilizer treatments from grave soils over a longer period of time.

As seen in the results section, not all classifiers can separate the data equally as well. The results indicate that the nearest neighbor classifier (knnc), linear (ldc) and quadratic functions (qdc) work well to differentiate between treated soil, reference soil and grave soil. It is arguable that the errors that are seen are benign and do not actually signify a major difference among the spectral signature. The use of fingerprints coupled with classification can help identify key differences found within different spectral signatures. In other words, confusion between the spectra of treated soil, non-treated soil and grave soil is limited and should not hinder the identification of grave though soil spectroscopy.

This research shows that both species of plants react to the presence of animal tissue. Both soybean and wheat, present differences in their growth pattern, namely slower growth for those that received liver treatment. The main goal was to determine if fertilized areas can be mistaken for graves; findings show the plants' spectral signatures under fertilizer treatment remain distinctive from those in contact with the swine liver.

The amount of liver used in each pot represents the amount that a single body would represent in the ground, therefore, the purpose of experimenting with different liver amounts tried to capture the effects of a different number of bodies found within the soil. In the case of mass graves it is likely the differentiation would be stronger. However, it is important to note that the use of swine liver as a proxy of human cadaver does not reflect entirely the reality of the grave. Liver being rich in nutrients will degrade at a faster pace than a body that contains tissue, muscle and bones.

The main finding of this research is that decomposition of tissue (swine liver) affects the spectral signatures of soil and vegetation. As liver decomposes it releases an array of nutrients and chemicals such as hydrocarbons. This affects plant growth and the spectral signature of vegetation and soils. Hydrocarbons, such as ethyl benzene and tetrachloroethane that are produced by a cadaver affect the spectra of soil to become more similar to soil from a grave. From this, it is possible to infer that these hydrocarbons are highly influential on the spectra of

the soil. However, these chemicals tend to be volatile and might only alter the soil during initial stages of decomposition.

Some of the changes seen in the spectral signatures can be attributed to changes in pigments; different fertilizers will have more impact on the chlorophyll concentration than other treatments. The decomposition of liver will actually affect plant growth and the internal structure of leaves as seen throughout the summer of 2011 and 2012, showing variation along the spectra past 750 nm.

Finally, the soil spectral signature of the different treatments can be separated from one another using the following three bands: 725, 1889 and 2058 nm. The bands around 1800 nm according to the literature are linked to phenolic O-H changes in the soil (Ben-Dor, Inbar et al. 1997; Ben-Dor 2002).

To conclude, this research provides some insights into the effects of decomposing animal tissue on vegetation and soil. The main observations that were made are that as animal tissue decomposes into the ground, it releases nutrients causing changes in nutrient and microbial composition of the soil. The internal structure of leaves for the soy bean plants are affected by the animal tissue decomposition in the soil, and finally that some of the hydrocarbons released through the decomposition process might be responsible for the changes seen in the spectral signature of soil.

APPENDIX A

Reflectance Index	*Acronym*	*Ratio*	*Use*	*References*
Simple Ratio	**SR**	**NIR/Red**	**Greenness**	(Jordan 1969)
Normalized difference pigment index	**NDPI**	**R680-R430/R680+R430**	**Carotenoids, chlorophylls**	(Penuelas and Filela 1998)
Normalized difference vegetation index	**NDVI**	**(NIR-Red)/(NIR+Red)**	**Greenness**	(Tucker 1979; Jackson, Slater et al. 1983; Sellers 1985)
Vogelmann Red Edge Index 1 **Vogelmann Red Edge Index 2** **Vogelmann Red Edge Index 3**	**VOG1** **VOG2** **VOG3**	**R740/R720** **R734-R747/R715+R726** **R734-R747/R715+R720**	**Chlorophyll**	(Vogelmann, Rock et al. 1993)
Photochemical reflectance index	**PRI**	**R531-R570/R531+R570**	**Absorption by leaf carotenoids**	(Gamon, Peñuelas et al. 1992; Gamon, Serrano et al. 1997)
Plant Senescence Reflectance Index	**PSRI**	**(R680/R500)/P750**	**Senescence/carotenoids**	(Merzlyak, Gitelson et al. 1999)
Yellow Index	**YI**	**(R580-2*R624+R668)/ ΔR^2**	**Chlorosis**	(Adams, Philpot et al. 1998)

Appendix A enumerates some common indices to assess the amount of pigments found within vegetation. Most of these indices use features of the spectral signatures to get a better understanding of the health of the plants or amount chlorophyll found within the leaves. For example, the simple ratio uses a band from the NIR over a band coming from the red region of the spectrum. Some of these indices can be used in order to assess the health of plants. Therefore, these indices might be useful when looking for plants affected by fertilizers or cadaver decomposition.

APPENDIX B

PHYTOTRON TREATMENT BREAKDOWN

PLANT	SOIL	TREATMENT	LIVER	REPLICATE
Soy	Clay soil	None	None	3
Soy	Clay soil	Manure	None	3
Soy	Clay soil	Bone meal	None	3
Soy	Clay soil	Blood meal	None	3
Soy	Clay soil	Inocculated	None	3
Soy	Clay soil	None	Yes	3
Soy	Clay soil	Manure	Yes	3
Soy	Clay soil	Bone meal	Yes	3
Soy	Clay soil	Blood meal	Yes	3
Soy	Clay soil	Inocculated	Yes	3
Soy	Black organic soil	None	None	3
Soy	Black organic soil	Manure	None	3
Soy	Black organic soil	Bone meal	None	3
Soy	Black organic soil	Blood meal	None	3
Soy	Black organic soil	Inocculated	None	3
Soy	Black organic soil	None	Yes	3
Soy	Black organic soil	Manure	Yes	3
Soy	Black organic soil	Bone meal	Yes	3
Soy	Black organic soil	Blood meal	Yes	3
Soy	Black organic soil	Inocculated	Yes	3
Wheat	Clay soil	None	None	3
Wheat	Clay soil	Manure	None	3
Wheat	Clay soil	Bone meal	None	3
Wheat	Clay soil	Blood meal	None	3
Wheat	Clay soil	None	Yes	3
Wheat	Clay soil	Manure	Yes	3
Wheat	Clay soil	Bone meal	Yes	3
Wheat	Clay soil	Blood meal	Yes	3
Wheat	Black organic soil	None	None	3
Wheat	Black organic soil	Manure	None	3
Wheat	Black organic soil	Bone meal	None	3
Wheat	Black organic soil	Blood meal	None	3
Wheat	Black organic soil	None	Yes	3
Wheat	Black organic soil	Manure	Yes	3
Wheat	Black organic soil	Bone meal	Yes	3
Wheat	Black organic soil	Blood meal	Yes	3
			Total wheat	48
			Total soy	60
			Total pots	108

This appendix shows the different treatments that were applied during the summer of 2011 at the Phytotron.

VAUDREUIL- DORION LIST OF TREATMENTS

ID	PLANT	SOIL	TREATMENT	LIVER	# Plants per pot	REPLICATE
1	Soy	VD Soil	None	None	5	10
2	Soy	VD Soil	Manure	None	5	10
3	Soy	VD Soil	Bone meal	None	5	10
4	Soy	VD Soil	Blood meal	None	5	10
5	Soy	VD Soil	50g	Yes	5	10
6	Soy	VD Soil	100g	Yes	5	10
7	Soy	VD Soil	200g	Yes	5	10
8	Soy	VD Soil	Manure	Yes	5	10
9	Soy	VD Soil	Bone meal	Yes	5	10
10	Soy	VD Soil	Blood meal	Yes	5	10
11	Wheat	VD Soil	None	None	5	10
12	Wheat	VD Soil	Manure	None	5	10
13	Wheat	VD Soil	Bone meal	None	5	10
14	Wheat	VD Soil	Blood meal	None	5	10
15	Wheat	VD Soil	50g	Yes	5	10
16	Wheat	VD Soil	100g	Yes	5	10
17	Wheat	VD Soil	200g	Yes	5	10
18	Wheat	VD Soil	Manure	Yes	5	10
19	Wheat	VD Soil	Bone meal	Yes	5	10
20	Wheat	VD Soil	Blood meal	Yes	5	10
				Total wheat	50	100
	VD Soil means Soil taken in Vaudreuil-Dorion			**Total soy**	50	100
				Total pots	100	200

This appendix shows the different treatments that were applied during the summer of 2012 in Vaudreuil-Dorion.

APPENDIX C

PROTOCOL FOR LEAF TEM PREPARATION

1. From the frozen leaves, cut a small piece as a sample.
2. Fixation in buffered aldehyde for at least 24 hours at4°C.
3. Wash three times with wash buffer. Let 10 minute for each time.
4. Post fixation in osmium tetroxide
    a. 1% osmium tetroxide
    b. 1.5% potassium ferrocyanide, 2 hours at 4° C
5. Wash three times with wash buffer , 10 minutes each
6. 2% tannic acid, 2 hours at 4° C
7. Wash three times, 10 minutes for each
8. Dehydration
    a. Acetone: 30%, 50%, 70%, 80%, 90%, 100% (15 minutes for each concentration, two times is more for 100%)
9. Embedding
    a. Acetone: epon 812 is 1 :1 overnight
    b. Acetone: epon 812 is 1: 2 all day
    c. Acetone: epon 812 is 1:3 Overnight
    d. Acetone: epon 812 1:3 all day
    e. Pure epon 812 Overnight Under vacuum
    f. Pure epon 812 All day Under vacuum
10. Polymerization
    a. 60 degrees Celsius For two days
11. Cutting and placement on mesh

APPENDIX D

MATLAB CODES

The code in this appendix was used in Matlab R2012a, this section shows the different codes used to analyze the data

ANALYSIS OF VARIANCE

- *1 WAY ANOVA*

  [p,tbl,stats]=anoval(growth2012);

  % Note that the groups have to be placed by columns

- *2 WAY ANOVA*

  [p,table,stats]=anova2(soyplant_height) SAVITZKY-

GOLAY SMOOTHING FILTER

The Savitzky-Golay smoothing filter allows you to smooth out noise in the signal.

CODE:

```
% VARIABLES
% A= ID_LEAFSPECTRA
SG_A=SGOLAYFILT (A, 3, 15)
% 3 IS DEGREE
% 15 IS THE SIZE OF THE WINDOW (FRAME).
```

CLASSIFICATION

```
%THIS DOCUMENT SERVES AS A REFERENCE FOR CLASSIFICATION DONE WITH
%SPECTRAL SIGNATURE OF LEAVES COLLECTED DURING THIS STUDY.
WRITTEN BY: CARRIE HERZOG
%%%%%%%%%%%%%%%%%%%%%%%%%%%%%%%%%%%%%%%%%%%%%%%%%%%%%%%%%%%%%%%%%%%%%%%%%%%%
%%%%%%%%
%STEP 1- CLEAN DATA AND IMPORT INRO MATLAB
%TEST 1: SOY CONTROL VS 50G LIVER TREATMENT
TRAIN_T1(:,1:5)=faf_ref(:,1:5);
TRAIN_T1(:,6:10)=fafrefLiver(:,1:5);
TEST_T1=faf_ref(:,6:10);
TEST_T1(:,6:10)=fafrefLiver(:,6:10);
%ONCE YOU HAVE CREATED THE TRAIN AND TEST MATRIX CREATE LABELS
LABEL_T1(1:5)=1;
LABEL_T1 (6:10)=2;
%TRANSPOSE DATA
TRAIN_T1=TRAIN_T1';
TEST_T1=TEST_T1';
LABEL_T1=LABEL_T1';
%CREATE DATASETS
A_T1=dataset(TRAIN_T1,LABEL_T1);
B_T1=dataset(TEST_T1,LABEL_T1);
%FEATURE SELECTION
%TEST FOR OPTIMAL WAVELENGTH RANGE
[W_T1 R_T1]=featself(A_T1,'NN'); % CHECK THE RESULT TO DETERMINE
%OPTIMIUM NUMBER OF WAVELENGTH
%REDUCE IF IT IS NECCESARY, [WR_T1, RR_T1]=featself(A_T1,'NN',
%#Wavelengths)
%CREATE MAPPING FOR CLASSIFICATION
C_T1=A_T1*W_T1;
D_T1=B_T1*W_T1;
%CLASSIFERS
W1_T1=ldc(C_T1);
W2_T1=qdc(C_T1);
W3_T1=parzenc(C_T1);
W4_T1=knnc(C_T1,3);
W5_T1=udc(C_T1);
train_res_T1=([testc(C_T1*W1_T1),testc(C_T1*W2_T1),testc(C_T1*W3_T
1),testc(C_T1*W4_T1),testc(C_T1*W5_T1)]);
test_res_T1=([testc(D_T1*W1_T1),testc(D_T1*W2_T1),testc(D_T1*W3_T1
),testc(D_T1*W4_T1),testc(D_T1*W5_T1)]);
```

MATLAB ARRAY TO ENVI IMAGE

```
%%STEPS TO FOLLOW TO CREATE ENVI IMAGE FROM MATLAB ARRAY
STEPS:
   1. OPEN AND CLASSIFY DATA
   2. CREATE ZERO MATRIX
   3. TRANSPOSE DATA
   4. CREATE 3D MATRIX
   5. ENVI IMAGE
\\\\\\\\\\\\\\\\\\\\\\\\\\\\\\\\\\\\\\\\\\\\\\\\\\\\\\\\\\\\
%CREATE ZERO MATRIX
      image=zeros(37,37,501);
      imageTxt=zeros(37,37,501);
%TRANSPOSE DATA
      June22dataT=June22data';
      % CONTINUE WITH ALL THE DATA
%CREATE 3D MATRIX
      %ENTER DATA AS FOLLOWS
      image(1,1:37,:)=June22dataT(1:37,:);
      image(2,1:37,:)=June22dataT(38:74,:);
      image(3,1:37,:)=June22dataT(75:111,:);
      image(4,1:37,:)=June22dataT(112:148,:);
      image(5,1:37,:)=June22dataT(149:185,:);
      image(6,1:37,:)=June22dataT(186:222,:);
      image(7,1:15,:)=June22dataT(223:237,:);
      % CONTINUE ENTERING DATA UNTIL ZERO MATRIX IS FILLED UP
      %KEEP RECORD OF THE DIFFERENT ENTRY
      imageTxt(1,1:37)=June22txtT(1:37);
      imageTxt(2,1:37)=June22txtT(38:74);
      imageTxt(3,1:37)=June22txtT(75:111);
      imageTxt(4,1:37)=June22txtT(112:148);
      imageTxt(5,1:37)=June22txtT(149:185);
      imageTxt(6,1:37)=June22txtT(186:222);
      imageTxt(7,1:15)=June22txtT(223:237);
%ENVI IMAGE
      %CREATE HEADER
      info=enviinfo(image);
      %WRITE IMAGE (DON'T FORGET TO NAVIGATE TO THE PROPER
      WORKING FOLDER
      enviwrite(image,info,'VD_image.dat');
```

APPENDIX E

Average Plant Height (cm) , Phytotron Summer 2011							
	05-Jul	**11-Jul**	**18-Jul**	**25-Jul**	**03-Aug**	**10-Aug**	**17-Aug**
soy with liver	3.0 +/- 1.9	4.2 +/- 1.6	8.1 +/- 1.7	5.1 +/- 3.2	7.0 +/- 3.2	11.9 +/- 3.3	49.9 +/- 3.4
soy without liver	13.4 +/- 1.0	17.6 +/- 2.2	22.9 +/- 3.5	30.2 +/- 3.3	43.6 +/- 3.2	52.2 +/- 3.3	53.1 +/- 3.5
wheat with liver	6.9 +/- 3.4	6.9 +/- 3.4	7.8 +/- 5.4	4.3 +/- 5.1	3.5 +/- 5.1	3.0 +/- 6.1	28.7 +/- 5.8
wheat without liver	23.0 +/- 3.3	23.0 +/- 3.6	26.9 +/- 4.4	25.3 +/- 5.3	33.9 +/- 5.6	36.0 +/- 6.7	37.3 +/- 5.3

Average Plant Height in Vaudreuil-Dorion

Treatment	*28-May*	*1-Jun*	*8-Jun*	*18-Jun*	*22-Jun*	*27-Jun*	*11-Jul*	*28-Jul*	*8-Aug*	*17-Aug*
None	13.00	16.90	23.09	51.11	74.13	80.00	107.43	108.00	109.43	116.60
Manure	12.60	16.30	22.43	58.00	68.50	81.29	98.25	102.00	104.83	120.50
Bone meal	14.00	18.70	26.22	58.67	71.89	90.00	111.50	104.00	114.75	119.80
Blood meal	9.50	10.80	27.67	61.75	62.00	74.25	85.83	98.67	116.00	120.00
Liver	14.20	17.80	24.13	36.63	43.13	45.86	48.00	50.40	59.67	76.50
Manure and Liver	13.70	19.00	26.40	44.38	51.75	52.00	53.43	64.00	68.33	73.50
Bone meal and Liver	14.00	16.80	21.83	40.22	57.14	80.80	82.00	91.50	94.40	95.00
Blood meal and Liver	11.80	15.20	21.78	32.50	52.00	53.00	54.00	57.80	65.00	66.00

Soy bean plant height for different liver amounts

Treatment	**28-May**	**1-Jun**	**8-Jun**	**18-Jun**	**22-Jun**	**27-Jun**	**11-Jul**	**28-Jul**	**8-Aug**	**17-Aug**
None	13.00	16.90	23.09	51.11	74.13	80.00	107.43	108.00	109.43	116.60
50g	14.20	17.80	24.13	36.63	43.13	45.86	48.00	50.40	59.67	76.50
100g	13.40	16.90	23.18	41.67	45.78	45.80	80.33	85.00	90.33	92.00
200g	13.50	15.20	24.25	41.00	52.40	53.00	53.00	72.50	78.67	79.00

Vacuole size in TEM Comparaison

ANOVA Table

Source	SS	df	MS	F	Prob>F
Columns	70670.4	1	70670.4	18.85	5.73608e-05
Error	217405.3	58	3748.4		
Total	288075.7	59			

Average size of vacuoles in um^2

Control	Treated with Liver
331.395	51.664
90.886	49.063
271.228	34.844
44.62	72.682
42.074	53.618
148.941	54.809
110.349	47.401
154.977	61.703
97.829	66.396
291.474	17.211
75.431	51.258
108.21	17.701
72.47	33.113
110.386	35.043
174.288	7.68
103.985	5.143
39.154	6.242
78.859	10.813
65.767	6.602
245.252	12.444
42.254	12.018
13.683	9.326
46.246	18.325
26.827	4.568
35.657	16.786
22.213	34.735
62.637	44.273
43.661	51.585
41.515	80
80.154	46.196
Average 102.4141	Average 33.77473333
Standard deviation 82.15432	Standard deviation 22.30494808

REFERENCES

Adams, M. L., W. D. Philpot, et al. (1998). "Yellowness index: an application of spectral second derviatives to estimate chlorosis of leaves in stressed vegetation." International Journal of Remote Sensing **20**(18): 3663-3675.

Aron, D., L (1949). "Copper enzymes in isolated Chloroplasts polyphenoxides in Beta vulgaris." Plant Physiology **24**: 1-15.

Bartholomeus, H. M., M. E. Schaepman, et al. (2008). "Spectral reflectance based indices for soil organic carbon quantification " Geoderma **145**: 28-36.

Bax, M. (1997). "MASS GRAVES, STAGNATING IDENTIFICATION, AND VIOLENCE: A CASE STUDY IN THE LOCAL SOURCES OF "THE WAR" IN BOSNIA HERCEGOVINA." Anthropological Quarterly **70**(1): 11-19.

Ben-Dor, E. (2002). "Quantitative remote sensing of soil properties." Advances in Agronomy **75**: 173-243.

Ben-Dor, E., Y. Inbar, et al. (1997). "The reflectance of organic matter in the visible near-infrared and short wave infrared region (400-2500)nm during a controlled decomposition process." Remote Sensing of Environment **61**(1): 1-15.

Bowers, S. A. and R. J. Hanks (1965). "Reflection of radiant energy from soil." Soil Science **100**: 130-138.

Bremmer, R. H., A. Nadort, et al. (2011). "Age estimation of blood stains by hemoglobin derivative determination using reflectance spectroscopy." Forensic Science International **206**(1–3): 166-171.

Bromba, M. U. A. and H. Ziegler (1981). "Application hints for Savitzky-Golay digital smoothing filters." Analytical Chemistry **53**(11): 1583-1586.

Campbell, N., J. Reece, et al. (2003). Biology: concepts and connections. San Francisco, Benjamin Cummings.

Carter, D. O., D. Yellowlees, et al. (2007). "Cadaver decomposition in terrestrial ecosystems." Naturwissenschaften **94**: 12-24.

Cheng, T., B. Rivard, et al. (2010). "Continuous wavelet analysis for the detection of green attack damage due to mountain pine beetle infestation." Remote Sensing of Environment **114**(4): 899-910.

Clemens, S., M. G. Palmgren, et al. (2002). "A long way ahead: understanding and engineering plant metal accumulation." Trends in Plant Science **7**(7): 309-315.

Dalva, M., M. Kalácska, et al. (2012). "Detecting graves with methane." Geoderma **189-190**: 18-27.

Daubechies, I. (1990). "The wavelet transform, time-frequency localization and signal analysis." Information Theory, IEEE Transactions on **36**(5): 961-1005.

Daubechies, I. (1992). Ten lectures on wavelets, SIAM.

Degea, J. (2011). Discriminating between Grave Sites and NonGrave Sites Using Conventional Remote Sensing Methods. Undergraduate Honours Thesis, McGill University.

Dematte, J. A. M., M. Nanni, R,, et al. (2010). "Soil density evaluated by spectral reflectance as an evidence of compaction effect." International Journal of Remote Sensing **31**(2): 405-422.
Dent, B. B., S. L. Forbes, et al. (2004). "Review of human decomposition processes in soil." Environmental Geology **45**: 576–585.
Dixon, A. F. G. (1998). Aphid Ecology An optimization approach: An Optimization Approach, Springer.
Dorriety, J. (2007). "Cadaver dogs as a forensic tool: an analysis of prior studies." Journal of Forensic Identification **57**: 717-725.
Duin, R. P. W., P. Juszczak, et al. (2007). PRTools4.1, A Matlab Toolbox for Pattern Recognition, Delft University of Technology.
Ellis, S. and A. Mellor (1995). Soils and Environement. New York, Routledge.
Emsley, J. (1998). The Elements, Oxford University press.
Fidêncio, P. H., R. J. Poppi, et al. (2002). "Determination of organic matter in soil using near-infrared spectroscopy and partial least squares regression." Communications in Soil Science and Plant Analysis **33**(9&10): 1607-1615.
Filella, I., L. Serrano, et al. (1995). "Evaluating wheat nitrogen status with canopy reflectance indices and discriminant analysis." Crop Science **35**(5): 1400-1405.
Forbes, S. L. (2008). Decomposition Chemistry in a Burial Environment. Soil analysis in forensic taphonomy : chemical and biological effects of buried human remains M. Tibbett and D. O. Carter. Boca Raton, CRC Press.
Freckman, D. W. (1982). Nematodes in soil ecosystems. Austin, University of Texas Press.
Gamon, J. A., J. Peñuelas, et al. (1992). "A narrow-waveband spectral index that tracks diurnal changes in photosynthetic efficiency." Remote Sensing of Environment **41**(1): 35-44.
Gamon, J. A., L. Serrano, et al. (1997). "The photochemical reflectance index: an optical indicator of photosynthetic radiation use efficiency across species, functional types, and nutrient levels." Oecologia **112**(4): 492-501.
Garrido-Varo, A., & De Pedro, E. (2008). The role of Near-Infrared Spectroscopy in Verifying Label Information in Agro-Forestry Products. Handbook of near-infrared analysis. D. A. Burns and Ciurczak. Boca raton, CRC Press, Francis and Taylor Group.
Gerendás, J., Z. Zhu, et al. (1997). "Physiological and Biochemical Processes Related to Ammonium Toxicity in Higher Plants." Zeitschrift für Pflanzenernährung und Bodenkunde **160**(2): 239-251.
Govender, M., P. Dye, et al. (2009). "Review of commonly used remote sensing and ground-based technologies to measure plant water stress." Water SA **35**: 741-752.
Grossmann, A., R. Kronland-Martinet, et al. (1989). Reading and Understanding Continuous Wavelet Transforms. Wavelets. J.-M. Combes, A. Grossmann and P. Tchamitchian, Springer Berlin Heidelberg**:** 2-20.
Harrison, M. and L. Donnelly (2009). Locating Concealed Homicide Victims: Developing the Role of Geoforensics. Criminal and Environmental Soil

Forensics. K. Ritz, L. Dawson and D. Miller, Springer Netherlands**:** 197-219.

Hiscox, J. D. and G. Israelstam (1979). "A Method for the extraction of chlorophyll leaf tissue without maceration." Canadian journal of botany **57**: 1332-1334.

Huete, A. R. and R. Escadafal (1991). "Assessment of biophysical soil properties through spectral decomposition techniques." Remote Sensing of Environment **35**(2–3): 149-159.

Jackson, R. D., P. N. Slater, et al. (1983). "Discrimination of Growth and Water Stress by Various Vegetation Indices Through Clear and Turbid Atmospheres." Remote Sensing of Environment **15**(187-208).

Jessee, E. and M. Skinner (2005). "A typology of mass grave and mass grave-related sites." Forensic Science International **152**(1): 55-59.

Jones, H. G. and R. A. Vaughan (2010). remote sensing of vegetation: principles , techniques, and applications. New York, Oxford University Press.

Jordan, C. F. (1969). "Derivation of leaf area index from quality of light on the forest floor." Ecology **50**(663-666).

Kabata-Pendias, A. and A. B. Mukherjee (2007). Plants. Trace Elements from Soil to Human, Springer Berlin Heidelberg**:** 57-65.

Kalacska, M. E., Bell, L. S., Sanchez-Azofeifa, G. A., & Caelli, T. (2009). "The application of remote sensing for detecting mass graves: An experimental animal case study from Costa Rica. ." Journal of forensic science **54**(1): 159-166.

Keller, T. and F. Pipitone (2010). "Inside Mexico's Drug War." World Policy Journal **27**(1): 29-37.

Khan, Z. and Y. H. Kim (2007). "A review on the role of predatory soil nematodes in the biological control of plant parasitic nematodes." Applied Soil Ecology **35**(2): 370-379.

Knipling, E. B. (1970). "Physical and Physiological Basis for the Reflectance of Visible and Near-Infrared Radiation from Vegetation." Remote Sensing of Environment **1**: 155-159.

Lajoie, P. and P. Stobbe (1951). Étude des soils des comtés de Soulanges et de Vaudreuil dans la province de Québec. e. c. a. l. m. d. l. A. d. Q. e. l. C. M. Services des fermes expérimentales ministère fédéral de l'Agriculture, Université McGill. Ottawa, ministère fédéral de l'Agriculture.

Larizza, M. (2010). Physical and Chemical Analysis of Pig Carcass Decomposition in a Fine Sand, University of Ontario Institute of Technology.

Larson, D. O., A. A. Vass, et al. (2011). "Advanced Scientific Methods and Procedures in the Forensic Investigation of Clandestine Graves." Journal of Contemporary Criminal Justice **27**(2): 149-182.

Leblanc, G., M. Kalacska, et al. (2012). "Detection of Single Graves by Airborne Hyperspectral Imaging." 33rd Canadian Symposium on Remote Sensing.

Lichtenthaler, H. K. (1987). [34] Chlorophylls and carotenoids: Pigments of photosynthetic biomembranes. Methods in Enzymology. R. D. Lester Packer, Academic Press. **Volume 148:** 350-382.

Mailloux, A. and G. Godbout (1954). Étude pédologique du comté de huntingdon et beauharnois. M. d. l'agriculture. Québec, Province de Québec-Ministère de l'agriculture **4**.

Melvern, L. (2006). Conspiracy to murder: The Rwandan genocide, Verso.

Merzlyak, J. R., A. A. Gitelson, et al. (1999). "Non-destructive Optical Detection of Pigment Changes During Leaf Senescence and Fruit Ripening." Physiologia Plantarum **106**: 135-141.

Penuelas, J. and I. Filela (1998). "Visible and near-infrared reflectance techniques for diagnosing plant physiological status." Trends in Plant Science **3**(4): 151-156.

Peñuelas, J. and I. Filella (1998). "Visible and near-infrared reflectance techniques for diagnosing plant physiological status." Trends in Plant Science **3**(4): 151-156.

Potvin, C. (1993). ANOVA: Experiments in Controlled Environments. Design and Analysis of Ecological Experiments. S. M.Scheiner and J. Gurevitch. New York, Chapman & Hall.

Rasband, W. (2012). Image J: Image Processing and Analysis in Java. N. I. o. Health.

Ruffell, A. and J. McKinley (2014). "Forensic geomorphology." Geomorphology **206**(0): 14-22.

Schultz, J. J. (2008). "Sequential Monitoring of Burials Containing Small Pig Cadavers Using Ground Penetrating Radar*." Journal of Forensic Sciences **53**(2): 279-287.

Sellers, P. J. (1985). "Canopy Reflectance, Photosynthesis and Transpiration." International Journal of Remote Sensing **6**: 1335-1372.

Stone, M., J. Solie, et al. (1996). "Use of spectral radiance for correcting in-season fertilizer nitrogen deficiencies in winter wheat." Transactions of the ASAE **39**(5): 1623-1631.

Stoner, E. R. and M. F. Baumgardner (1981). "Characteristic variations in reflectance on surface soils." soil science society of America journal **45**(6): 1161-1165.

Swann, L. M., S. L. Forbes, et al. (2010). "Observations of the temporal variation in chemical content of decomposition fluid: A preliminary study using pigs as a model system." Australian Journal of Forensic Sciences **42**(3): 199-210.

Tibbett, M. and D. O. Carter (2009). Research in Forensic Taphonomy: A Soil-Based Perspective. Criminal and Enviromental Soil Forensics K. Rittz, L. Dawson and D. Miller. Aberdeen, Springer Science + Business Media**:** 529.

Tucker, C. J. (1979). "Red and Photographic Infrared Linear Combinations for Monitoring Vegetation." Remote Sensing of Environment **8**: 127-150.

Vass, A., A. (2008). "Decompositional Odor Analysis Database." Journal of forensic science **March 53**(2): 384-391.

Vass, A. A. (2011). "The elusive universal post-mortem interval formula." Forensic Science International **204**: 34-40.

Vogelmann, J. E., B. N. Rock, et al. (1993). "Red edge spectral measurements from sugar maple leaves." International Journal of Remote Sensing **14**(8): 1563-1575.

Watts, S. J. (1999). Epidemics and history: disease, power and imperialism, Yale University Press.

Wessman, C. (1991). "Remote sensing of soil processes." Agriculture, Ecosystems & Environment **34**(1-4): 479-493.